Department of Physics

TITLE PAGE

Formation of thin film of *AB* compound layer under irradiation

By

Samuel Oluwafemi Akintunde

Submitted in partial fulfilment of the requirements for the degree

Doctor of Philosophy (in Physics)

In the

Department of Physics
Faculty of Natural and Agricultural Sciences
University of Pretoria

Supervisor: Prof. P.A. Selyshchev

September 2016

© University of Pretoria

Department of Physics

DECLARATION PAGE

I, Samuel Oluwafemi Akintunde, declare that the thesis which I hereby submit for the degree of Doctor of Philosophy (in Physics) at the University of Pretoria is my original work which has not been previously submitted by me for a degree at this university or any other tertiary institution.

Student signature:..................................

Student number: 14008590

Supervisor's signature:............................

Supervisor's name: Prof. P.A. Selyshchev

H.O.D. signature:.....................................

Prof. C. C. Theron

Copyright © 2016 University of Pretoria

© University of Pretoria

ACKNOWLEDGMENTS

I would like to thank the following people and institutions for their immense contribution towards the completion of my PhD study.

- My academic supervisor, Prof. P.A Selyshchev for his continued support, incessant advice, guidance and encouragement.
- The South African National Research Foundation and UP postgraduate scholarship scheme that gives me the opportunity of studying at no cost.
- The head of the department, Prof. C.C. Theron for creating job opportunity on a part-time basis for me and other students in the department.
- My fellow research students and all those who happen to be the source of inspiration to me.
- My wife Mrs Akintunde, my daughters Ms Eniola Akintunde and Oluwashikemi Akintunde, and my son Master Daniel Akintunde for their prayer, understanding, and support that I received from them during the period of my studies.

© University of Pretoria

UNIVERSITEIT VAN PRETORIA
UNIVERSITY OF PRETORIA
YUNIBESITHI YA PRETORIA

Department of Physics

ABSTRACT

In this research study, we proposed a model that describes the formation of thin-film of an *AB* compound layer at the interfaces of two immiscible solid layers *A* and *B* under the influence of irradiation. However, we begin our study with a non-irradiation process where we investigate the growth kinetics of an *AB* compound layer under the diffusion of one and two kinds of species. This diffusion process takes place by means of one or two transport mechanisms during an *AB* compound layer formation process. The results that follow from this investigation reveal a complex growth kinetics of an *AB* compound layer under the diffusion of two kinds of species by means of two transport mechanisms. However, the complex growth behaviour transforms to simple linear-parabolic or parabolic growths when only one kind of species diffuse by means of one transport mechanism.

In the irradiation aspect of the study, the *A* and *B* solid layers (bilayer system) are considered to be bombarded by a beam of light and heavy energetic particles independently under different considerations. We take into account two possibilities during the irradiation of this bilayer system. Firstly, the majority of the kinetic energy of the radiation particles is considered to be converted into heat energy which subsequently results in the heating of the irradiated layers. We assume that the energy transferred from the incident particles to the atoms of the irradiated materials during the course of irradiation is less than their lattice threshold displacement energy. Thus, no defects are generated during this process. The influence of heating that accompanies the irradiation process is investigated to see if it could accelerate the growth of an *AB* compound layer at the interfaces of the *A* and *B* layers.

© University of Pretoria

The second possibility is considered under the presupposition that the kinetic energy transferred by the radiation particles is greater than the lattice threshold displacement energy of the *A* and *B* layers; therefore, this process results in defects generation.

The contribution of the two basic point defects (i.e. interstitial and vacancy defects), induced by irradiation, towards the growth of an *AB* compound layer is studied independently.

The results that follow from this study show that the rate of growth of an *AB* compound layer at the interfaces depends on the defect generation rate. The growth rate increases proportionally with the defect generation rate. At high-temperature irradiation, the growth rate depends strongly on both temperature and defect generation rate while at low-temperature irradiation it depends strongly only on defect generation rate. On the other hand, the radiation heating makes no significant contribution towards the growth of an *AB* compound layer at low temperature; this is because the dimensions of the *A* and *B* layers that are considered in this study are in the order of a few tens of nanometers. Considering the fact that the amount of energy deposited by the radiation particles increases with the thickness of the irradiated layer, less energy is, therefore, deposited in the irradiated layers under the thin film consideration. This reason makes radiation heating a less probable process for an *AB* compound layer formation under the influence of irradiation.

© University of Pretoria

UNIVERSITEIT VAN PRETORIA
UNIVERSITY OF PRETORIA
YUNIBESITHI YA PRETORIA

TABLE OF CONTENTS

TITLE PAGE…..1

DECLARATION PAGE………………………………………………………………........2

ACKNOWLEDGMENTS…………………………………………………………………..3

ABSTRACT……………………………………………………………………………....4-5

TABLE OF CONTENTS……………………………………………………………………6-7

LIST OF TABLES………………………………………………………………………..8-9

LIST OF FIGURES………………………………………………………………………10-12

CHAPTER 1: INTRODUCTION……………………………………………………13

1.1 Review of experimental works…………………………………...13-16

1.2 Introduction to the present theoretical approach………………….16-18

1.3 Aim of the research study………………………………………...18-20

1.4 The contents of the thesis…………………………………………20-21

CHAPTER 2: *AB* COMPOUND LAYER FORMATION AS A RESULT OF CHEMICAL TRANSFORMATION CONTROLLED BY DIFFUSION…………………………………………………………22

2.1 Introduction……………………………………………………22-23

2.2 Physical process for an *AB* compound layer formation under non-irradiation process……………………………………………23-25

2.3 Basic equations for an *AB* compound layer formation under non-irradiation process………………………..……………….25-32

2.4 Results and discussion on non-irradiation process……………..…32-47

2.5 Conclusion……………………………………………….…………..47

CHAPTER 3: INFLUENCE OF IRRADIATION ON *AB* COMPOUND LAYER FORMATION………...…………………………………………..48

3.1 Introduction……………….………………………………………...48-49

3.2 Physical process for an *AB* compound layer formation under the influence of radiation-induced heating…………………….....50-51

© University of Pretoria

UNIVERSITEIT VAN PRETORIA
UNIVERSITY OF PRETORIA
YUNIBESITHI YA PRETORIA

3.2.1 Basic equations for an *AB* compound layer formation under the influence of radiation-induced heating………………………..52-62

3.2.2 Results and discussion on radiation-induced heating…….……....62-68

3.3 The influence of radiation-induced vacancies on the formation of an *AB* compound layer……………………………………………68-69

3.3.1 Basic equations for an *AB* compound layer formation due to radiation-induced vacancy mechanism……..…...………..69-77

3.3.2 Results and discussion on radiation-induced vacancy mechanism……………………………………………77-89

3.4 The role of radiation-induced interstitial mechanism on the formation of an *AB* compound layer……………………………..89-90

3.4.1 Basic equations for an *AB* compound layer formation due to radiation-induced interstitial mechanism…………..…….………91-95

3.4.2 Results and discussion on radiation-induced interstitial mechanism…………………………………………...96-107

3.5 Conclusion……………………………………..……………107-108

CHAPTER4: SUMMARY, CONCLUSION, AND RECOMMENDATION……………………………..……....109-111

REFERENCES ……………………………………………………………………...112-116

ARTICLES…………………………………………………………………………117-128

© University of Pretoria

LIST OF TABLES

1-1 Silicides growth parameters measured from experiment under non-irradiation process……………………………………………………………………15

1-2 Silicides growth parameters measured from experiment under the influence of irradiation……………………………………………………………………16

2-1 Useful information on growth kinetics of WSi_2, VSi_2, Co_2Si, and Ni_2Si……………...35

2-2 Data used for WSi_2, VSi_2, Co_2Si, and Ni_2Si layer thickness estimation………………36

2-3 Critical thickness and time of WSi_2, VSi_2, Co_2Si, and Ni_2Si layer……………………37

2-4 Activation energy and pre-exponential factor for the growth kinetics of WSi_2, VSi_2, Co_2Si, and Ni_2Si……………………………………………………………………38

3-1 Useful parameters for estimation of temperature rise in the irradiated layers……….64

3-2 Estimated values for light particle stopping power, light particle penetration depth, volumetric heat generation rate, and temperature rise in metal-silicon bilayer system at a given energy of 20 keV……………………………………………65

3-3 Estimated values for heavy particle stopping power, heavy particle penetration depth, volumetric heat generation rate, and temperature rise in metal- silicon bilayer system at a given energy of 110 keV and120 MeV…………………………..…………66

3-4 Estimated values for the diffusion coefficients of reactant species under the influence of radiation heating……………..………………………………….……………66

3-5 Estimation of diffusivity of palladium and silicon species via vacancy mechanism in the Pd_2Si layer together with the speed of growth and reaction rate of the layer…...80

3-6 Estimation of speed of growth and reaction rate of Ni_2Si layer with the diffusivity of nickel and silicon species via vacancy mechanism in the Ni_2Si layer………………80

3-7 Estimation of reaction rate, growth speed, and diffusivity of platinum and silicon species via vacancy mechanism in the Pt_2Si layer…………………………………..80

3-8 Estimation of diffusivity of cobalt and silicon species via vacancy mechanism in the $CoSi$ layer together with the speed of growth and reaction rate of the layer……….81

© University of Pretoria

3-9 Estimation of the speed of growth, reaction rate, the diffusivity of tungsten and silicon species via vacancy mechanism in the WSi_2 layer……………………………………81

3-10 Estimated density of silicide layers and their formation temperatures under non-irradiation process……………………………………………………………………84

3-11 Parameters used for estimation of thermal self-diffusion coefficients of *Pd*, *Si*, *Ni*, *Pt*, *Co* and *W* in their respective silicides…………………………………………………..88

3-12 Useful parameters for estimation of diffusivity via vacancy mechanism at temperature of 298 K……………………………………………………………………………89

3-13 Parameters used for estimation of interstitial diffusivity at a temperature of 298 K together with the density of atomic species and *AB* molecule………………………98

3-14 Estimation of speed of growth, the rate of reaction, and interstitial density of palladium and silicon species in their respective layers………….……………………99

3-15 Estimation of speed of growth and reaction rate of Ni_2Si layer with the interstitial density of nickel and silicon species in their respective layers………………………99

3-16 Estimation of interstitial density of platinum and silicon species in their respective layers together with the speed of growth and reaction rate of the Pt_2Si layer………100

3-17 Estimation of interstitial density of cobalt and silicon species, the speed of growth and reaction rate of *CoSi* layer……………………………………………………………100

3-18 Estimation of interstitial density of tungsten and silicon species in their respective layers together with the speed of growth and reaction rate of the WSi_2 layer………101

© University of Pretoria

LIST OF FIGURES

2-1 Schematic diagram of the A-B bilayer system at time $t = 0$ before the commencement of heating……..24

2-2 Schematic diagram of the A-B bilayer system showing an AB layer formation at time $t > 0$ after the commencement of heating……25

2-3 The growth kinetics of tungsten disilicide (WSi_2) at 1033 K under a non-irradiation process……..39

2-4 The growth kinetics of vanadium disilicide (VSi_2) at 873 K under a non-irradiation process……40

2-5 The growth kinetics of cobalt silicide (Co_2Si) at 763 K under a non-irradiation process……..41

2-6 The growth kinetics of nickel silicide (Ni_2Si) at 573 K under a non-irradiation process……..42

2-7 The growth kinetics of palladium silicide (Pd_2Si) at 473 K under the concurrent diffusion of both palladium and silicon species in the silicide layer……45

2-8 The growth kinetics of palladium silicide (Pd_2Si) at 473 K when only palladium species diffuse in the silicide layer……...46

2-9 The growth kinetics of Palladium silicide (Pd_2Si) at 473 K under the consideration of three different diffusion possibilities over a period of 3600 s……..47

3-1 Schematic diagram of the A-B bilayer system during radiation heating process…….51

3-2 Schematic diagram showing the formation of an AB layer under a radiation-induced vacancy mechanism……..69

3-3 The growth kinetics of palladium silicide Pd_2Si at room temperature under the influence of radiation-induced vacancy at defect generation rates of $K = 10^{-9}$, 10^{-8} and 10^{-7} dpa/s ……83

© University of Pretoria

3-4 The growth kinetics of nickel silicide Ni_2Si at room temperature under the influence of radiation-induced vacancy at defect generation rates of $K = 10^{-9}$, 10^{-8} and 10^{-7} dpa/s....84

3-5 The growth kinetics of platinum silicide Pt_2Si at room temperature under the influence of radiation-induced vacancy at defect generation rates of $K = 10^{-9}$, 10^{-8} and 10^{-7} dpa/s....85

3-6 The growth kinetics of cobalt silicide $CoSi$ at room temperature under the influence of radiation-induced vacancy at defect generation rates of $K = 10^{-9}$, 10^{-8} and 10^{-7} dpa/s....86

3-7 The growth kinetics of tungsten disilicide WSi_2 at room temperature under the influence of radiation-induced vacancy at defect generation rates of $K = 10^{-9}$, 10^{-8} and 10^{-7} dpa/s....87

3-8 Schematic diagram showing the formation of an AB layer under a radiation-induced interstitial mechanism....90

3-9 The growth kinetics of palladium silicide Pd_2Si at room temperature under the influence of radiation-induced interstitial at defect generation rates of $K = 10^{-9}$, 10^{-8} and 10^{-7} dpa/s....102

3-10 The growth kinetics of nickel silicide Ni_2Si at room temperature under the influence of radiation-induced interstitial at defect generation rates of $K = 10^{-9}$, 10^{-8} and 10^{-7} dpa/s....103

3-11 The growth kinetics of platinum silicide Pt_2Si at room temperature under the influence of radiation-induced interstitial at defect generation rates of $K = 10^{-9}$, 10^{-8} and 10^{-7} dpa/s....104

3-12 The growth kinetics of cobalt silicide $CoSi$ at room temperature under the influence of radiation-induced interstitial at defect generation rates of $K = 10^{-9}$, 10^{-8} and 10^{-7} dpa/s....105

© University of Pretoria

3-13 The growth kinetics of tungsten disilicide WSi_2 at room temperature under the influence of radiation-induced interstitial at defect generation rates of $K = 10^{-9}$, 10^{-8} and 10^{-7} dpa/s……106

© University of Pretoria

UNIVERSITEIT VAN PRETORIA
UNIVERSITY OF PRETORIA
YUNIBESITHI YA PRETORIA

CHAPTER 1

INTRODUCTION

The reaction-diffusion kinetics has proven very useful in solid state reaction, providing the necessary insight into the compound layer formation at the interface(s) of a bilayer system. This bilayer system could be a solid-solid, solid-liquid, or solid-gas system. The technological importance and other useful applications of these compounds have been the motivation behind the investigation carried out on their formation processes. These investigations have been conducted under both irradiation and non-irradiation processes.
The results of these investigations showed that the layer growth kinetics under both processes are usually the same, and they are often identified as parabolic [1].

1.1 Review of experimental works

The growth kinetics of different silicides are investigated at different temperatures ranging from 200 – 650^{0} C [2, 3] under a non-irradiation process. The activation energies for the growth of these silicides are determined from the experimental measurements, and the values are shown in Table 1-1. The interdiffusion coefficients of the silicides are calculated based on the measured activation energies and temperatures at which the silicides are formed.

The growth rates of these silicides are determined from the ratio of the square of the thickness of the silicide to the annealing time. The growth rate remains constant at a particular annealing temperature. As annealing temperature changes, the growth rate changes correspondingly.
The diffusion coefficients of metal and silicon species are usually found to be smaller than the interdiffusion coefficients of the growing silicides [4]. This observation suggests that the growth of the silicide occurs at a rate faster than the diffusion of both metal and silicon species in the metal-silicon bilayer system.

© University of Pretoria

The growth kinetics of the silicides is often determined as parabolic. However, there are silicides that are found to have two growth kinetics as shown in Table 1-1.

Examples of such silicides are nickel silicide, tungsten disilicide and vanadium disilicide. Their growth kinetics begins as linear and later change into parabolic after a certain period of time. The thickness of silicide is generally found to increase with annealing temperature and time.

The experimental studies of the growth of silicides under irradiation are mostly carried out by ion beam mixing technique at a room temperature. The studies reveal that the stoichiometry of the silicide formed under irradiation in most cases is the same as that of the non-irradiation process. The growth kinetics of the silicide under irradiation is usually found to be similar to that of the non-irradiation process. The growth kinetics is parabolic for most of the silicides as depicted in Table 1-2.

The metal/silicon interface is usually irradiated with an ion beam to different doses at a particular ion energy.

The dose dependence of mixing variance of each diffusing species is found to be the product of diffusion coefficient and irradiation time [5]. The interfacial mixing is found to increase with ion dose. The thickness of the silicide layer increases in proportion to the square root of the ion dose with nearly constant composition [6].

The growth of the silicide layer in the metal/silicon bilayer system is suggested to be due to isotropic cascade mixing, thermal spike, and radiation enhanced diffusion of both metal and silicon species. The growth of the silicide is found to depend on the fluence rate.

The palladium silicide (Pd_2Si), nickel silicide (Ni_2Si), cobalt silicide (Co_2Si), tungsten disilicide (WSi_2), vanadium disilicide (VSi_2), and platinum silicide (Pt_2Si) growth measured from experiment under irradiation and non-irradiation process are shown in Tables 1-1 and 1- 2 below:

© University of Pretoria

UNIVERSITEIT VAN PRETORIA
UNIVERSITY OF PRETORIA
YUNIBESITHI YA PRETORIA

Table 1-1. Silicides growth parameters measured from experiment under non-irradiation process

Silicide	Activation energy (eV)	Formation temperature (^{0}C)	Pre-exponential factor (m^2 /s)	Growth kinetics	The cause of growth of the silicide
Pd_2Si	1.50 [7]	200 - 275 [7]	7.90 x 10^{-4} [7]	Parabolic [7]	Heating and atomic diffusion
Ni_2Si	0.80 [8]	200 - 350 [8]	2.50 x 10^{-5} [8]	Linear [8]	Heating and atomic diffusion
Ni_2Si	1.50 [8]	200 - 350 [8]	1.67 x 10^{-4} [8]	Parabolic [8]	Heating and atomic diffusion
Co_2Si	1.50 [9]	350 - 500 [9]	-	Parabolic [9]	Heating and atomic diffusion
WSi_2	3.00 [2, 3]	650 [2, 3]	-	Linear [2, 3]	Heating and atomic diffusion
WSi_2	1.90 [2, 3]	650 [2, 3]	-	Parabolic [2, 3]	Heating and atomic diffusion
VSi_2	2.90 [2, 3]	600 [2, 3]	-	Linear [2, 3]	Heating and atomic diffusion
VSi_2	1.80 [2, 3]	600 [2, 3]	-	Parabolic [2, 3]	Heating and atomic diffusion
Pt_2Si	1.49 [10]	200 - 500 [10]	5.50 x 10^{-4} [10]	Parabolic [10]	Heating and atomic diffusion

© University of Pretoria

Table 1-2. Silicides growth parameters measured from experiment under the influence of irradiation

Silicide	Fluence (ions/cm^2)	Formation temperature (^{0}C)	Type of ion used for irradiation	Ion energy (eV)	The cause of growth of the silicide	Growth kinetics
Pd_2Si	1.0 - 15 x 10^{15} [5]	25 [5]	Argon ion [5]	78 x 10^3 [5]	Isotropic cascade mixing and radiation enhanced diffusion [9]	Parabolic [5]
Ni_2Si	4.7 – 8.9 x 10^{17} [11]	25 [11]	Argon ion [11]	2 – 20 x 10^3 [11]	Isotropic cascade mixing and thermal spike [11]	Parabolic [11]
Co_2Si	1.0 – 10 x 10^{13} [12]	25 [12]	Gold ion [12]	120 x 10^6 [12]	Thermal spike [12]	Parabolic [12]
WSi_2	1.0 – 100 x 10^{12} [13]	25 [13]	Gold ion [13]	120 x 10^6 [13]	Thermal spike [13]	Parabolic [13]
VSi_2	2.0 – 2.7 x 10^{16} [14]	25 [14]	Argon ion [14]	3 x 10^3 [14]	Isotropic cascade mixing and radiation enhanced diffusion [14]	Parabolic [14]
Pt_2Si	1.0 – 11 x 10^{16} [15]	25 [15]	Argon ion[15]	150 x 10^3 [15]	Isotropic cascade mixing [15]	Parabolic [15]

1.2 Introduction to the present theoretical approach

A number of theoretical approaches had been developed in the past, among them are the physicochemical approach, linear-parabolic approach, interfacial reaction barrier approach and the conventional diffusion approach [16-18] in which all have a common goal of describing the formation of intermediate compound layer(s) in the bilayer systems.

© University of Pretoria

UNIVERSITEIT VAN PRETORIA
UNIVERSITY OF PRETORIA
YUNIBESITHI YA PRETORIA

The results of these theoretical approaches were compared with those predicted in the equilibrium phase diagrams.

The results show that the simultaneous growth of three or more compound layers at the interface(s) of bilayer system (under thin film consideration) is very unlikely in contrast to the prediction of equilibrium phase diagrams. Therefore, the maximum number of compound layers that are most likely to grow simultaneously under experimental conditions is shown to be two [19].

The theoretical approaches described in the previous models are limited to non-irradiation processes. However, the present approach provides a logical explanation for the kinetics of growth of the compound layer under both irradiation and non-irradiation processes.

In the present approach, we take into account the simultaneous contributions of both diffusion and chemical reaction to the formation process of the compound layer. This approach is different from that of the physicochemical model described in [19] where chemical reaction contribution is considered separately from that of diffusion.

With the present approach, it is possible to consider different diffusion mechanisms and chemical transformation simultaneously in the bilayer system. The contribution of each diffusion mechanism to the growth of the compound layer can be determined by the density of reactant species that diffuse from different reactant layers to the reaction interface(s). On the other hand, chemical transformation contributes to the formation process of the compound layer at the reaction interface(s) through the chemical interaction between the diffusing and surface reactant species.

The connection between the flux of diffusion and the reaction rate at the interface(s) of the bilayer system can be established in accordance with mass action principle. This connection, in turn, is linked with the growth rate of the compound layer. The reaction rate is shown in this model as the product of the density of the reactant species at the reaction interface(s).

The influence of diffusion of atomic species on the motion of surface boundary can also be established during the compound layer formation process. The position of surface boundary changes as the AB compound layer grows at the interface(s).

© University of Pretoria

UNIVERSITEIT VAN PRETORIA
UNIVERSITY OF PRETORIA
YUNIBESITHI YA PRETORIA

The diffusion of species determines the rate of change of position of the surface boundary.
For example, as more reactant species diffuse to the reaction interface(s) the chance of chemical transformation between the diffusing and surface reactant species increases.
The growth of the compound layer increases as a result of this chemical transformation and the layer growth, in turn, enhances the motion of the surface boundary.

The distribution of reactant species in the compound layer can be obtained mathematically from the present approach. This approach makes it feasible to obtain the density of reactant species actively participating in the formation process of the compound layer. The spatial dependence of the density of each reactant species in the growing layer is explicitly presented for different growth stages.

1.3 Aim of the research study

The aim of this research is to develop a theoretical model that would describe the compound layer formation under irradiation. The model in [19] is inappropriate for this case because it cannot account for the simultaneous diffusion of reactant species via different transport mechanisms together with the chemical transformation occurring at the interface(s) of the bilayer system.

By specific consideration of each radiation-induced process, we can possibly identify the process responsible for the compound layer formation. This consideration is important because there are a lot of processes that occur almost at the same time under irradiation. These processes include excitation of electron and phonon subsystems, radiation induced defect generation, nuclear transformation, interaction between defects: recombination of point defects (for example, recombination between interstitial and vacancy defects); formation of complexes, clusters, vacancy and interstitial loops; absorption of point defects by dimensional ones, for example, by dislocations and voids, and so on.
It is clear that radiation heating and production and absorption of defects have the most significant influence on diffusion and growth of compound layer.

© University of Pretoria

UNIVERSITEIT VAN PRETORIA
UNIVERSITY OF PRETORIA
YUNIBESITHI YA PRETORIA

To examine the influence of each process on the compound layer formation we consider the influence of vacancy and interstitials, and influence of radiation heating separately. It is the first approximation of course, but it shows the main tendencies.

The influence of heating on the compound layer formation is investigated under irradiation. This investigation is done by examining the role of temperature induced by heating under irradiation on the chemical reaction and diffusion of reactant species.

Inasmuch as chemical reaction and diffusion phenomena, which play an important role in the compound layer formation process, depend strongly on temperature.

The role of temperature on these two key players during irradiation cannot be ignored. Therefore, it is crucial to investigate the contribution of heating to these two phenomena under irradiation. For example, if sufficiently high temperature accompanies the heating process, this can activate the diffusion of species from the reactant layers to the reaction interface(s) and at the interface(s), chemical reaction will occur at different rates because the temperature at each interface will be different due to the different quantities of heat energy generated in each irradiated layer.

However, if extremely low temperature accompanies the process, the contribution of heating under irradiation become insignificant, and layer formation is less probable under such consideration.

On the other hand, the radiation-induced defect generation process is considered under two independent mechanisms. These mechanisms are interstitial and vacancy mediated processes. The vacancy mechanism under irradiation is similar to that of the non-irradiation process. The only difference between them is the disparity in vacancy density. There are more vacancies under irradiation than non-irradiation process.

The interstitial mechanism under irradiation occurs faster than radiation-induced vacancy mechanism due to low migration energy of interstitial atoms. The density of interstitial atoms generated under irradiation is approximately the same as that of vacancy. Therefore, the interstitial mechanism may be regarded as an effective diffusion mechanism for reactant species under irradiation in terms of mobility of species to the reaction interface(s).

© University of Pretoria

UNIVERSITEIT VAN PRETORIA
UNIVERSITY OF PRETORIA
YUNIBESITHI YA PRETORIA

The commonly used theoretical models on irradiation are the thermal spike and displacement cascade model. These models are used to describe the extent of damage caused by irradiation in the target materials.

They are mostly used by experimental investigators that usually irradiate materials with heavy particle radiation, such as ion radiation to explain their empirical results. Most of the experimental works on compound layer formation like those shown in Table 2-1 are explained in terms of these models because these compounds are also formed by ion irradiation.

However, there are other experimental studies that confirmed the formation of compound layer, such as silicide with beam of light particles radiation (e.g. electron radiation) and non-particles radiation (e.g. laser radiation) [20, 21].

The theory of thermal spike and cascade displacement may not be appropriate for these cases, especially at low radiation energy considered in these studies, this is because the mass of radiation particle is smaller than that of the target atom. Therefore, translational displacement of atoms out of their lattice sites with the energy of a few of tens of kiloelectron volts is difficult in this situation. However, the radiation-induced approach developed in this study is applicable to all kinds of irradiation techniques. Since radiation-induced defect and heating occur in all irradiated materials under the application of different irradiation techniques, therefore, this approach can explain compound layer formation under any kind of irradiation.

The model proposed in this study sheds new light on the contribution of radiation-induced heating and defect generation process toward the formation of the compound layer at the interface of two different material samples.

1.4 The contents of the thesis

The content of this thesis is divided into four chapters.

In chapter one, we introduce the formation of the compound layer under both irradiation and non-irradiation processes with a brief review of experimental work on the subject.

© University of Pretoria

UNIVERSITEIT VAN PRETORIA
UNIVERSITY OF PRETORIA
YUNIBESITHI YA PRETORIA

In chapter two, we tailored our theoretical model toward the compound layer formation under non-irradiation process. We divide this chapter into five sections.

The first section introduces an AB compound layer formation under non-irradiation process. The second section presents the physical process for an AB compound layer formation. The third section describes the model and basic equations for an AB compound layer formation under non-irradiation process.

The fourth section presents results and discussion of an AB compound layer formation under non-irradiation process. These results are compared with experimental results. The fifth section presents a brief conclusion on the compound layer formation under non-irradiation process.

In chapter three, we tailored the physical model developed in this study toward the compound layer formation under irradiation. We divide this chapter into five sections and two subsections. The first section introduces an AB compound layer formation under irradiation.

The second section describes a physical model for an AB compound layer formation under radiation-induced heating. The third section describes a physical model tailored toward an AB compound layer formation under radiation-induced vacancy mechanism.

The fourth section describes a theoretical model tailored toward the formation of an AB compound layer under the radiation-induced interstitial mechanism. The first subsection presents the model and basic equations for an AB compound layer formation under each radiation-induced process. The second subsection presents the results and discussion of an AB compound layer formation under each radiation-induced process.

The results are compared with experimental results. Each of the subsection is discussed under each section. The fifth section present a concise conclusion on the formation of an AB compound layer under radiation-induced heating and defects.

In chapter four, we give a general conclusion on the compound layer formation under irradiation and non-irradiation processes followed by a recommendation. We end the thesis with a list of references.

© University of Pretoria

UNIVERSITEIT VAN PRETORIA
UNIVERSITY OF PRETORIA
YUNIBESITHI YA PRETORIA

CHAPTER 2

AB COMPOUND LAYER FORMATION AS A RESULT OF CHEMICAL TRANSFORMATION CONTROLLED BY DIFFUSION.

2.1 Introduction

A number of works in the literature report the formation and growth kinetics of the thin film of an *AB* compound layer such as silicide layer [22-25]. The compound layer formation can be explained from two approaches: diffusion approach (which is considered as the conventional approach) and physicochemical approach (an alternative approach to the former). From diffusion approach, the thin film of an *AB* compound is formed as a result of intermixing of *A* with *B* species after the diffusion of either *A* atoms into *B* layer or *B* atoms into *A* layer. This intermixing is initiated by heat treatment process. Diffusion approach usually leads to loss of reaction controlled stage [19] due to lack of consideration for the chemical reaction between *A* and *B* species**.**

Unlike diffusion approach, physicochemical approach incorporates two processes: diffusion and chemical reaction. It describes *A* and *B* layers as two immiscible layers with the interface(s) separating them. A chemical reaction takes place between *A* and *B* atoms at the interface(s). The *A* atoms or *B* atoms or both are brought to the interface(s) by means of diffusion. This approach creates room for the possibility of accounting for chemical reaction contributions to the thin film of an *AB* compound layer growth during reaction controlled stage.

The interfacial barrier approach described by Gosele and Tu [18] predicts the number of compound phases that can grow sequentially at the reaction interface in both thin film and bulk reaction couple taking into account a certain minimum thickness (called critical thickness).

© University of Pretoria

UNIVERSITEIT VAN PRETORIA
UNIVERSITY OF PRETORIA
YUNIBESITHI YA PRETORIA

This approach is limited to non-irradiation process, unlike the present approach that can account for the growth of compound phase(s) under and without irradiation.

In this chapter, we present a physical model that is tailored toward an *AB* compound layer formation under non-irradiation process.

This model describes the growth kinetics of an *AB* compound layer based on the first approximation of reaction rate, which is expressed as the product of reactant species' densities. This approximation is in accord with mass action law.

The speed of growth is proportional to reaction rate during the reaction controlled and diffusion limited stages.

The *AB* compound layer growth kinetics that follows from this approach show that the growth behaviour of the growing layer can be explained from the viewpoint of the number of kinds of atomic species actively diffusing into an *AB* layer during the formation process.

This model is discussed in light of the number of kinds of active and dominant diffusing species in an *AB* compound layer during a non-irradiation process. The results of this theoretical approach are compared with experimental results.

2.2 Physical process for an *AB* compound layer formation under non-irradiation process

Let us consider *AB* compound formation for time $t > 0$. Suppose that at time $t = 0$ the *A* layer occupies space $x < 0$ and *B* layer occupies space $x > 0$ in the *A*-*B* bilayer system as illustrated in Figure 2-1. At time $t > 0$ heat treatment process commences in the *A* and *B* layers. The *AB* compound layer arises due to the chemical reaction between *A* and *B* atoms. The interfaces *A/AB* and *AB/B* spatially separates *A* and *B* layers after the formation of the *AB* compound. The *A* atoms diffuse from the *A* layer through an *AB* layer to interface *A/AB,* and *B* atoms diffuse from the *B* layer via an *AB* layer to interface *AB/B*. At both interfaces, *A/AB* and *AB/B*, diffuse *A* and *B* atoms chemically react with *B* and *A* surface atoms respectively to form additional *AB* compound.

© University of Pretoria

An *AB* layer occupies space from $x = -h_A(t)$ to $x = h_B(t)$ as shown in Figure 2-2. The thickness of the compound layer formed at interface *A/AB* is denoted by $h_A(t)$ and at interface *AB/B* by $h_B(t)$. The total thickness of an *AB* compound layer formed between the *A* and *B* layers is designated by $h(t) = h_A(t) + h_B(t)$.

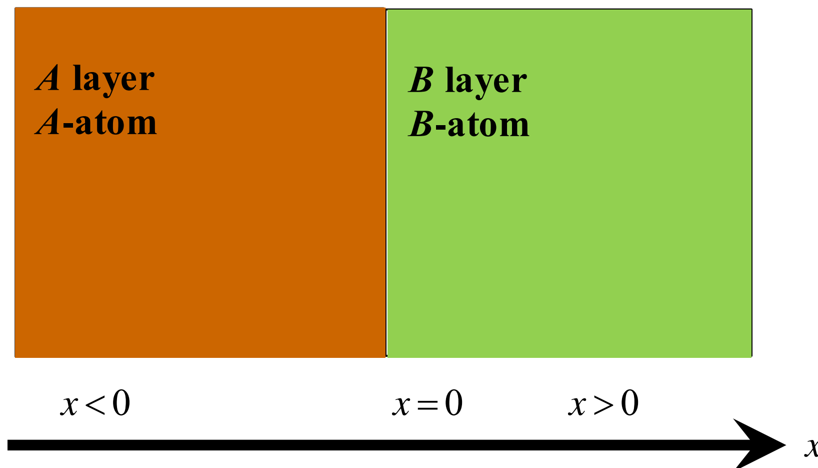

Figure 2-1: Schematic diagram of the *A*-*B* bilayer system at time $t = 0$ before the commencement of heating.

© University of Pretoria

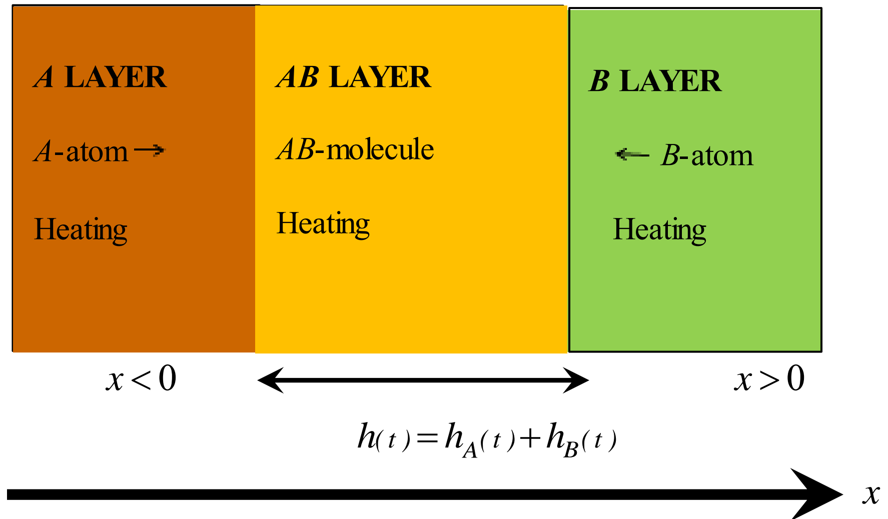

Figure 2-2: Schematic diagram of the A-B bilayer system showing an AB layer formation at time $t>0$ after the commencement of heating.

2.3 Basic equations for an AB compound layer formation under a non-irradiation process

The chemical reaction between A and B atom, is represented as thus:

$$\nu_a A + \nu_b B \rightarrow A_{\nu_a} B_{\nu_b} \qquad (2.1)$$

Where

ν_a and ν_b are the stoichiometric coefficients for the A and B atoms respectively.

The rate of chemical transformation depends on density of the reactant species. If one of the reactant species is in excess, the rate of reaction remains constant with a change of density of the species that are present in excess at the interface [26].

© University of Pretoria

UNIVERSITEIT VAN PRETORIA
UNIVERSITY OF PRETORIA
YUNIBESITHI YA PRETORIA

But, if the density of the reacting species is approximately the same, the rate of chemical transformation can be delineated in the first approximation as the product of reactant species' densities.

Thus, the rate of chemical reaction between *A* and *B* atoms, at reaction interfaces *A/AB* and *AB/B* can be approximately defined as thus:

$$R_a = \begin{cases} \gamma\left(n_a^0\right)^2 = \text{const} & n_b\left(x = -h_{A(t)}\right)v_b \geq n_a^0 v_a \\ \gamma n_a^0 n_b\left(x = -h_{A(t)}\right) & n_b\left(x = -h_{A(t)}\right)v_b \leq n_a^0 v_a \end{cases} \tag{2.2a}$$

and

$$R_b = \begin{cases} \gamma\left(n_b^0\right)^2 = \text{const} & n_a\left(x = h_{B(t)}\right)v_a \geq n_b^0 v_b \\ \gamma n_b^0 n_a\left(x = h_{B(t)}\right) & n_a\left(x = h_{B(t)}\right)v_a \leq n_b^0 v_b \end{cases} \tag{2.2b}$$

where

$n_a\left(x = h_{B(t)}\right)$ and $n_b\left(x = -h_{A(t)}\right)$ are the densities of *A* and *B* atoms which diffuse to reaction interfaces *AB/B* and *A/AB,*

γ is the reaction rate constant, and

R_a and R_b are the reaction rates at interfaces *A/AB* and *AB/B.*

Due to this approximation, the growth of an *AB* layer can be described in two stages. The first growth stage occurs when there is an excess of one kind of diffusing atoms.

For example, excess *A* atoms at interface *AB/B* or excess *B* atoms at interface *A/AB* and the second growth stage takes place when there is no excess of any kind of atoms at the corresponding interfaces.

The growth rate of an *AB* layer is determined by the rate of *AB* compound formation at both interfaces:

$$\frac{dh_{(t)}}{dt} = V_{ab}\left(R_a + R_b\right) \tag{2.3}$$

© University of Pretoria

We give the details of eqn. (2.3) for all possible situations at interfaces of *A*-*B* bilayer system as thus:

If there are no excess diffusing atoms at the corresponding interfaces (*AB/B* and *A/AB*), we obtain

$$\frac{dh_{(t)}}{dt} = V_{ab}\left(\gamma n_a^0 n_b\left(x = -h_{A(t)}\right) + \gamma n_b^0 n_a\left(x = h_{B(t)}\right)\right) \tag{2.3a}$$

If *A* atoms are in excess at interface *AB/B,* we obtain

$$\frac{dh_{(t)}}{dt} = V_{ab}\left(\gamma\left(n_b^0\right)^2 + \gamma n_a^0 n_b\left(x = -h_{A(t)}\right)\right) \tag{2.3b}$$

If *B* atoms are in excess at interface *A/AB,* we obtain

$$\frac{dh_{(t)}}{dt} = V_{ab}\left(\gamma\left(n_a^0\right)^2 + \gamma n_b^0 n_a\left(x = h_{B(t)}\right)\right) \tag{2.3c}$$

Where V_{ab} is the volume of one molecule of *AB* compound.

The above consideration (in eqns. (2.3b) and (2.3c)) exhaust all possible cases since an excess of both *A* atoms and *B* atoms at the same time at the respective interfaces is impossible.

Note that if there is an excess of *A* (or *B*) atoms at some moment of time (for case (2.3b) or case (2.3c)), then the excess atoms decreases as *AB* layer grows. Stoichiometric equilibrium is reached at some time called critical time, t_c after that, case (2.3a) takes place.

Suppose that all *A* atoms at *AB/B* interface and all *B* atoms at *A/AB* interface reacted at once. Therefore, the growth of an *AB* compound layer is determined by the flux of *A* atoms toward *B* layer and flux of *B* atoms toward *A* layer.

© University of Pretoria

Thus, we consider the diffusion of *A* and *B* atoms inside the *AB* compound layer.

Diffusion of *A* and *B* atoms inside the *AB* layer is described by Fick's second law under a stationary condition as thus:

$$D_{a(b)}\frac{\partial^2 n_{a(b)(x)}}{\partial x^2}=0 \tag{2.4}$$

With corresponding boundary conditions:

$$J_a\left(h_{B(t)}\right)=-D_a\frac{dn_{a(x)}}{dx}=v_a\gamma n_b^0 n_a\left(h_{B(t)}\right),$$

$$J_b\left(-h_{A(t)}\right)=-D_b\frac{dn_{b(x)}}{dx}=v_b\gamma n_a^0 n_b\left(-h_{A(t)}\right),$$

$n_a\left(x=-h_{A(t)}\right)=n_a^0$ and

$n_b\left(x=h_{B(t)}\right)=n_b^0$.

where

$J_a\left(h_{B(t)}\right)$ and $J_b\left(-h_{A(t)}\right)$ are fluxes of *A* and *B* atoms toward interfaces AB/B and A/AB respectively,

D_a and D_b are diffusivities of *A* and *B* atoms.

Solving eqn. (2.4) with boundary conditions for the first stage of layer growth (before critical time). We obtain an expression for the distribution of *A* and *B* atoms inside the *AB* compound layer when *A* atom is in excess at *AB/B* interface:

$$n_a(x,t)=-\frac{\gamma\left(n_b^0\right)^2}{D_a}\left(x+h_{A(t)}\right)+n_a^0 \tag{2.5a}$$

and

© University of Pretoria

UNIVERSITEIT VAN PRETORIA
UNIVERSITY OF PRETORIA
YUNIBESITHI YA PRETORIA

$$n_b(x,t) = \frac{v_b \gamma n_a^0 n_b^0}{D_b + v_b \gamma n_a^0 h(t)} \left(x - h_{B(t)}\right) + n_b^0 \tag{2.5b}$$

and for excess B atoms at A/AB interface, the distribution of A and B atoms in the AB layer is described by:

$$n_a(x,t) = \frac{v_a \gamma n_a^0 n_b^0}{D_a + v_a \gamma n_b^0 h(t)} \left(x + h_{A(t)}\right) + n_a^0 \tag{2.6a}$$

and

$$n_b(x,t) = -\frac{\gamma \left(n_a^0\right)^2}{D_b} \left(x - h_{B(t)}\right) + n_b^0 \tag{2.6b}$$

Density of A atoms at interface AB/B and B atoms at interface A/AB during second growth stage are:

$$n_a(h_{B(t)}) = \frac{D_a n_a^0}{D_a + v_a \gamma n_b^0 h(t)} \tag{2.7a}$$

and

$$n_b(-h_{A(t)}) = \frac{D_b n_b^0}{D_b + v_b \gamma n_a^0 h(t)} \tag{2.7b}$$

If there are excess A atoms at reaction interface AB/B at time $t < t_c$, an AB layer at this interface grow under reaction controlled process and at A/AB interface the growth is diffusion limited and vice-versa for excess B atoms at interface A/AB.

Therefore, the relationship between time and layer thickness can be found by solving either eqn. (2.3b) or (2.3c) for excess A or B atoms at the reaction interface.

© University of Pretoria

UNIVERSITEIT VAN PRETORIA
UNIVERSITY OF PRETORIA
YUNIBESITHI YA PRETORIA

$$t = \frac{h(t)}{\gamma V_{ab}\left(n_b^0\right)^2} - \frac{D_b v_a^2}{\gamma^2 v_b^3 V_{ab}\left(n_b^0\right)^3} \ln\left[\frac{\gamma n_a^0 n_b^0 v_b^2 h(t)}{D_b\left(n_a^0 v_a + n_b^0 v_b\right)} + 1\right] \quad (2.8a)$$

$$t = \frac{h(t)}{\gamma V_{ab}\left(n_a^0\right)^2} - \frac{D_a v_b^2}{\gamma^2 v_a^3 V_{ab}\left(n_a^0\right)^3} \ln\left[\frac{\gamma n_a^0 n_b^0 v_a^2 h(t)}{D_a\left(n_a^0 v_a + n_b^0 v_b\right)} + 1\right] \quad (2.8b)$$

Solutions to eqns. (2.3b) and (2.3c) are expressed in eqns. (2.8a) and (2.8b) respectively.

However, if there are no excess of *A* or *B* atoms at the reaction interfaces no reaction controlled growth would occur at either *AB/B* or *A/AB* interface. The growth at both interfaces would be predominantly diffusion limited at all time.

At critical time t_c, $h(t) = h_c(t_c)$:

$$n_a\left(h_B(t_c)\right) v_a = n_b^0 v_b \text{ or } n_b\left(-h_A(t_c)\right) v_b = n_a^0 v_a \quad (2.9)$$

where

$$n_a\left(h_B(t_c)\right) = \frac{D_a n_a^0}{D_a + \gamma v_a n_b^0 h_c(t_c)} \quad \text{and}$$

$$n_b\left(-h_A(t_c)\right) = \frac{D_b n_b^0}{D_b + \gamma v_b n_a^0 h_c(t_c)}$$

Critical thickness, $h_c(t_c)$ is obtained from eqn. (2.9) as follows:

$$h_c(t_c) = \frac{D_a\left(n_a^0 v_a - n_b^0 v_b\right)}{\gamma v_a v_b \left(n_b^0\right)^2} \text{ or} \quad (2.10a)$$

© University of Pretoria

UNIVERSITEIT VAN PRETORIA
UNIVERSITY OF PRETORIA
YUNIBESITHI YA PRETORIA

$$h_{c(t_c)} = \frac{D_b\left(n_b^0 v_b - n_a^0 v_a\right)}{\gamma v_a v_b \left(n_a^0\right)^2} \tag{2.10b}$$

Eqn. (2.10a) holds at interface *AB/B* under reaction controlled process or eqn. (2.10b) at *A/AB* under the same process. It is worth noting that critical thickness cannot take place at two interfaces at the same time. It can only occur at the interface that has excess atomic species. For the critical time, substitute $t = t_c$, and $h(t) = h_{c(t_c)}$ in eqn. (2.8a) or (2.8b)

$$t_c = \frac{h_{c(t_c)}}{\gamma V_{ab}\left(n_b^0\right)^2} - \frac{D_b v_a^2}{\gamma^2 v_b^3 V_{ab}\left(n_b^0\right)^3} \ln\left[\frac{\gamma n_a^0 n_b^0 v_b^2 h_{c(t_c)}}{D_b\left(n_a^0 v_a + n_b^0 v_b\right)} + 1\right] \tag{2.11a}$$

$$t_c = \frac{h_{c(t_c)}}{\gamma V_{ab}\left(n_a^0\right)^2} - \frac{D_a v_b^2}{\gamma^2 v_a^3 V_{ab}\left(n_a^0\right)^3} \ln\left[\frac{\gamma n_a^0 n_b^0 v_a^2 h_{c(t_c)}}{D_a\left(n_a^0 v_a + n_b^0 v_b\right)} + 1\right] \tag{2.11b}$$

Eqn. (2.11a) is the corresponding critical time of eqn. (2.10a) and eqn. (2.11b) is the corresponding critical time of eqn. (2.10b)

The growth rate of an *AB* compound layer after critical time (second stage of growth) is described by:

$$\frac{dh(t)}{dt} = \gamma V_{ab}\left(n_a^0 n_b\left(-h_{A(t)}\right) + n_b^0 n_a\left(h_{B(t)}\right)\right) \tag{2.12}$$

Substitute eqns. (2.7a) and (2.7b) into eqn. (2.12) and integrate the resulting equation.

© University of Pretoria

A connection between time and layer thickness is established:

$$\varphi_1 h^2(t) + \varphi_2 h(t) - \left(\varphi_1 h_c^2 + \varphi_2 h_c(t_c)\right) - \varphi_3 \ln\left[\frac{\varphi_4 h(t) + 1}{\varphi_4 h_c(t_c) + 1}\right] - (t - t_c) = 0 \qquad (2.13)$$

Where

$$\varphi_1 = \left[2V_{ab}\left(D_b n_b^0 + D_a n_a^0\right)\right]^{-1},$$

$$\varphi_2 = \left[\left(D_a n_a^0\right)^2 + \left(D_b n_b^0\right)^2\right]\left[\gamma V_{ab} n_a^0 n_b^0 \left(D_b n_b^0 + D_a n_a^0\right)^2\right]^{-1}$$

$$\varphi_3 = D_a D_b \left(D_a n_a^0 - D_b n_b^0\right)^2 \left[\gamma^2 V_{ab} n_a^0 n_b^0 \left(D_a n_a^0 + D_b n_b^0\right)^3\right]^{-1}, \text{and}$$

$$\varphi_4 = \frac{\gamma\left(D_a n_a^0 + D_b n_b^0\right)}{D_a D_b}$$

2.4 Results and discussion on non-irradiation process

The kinetics of the first stage of growth of an *AB* compound layer expressed in eqns. (2.8a) and (2.8b) shows time as both partly linear and partly natural logarithmic functions of layer thickness. Eqn. (2.13) depicts time as partly parabolic and partly natural logarithmic function of thickness. The natural logarithmic function in eqns. (2.8a), (2.8b) and (2.13) is attributed to the simultaneous diffusion of *A* and *B* atomic species in the *AB* compound layer.

It is important to mention that the layer growth kinetic would be linear under reaction controlled process and parabolic under diffusion limited process if only one kind of atomic species diffuses in the *AB* compound layer.

© University of Pretoria

If, for example, only *A* species diffuse in the *AB* layer when there is an excess of *A* species at *AB/B* interface during the first stage of growth (i.e., reaction controlled growth). Eqn. (2.8a) transforms to a linear equation (when $D_b = 0$)

$$h(t) = V_{ab}\gamma\left(n_b^0\right)^2 t \tag{2.14a}$$

And eqn. (2.13) reduces to parabolic equation

$$\gamma v_a n_b^0\left(h^2(t) - h_c^2(t)\right) + 2D_a\left(h(t) - h_c(t)\right) - 2\gamma V_{ab} D_a n_a^0 n_b^0 (t - t_c) = 0 \tag{2.14b}$$

The critical thickness under this condition remains the same since it depends on the diffusivity of the atomic species (that is in excess) at one of the reaction interfaces during the reaction controlled growth stage.
However, the corresponding critical time has a different expression under this situation.

$$t_c = \frac{h_c(t_c)}{\gamma V_{ab}\left(n_b^0\right)^2} \tag{2.14c}$$

Likewise, if only *B* atom diffuses in the *AB* layer when there is an excess of *B* atoms at *A/AB* interface during the same stage of growth. Eqn. (2.8b) also changes to a linear equation (when $D_a = 0$)

$$h(t) = V_{ab}\gamma\left(n_a^0\right)^2 t \tag{2.15a}$$

and eqn. (2.13) reduces to parabolic equation

© University of Pretoria

UNIVERSITEIT VAN PRETORIA
UNIVERSITY OF PRETORIA
YUNIBESITHI YA PRETORIA

$$\gamma v_b n_a^0\left(h^2(t)-h_c^2(t)\right)+2D_b\left(h(t)-h_c(t)\right)-2\gamma V_{ab}D_b n_a^0 n_b^0(t-t_c)=0 \tag{2.15b}$$

The critical thickness remains invariant under this condition due to the same reason as the one mentioned before. But the corresponding critical time is not of the same expression as the one obtained in eqn. (2.11b)

$$t_c=\frac{h_c(t_c)}{\gamma V_{ab}\left(n_a^0\right)^2} \tag{2.15c}$$

However, if there are no excess of *A* or *B* atoms at either *AB/B* or *A/AB* interface, first growth stage would be absent. In other words, there would be no reaction controlled process and linear growth would not take place.

Thus, only parabolic growth (diffusion limited growth) would be feasible. Eqn. (2.16a) would hold if there are only *A* species diffusing in the *AB* layer and eqn. (2.16b) would also hold if there are only *B* species diffusing in the *AB* layer under the second stage of growth.

$$\gamma v_a n_b^0 h^2(t)+2D_a h(t)-2\gamma V_{ab}D_a n_a^0 n_b^0 t=0 \tag{2.16a}$$

$$\gamma v_b n_a^0 h^2(t)+2D_b h(t)-2\gamma V_{ab}D_b n_a^0 n_b^0 t=0 \tag{2.16b}$$

The growth kinetics of four silicides (tungsten disilicide WSi_2, vanadium disilicide VSi_2, cobalt silicide Co_2Si, and Nickel silicide Ni_2Si) are studied based on the result of this model. The experimental data are taken from the literature [24-28] to determine the interdiffusion coefficients of silicide layers under conventional furnace annealing process. We assume that the diffusivity of dominant species is the same as that of interdiffusion coefficient of the growing silicides (since only one kind of species diffuses in the silicide layer). The diffusing species in each silicide layer are shown in Table 2-1.

© University of Pretoria

UNIVERSITEIT VAN PRETORIA
UNIVERSITY OF PRETORIA
YUNIBESITHI YA PRETORIA

Table 2-1. Useful information on growth kinetics of WSi_2, VSi_2, Co_2Si, and Ni_2Si

AB layer (Silicide layer)	Diffusing species under annealing condition in the *AB* layer (Silicide layer)	Formation temperature *T* (K) used in this work	Growth kinetics (from this study)	Growth kinetics (from experiment)
WSi_2	*Si* [2, 3]	1033 [27]	Linear and parabolic.	Linear and parabolic [2, 3]
VSi_2	*Si* [2, 3]	873 [28]	Linear and parabolic.	Linear and parabolic [3].
Co_2Si	*Co* [2, 3]	763 [9]	Linear and parabolic.	Parabolic [2, 3].
Ni_2Si	*Ni* [2, 3]	573 [8, 29]	Linear and parabolic.	Linear and parabolic[8]

The results of interdiffusion coefficients for four silicides are depicted in Table 2-2 and they are obtained from Arrhenius equation described in eqn. (2.17) based on the data available on D_0 and E_a in Table 2-4 at formation temperatures shown in Table 2-1.

$$D_{int} = N_{a(b)} D_{a(b)} = N_{a(b)} D_0 \exp\left(\frac{-E_a}{K_B T}\right) \tag{2.17}$$

where

D_{int} is the interdiffusion coefficient of *AB* layer,

$N_{a(b)}$ is the atomic fraction of *A* or *B* atoms (which is equal to unity in the case of one kind of diffusing species) in the *AB* layer,

D_0 is the pre-exponential factor,

E_a is the activation energy,

K_B (8.617 x 10^{-5} eV) is the Boltzmann constant, and

T is the absolute temperature.

© University of Pretoria

Table 2-2. Data used for WSi_2, VSi_2, Co_2Si, and Ni_2Si layer thickness estimation

AB layer (Silicide layer)	Interdiffusion coefficient, D_{int} of AB layer (Silicide layer) (10^{-17} m^2/s)	Reaction rate constant, γ (10^{-38} m^4/s)	Volume of AB compound per Molecule, V_{ab} (10^{-29} m^3)	Number density of A and B atoms in the A and B layers, $n^0_{a(b)}$ (10^{28} atoms/m^3)
WSi_2	1.000 [27]	4.700	4.300	W (6.300), Si (5.000)
VSi_2	0.029 [28]	0.910	4.000	V (5.200), Si (5.000)
Co_2Si	3.000 [9]	1.200	5.000	Co(9.100), Si (5.000)
Ni_2Si	1.100 (Estimated)	0.620	3.300	Ni(9.140), Si (5.000)

The layer thickness of WSi_2 and VSi_2 is estimated with eqn. (2.15a) (for reaction controlled growth) and eqn. (2.15b) (for diffusion limited growth). The critical thickness between the two growth stages is obtained with eqn. (2.10b) and the corresponding critical time, t_c (when $D_a = 0$) is estimated with eqn. (2.11b).

In a similar vein, the thickness of Co_2Si and Ni_2Si is obtained from eqn. (2.14a) (for reaction controlled growth) and eqn. (2.14b) (for diffusion limited growth). The critical thickness and time are estimated with eqn. (2.10a) and (2.11a) respectively (when $D_b = 0$). The results of critical thickness and time of the silicide layers are shown in Table 2-3.

The results show that critical thickness is strongly dependent on the diffusivity of the active moving species in the silicide layer. The higher the diffusing rate of the active species the thicker the thickness become at the transition point.

© University of Pretoria

Table 2-3. Critical thickness and time of WSi_2, VSi_2, Co_2Si, and Ni_2Si layer.

AB layer (Silicide layer)	h_c (10^{-9} m)	t_c (s)
WSi_2	0.990	0.124
VSi_2	0.280	0.285
Co_2Si	66.000	44.000
Ni_2Si	47.000	92.000

The growth kinetics of four silicides considered in this study reveals a linear-parabolic relationship between layer thickness and time. The linear growth in both WSi_2 and VSi_2 layer is due to the reaction rate dependence on tungsten density at W/WSi_2 interface and vanadium density at V/VSi_2 interface during reaction controlled stage. Parabolic growth, on the other hand, is due to reaction rate dependence on both densities of tungsten and silicon atoms at both interfaces in tungsten-silicon system. The same explanation applies to vanadium-silicon system. Linear growth in the Co_2Si layer occurs as a result of excess cobalt atoms at Co_2Si/Si interface during reaction controlled stage and parabolic growth arises in the Co_2Si layer due to the active diffusion of cobalt as the only moving species during diffusion limited stage in the Co_2Si layer. The same explanation holds for linear-parabolic growth in the Ni_2Si layer where nickel is the only active diffusing species.

© University of Pretoria

UNIVERSITEIT VAN PRETORIA
UNIVERSITY OF PRETORIA
YUNIBESITHI YA PRETORIA

Table 2-4. Activation energy and pre-exponential factor for the growth kinetics of WSi_2, VSi_2, Co_2Si, and Ni_2Si

AB layer (Silicide layer)	E_a (eV)	D_0 (m^2/s)
WSi_2	3.400 [27]	0.400 (Estimated)
VSi_2	2.900 [28]	0.016 (Estimated)
Co_2Si	-	-
Ni_2Si	1.500 [8, 29]	1.670×10^{-4} [8, 29]

© University of Pretoria

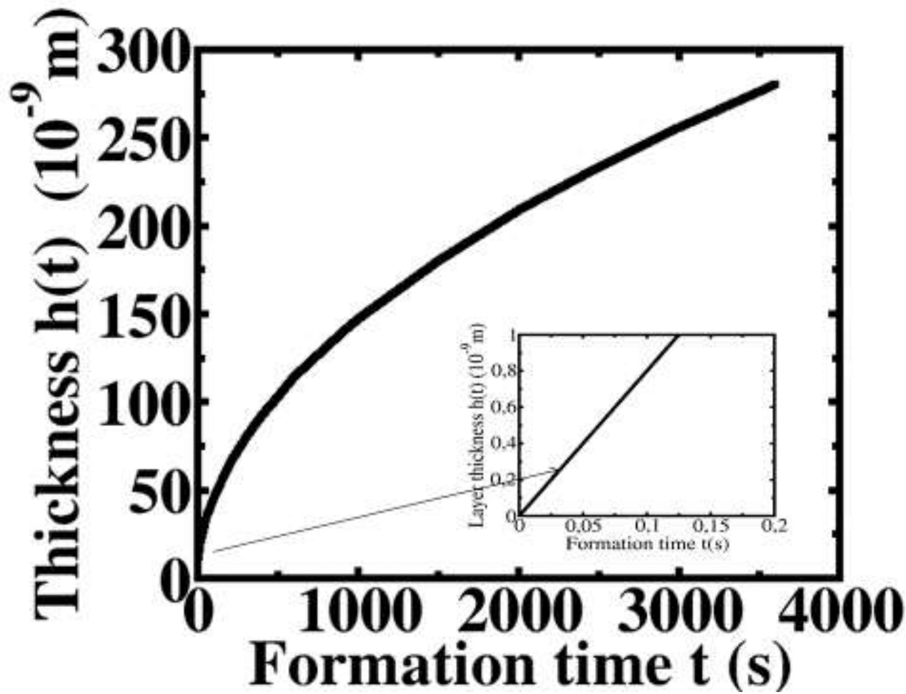

Figure 2-3: The growth kinetics of tungsten disilicide (WSi_2) at 1033 K under a non-irradiation process. The arrow shows the linear growth regime of WSi_2 under a reaction controlled process. The estimated time for the linear growth of WSi_2 is 0.124 s.

© University of Pretoria

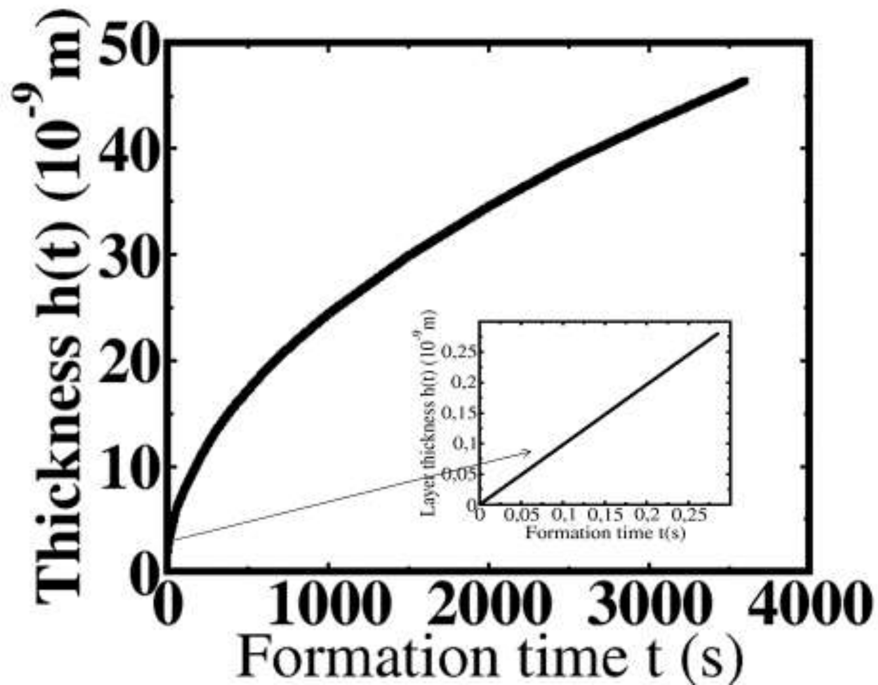

Figure 2-4: The growth kinetics of vanadium disilicide (VSi_2) at 873 K under a non-irradiation process. The arrow shows the linear growth region of VSi_2 over an estimated period of 0.285 s.

© University of Pretoria

UNIVERSITEIT VAN PRETORIA
UNIVERSITY OF PRETORIA
YUNIBESITHI YA PRETORIA

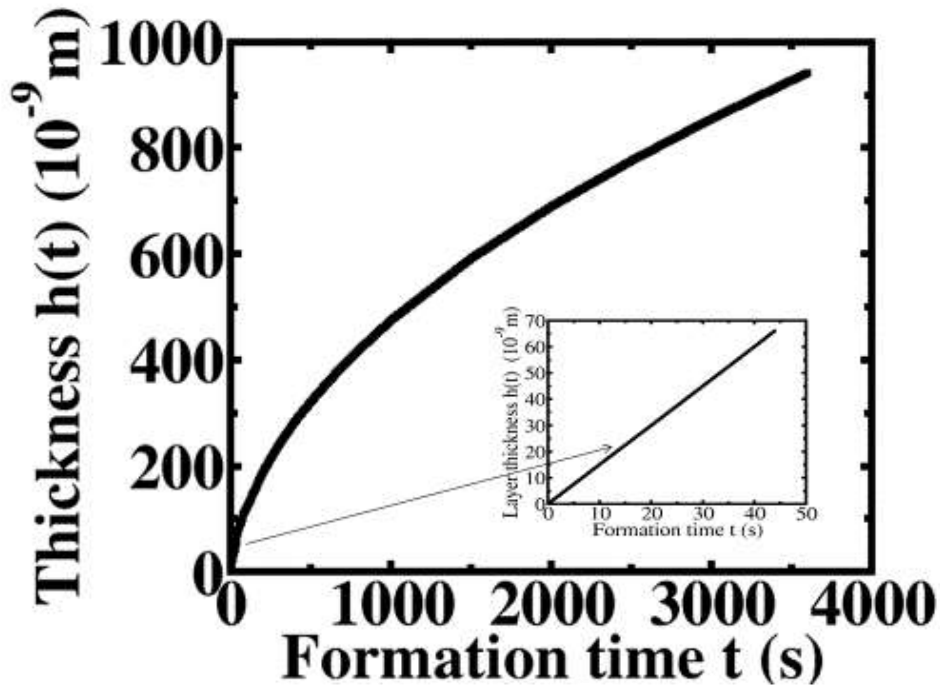

Figure 2-5: The growth kinetics of cobalt silicide (Co_2Si) at 763 K under a non-irradiation process. The arrow shows the linear growth regime of Co_2Si over a period of 44 s.

© University of Pretoria

UNIVERSITEIT VAN PRETORIA
UNIVERSITY OF PRETORIA
YUNIBESITHI YA PRETORIA

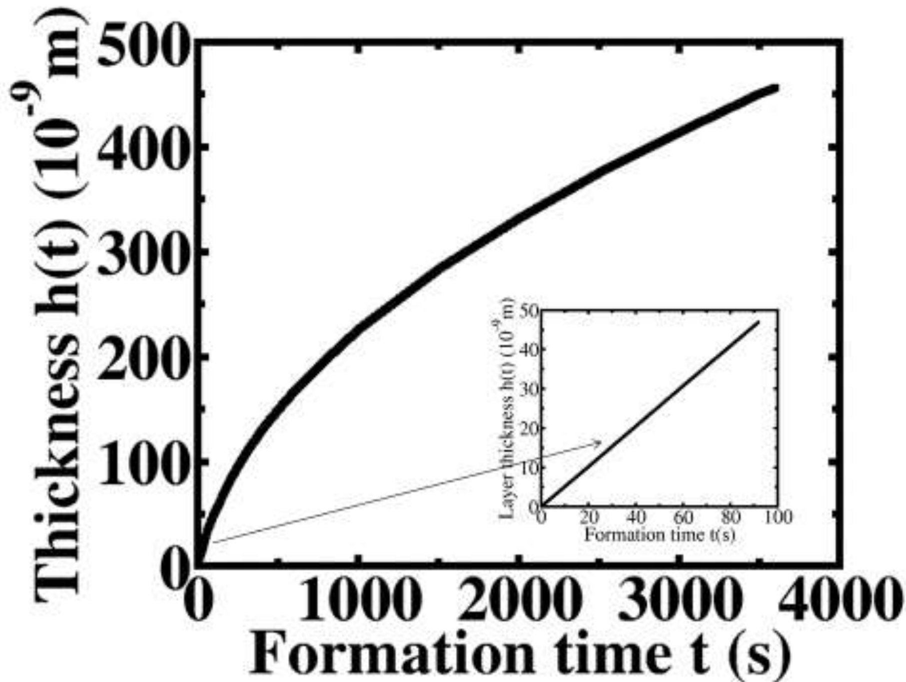

Figure 2-6: The growth kinetics of nickel silicide (Ni_2Si) at 573 K under a non-irradiation process. The dotted arrow indicates the linear growth regime of Ni_2Si over a period of 92 s.

Due to the small magnitude of layer thickness formed over a very short period of time during reaction controlled growth as shown in Table 2-3, the linear section of this curve is correspondingly small that the growth kinetics appear to be predominantly parabolic in Figures 2-3 to 2-6. The silicide growth is considered over a period of 3600 s in all the layers. The comparison between the growth kinetics predicted from this model and that of the experiment as depicted in Table 2-1 shows that the results of this theoretical approach are in good agreement with experiment.

The expressions in eqns. (2.8a), (2.10a), and (2.13) are used for the investigation of growth kinetics of palladium silicide; where both palladium and silicon are considered as diffusing species in the palladium silicide Pd_2Si layer.

© University of Pretoria

Since *Pd2Si* layer is a metal rich silicide phase, we assume that palladium species are in excess at the reaction interface *Pd2Si/Si* during the reaction controlled stage.

The diffusion coefficient of palladium and silicon species in the palladium silicide layer is determined through the application of Darken's equation:

$$D_{\mathrm{Pd2Si}} = D_{Pd} N_{Si} + D_{Si} N_{Pd} \tag{2.18}$$

where

D_{Pd2Si} is the chemical diffusion coefficient of palladium silicide,

D_{Pd} and N_{Pd} are the diffusion coefficient and atomic fraction of palladium species,

D_{Si} and N_{Si} are the diffusion coefficient and atomic fraction of silicon species.

The atomic fraction of both palladium and silicon species is determined by:

$$N_{Pd(Si)} = \frac{n^0_{Pd(Si)}}{n^0_{Pd} + n^0_{Si}} \tag{2.19}$$

Where

n^0_{Pd} is the density of palladium species (6.8 x 10^{28} atoms/m^3) in the palladium layer,

n^0_{Si} is the density of silicon species (5.0 x 10^{28} atoms/m^3) in the silicon layer.

$N_{Pd} = 0.58$, $N_{Si} = 0.42$, and $V_{\mathrm{Pd2Si}} = 4.2 \times 10^{-29}$ m^3.

V_{Pd2Si} is the volume of one molecule of palladium silicide.

The diffusion coefficient of palladium species is estimated to be about 3.9 times faster than that of silicon species in the palladium silicide layer based on the empirical data in [4].

© University of Pretoria

UNIVERSITEIT VAN PRETORIA
UNIVERSITY OF PRETORIA
YUNIBESITHI YA PRETORIA

The chemical diffusion coefficient of palladium silicide is estimated from the well-known Arrhenius equation:

$$D_{\mathrm{Pd2Si}} = D_0 \, exp\left(\frac{-E_a}{K_B T}\right) \tag{2.20}$$

E_a = 1.5 eV/atom [33], D_0 = 7.9 x 10^{-4} m^2/s [33], T = 473 K [33], and γ = 6.8 x 10^{-40} m^4/s. The estimated values of D_{Pd2Si} , D_{Pd} and D_{Si} are 8.2 x 10^{-20} m^2/s, 14.4 x 10^{-20} m^2/s, and 3.7 x 10^{-20} m^2/s respectively using eqns. (2.20) and (2.18).

The palladium silicide, Pd_2Si critical thickness is estimated with eqn. (2.10a) and we obtain 2.07 nm at a temperature of 473 K and the corresponding critical time is calculated using eqn. (2.11a) and a critical time of 19.78 s is obtained. These results are obtained under the consideration of two kinds of diffusing species in the palladium silicide layer. These species are palladium and silicon, and they are both assume to diffuse concurrently in the silicide layer. The growth kinetics of palladium silicide under this type of consideration is depicted in Figure 2-7.

There are different viewpoints on the diffusing species in the palladium silicide layer from experimental reports [31-36]. We, therefore, investigate the diffusing species in the palladium silicide layer looking at two more diffusion possibilities. This investigation is done based on the result obtained from this model.

The other two diffusion possibilities considered are when:

1. Silicon diffuses as the only species and
2. Palladium diffuses as the only species in the palladium silicide layer.

We, then estimate the thickness of palladium silicide under each diffusion consideration and compared the results with that of the experiment [7].

© University of Pretoria

UNIVERSITEIT VAN PRETORIA
UNIVERSITY OF PRETORIA
YUNIBESITHI YA PRETORIA

The palladium silicide thickness in [7] is estimated with equation of the form:

$$h^2(t) = 4D_{\mathrm{Pd2Si}}\,t \qquad (2.21)$$

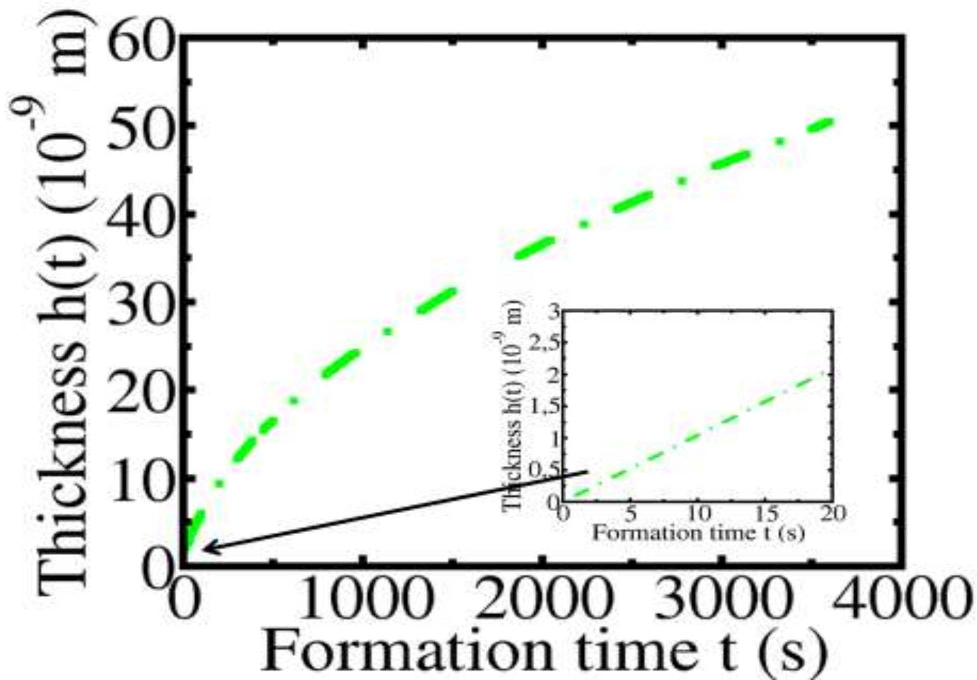

Figure 2-7: The growth kinetics of palladium silicide (Pd_2Si) at 473 K under the concurrent diffusion of both palladium and silicon species in the silicide layer. The arrow shows the linear growth regime of Pd_2Si over a period of 19.78 s.

The growth kinetics of palladium silicide when palladium is considered as the only diffusing species in the silicide layer is depicted in Figure 2-8. A linear-parabolic relationship is established under this consideration. The linear section of the growth stage is obscured due to reaction controlled process that dominates for a very short time compared to diffusion limited process. A reason similar to the one given previously.

© University of Pretoria

The critical thickness of 2.07 nm is obtained, using eqn. (2.10a), which is of the same magnitude as the one estimated under the concurrent diffusion of silicon and palladium species. The corresponding critical time of 29 s is obtained with eqn. (2.14c).

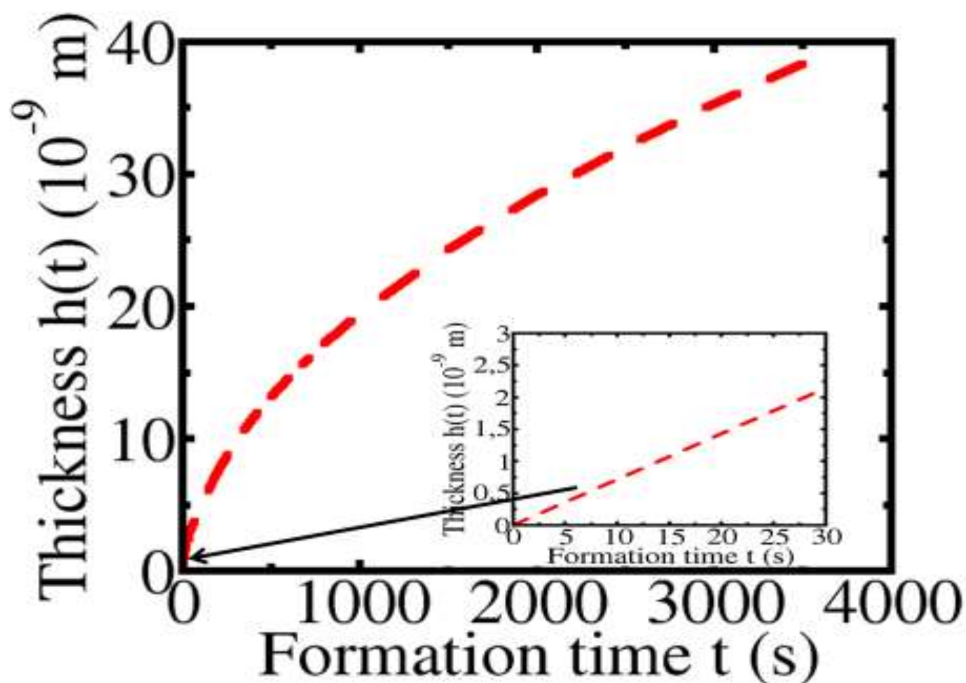

Figure 2-8: The growth kinetics of palladium silicide (Pd_2Si) at 473 K when only palladium species diffuse in the silicide layer. The arrow shows the linear growth regime of Pd_2Si over a period of 29 s.

The results in Figure 2-9 depict silicon as the dominant species during the palladium silicide growth; this is because the curve of palladium silicide under the diffusion of silicon is closer to the experimental curve than the other two curves.

The result also shows that the concurrent diffusion of palladium and silicon species is unlikely in the Pd_2Si layer; since the thickness of palladium silicide estimated under this consideration is more than that of the experimental value.

© University of Pretoria

UNIVERSITEIT VAN PRETORIA
UNIVERSITY OF PRETORIA
YUNIBESITHI YA PRETORIA

However, we cannot rule out the possibility of palladium species participation in the mass transport process during the silicide growth; this can only occur, if the diffusion of silicon is obstructed [37] during the silicide growing process.

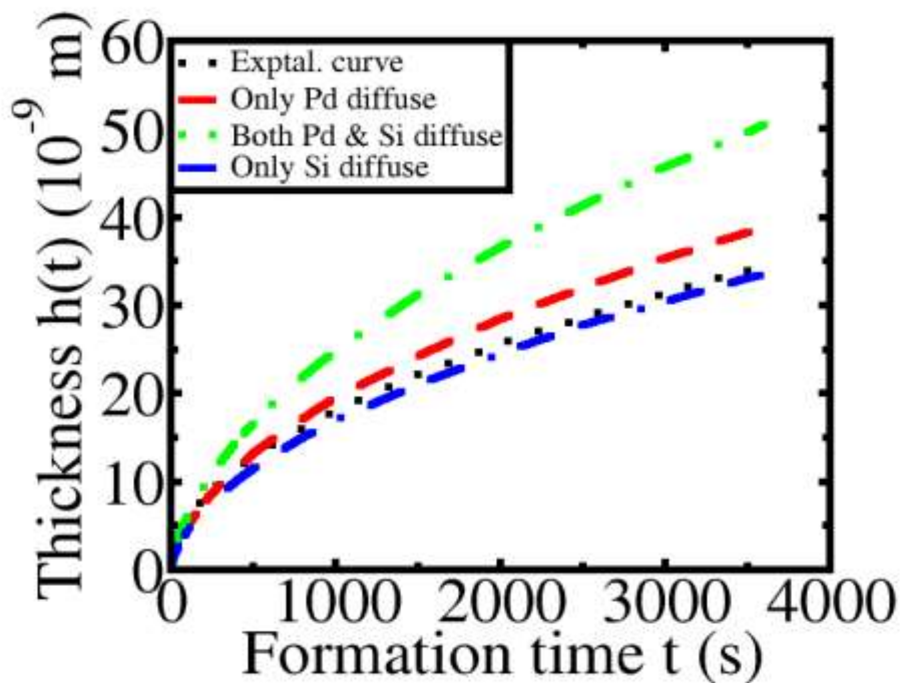

Figure 2-9: The growth kinetics of Palladium silicide (Pd_2Si) at 473 K under the consideration of three different diffusion possibilities over a period of 3600 s.

2.5 Conclusion

The model shows a good agreement with experimental results. The silicides considered in this study have two growth stages. Reaction controlled stage and diffusion limited stage.
The growth kinetics show a linear growth under a reaction controlled stage and parabolic growth under a diffusion limited stage. The reason for this kinetic of growth is ascribed to the diffusion of dominant species by means of one transport mechanism.

© University of Pretoria

UNIVERSITEIT VAN PRETORIA
UNIVERSITY OF PRETORIA
YUNIBESITHI YA PRETORIA

CHAPTER 3

INFLUENCE OF IRRADIATION ON *AB* COMPOUND LAYER FORMATION

3.1 Introduction

Experiments have shown the feasibility of the compound layer formation particularly at the interface of two immiscible solid layers under the influence of irradiation at a low temperature [11-15, 21, 38-40]. Most of the reported works were carried out independently with either heavy or light particle beam irradiation. For example, nickel silicide is produced at the interface of nickel/silicon system under argon ion irradiation [11, 39], cobalt silicide is formed at the interface of cobalt/silicon system under gold ion irradiation [12], tungsten disilicide is produced at the interface of tungsten/silicon system under gold ion irradiation, and vanadium disilicide is formed at the interface of vanadium/silicon system under argon ion irradiation [14]. The same set of silicides are also produced under electron and laser irradiation [20, 21].

The reports show that the compound layers were formed via cascade mixing under heavy particle irradiation, such as ion irradiation. However, this explanation is not applicable to light particle irradiation, such as electron irradiation due to mass difference between electrons and target atoms.

In this study, we proposed a different approach which intends to explain the compound layer formation from the viewpoint of the radiation-induced process which is fundamental to all irradiation techniques. Radiation-induced processes are many, and they occur only within a transient time during the period of irradiation. Examples of such process include radiation induced heating, radiation-induced defect generation process, radiation-induced excitation and ionization process, radiation-induced recombination, and annihilation of defects, etc.

Due to a number of these processes, it remains unclear which of them is actually responsible for the compound layer formation at the interface of an irradiated bilayer system, such as metal-silicon system.

© University of Pretoria

UNIVERSITEIT VAN PRETORIA
UNIVERSITY OF PRETORIA
YUNIBESITHI YA PRETORIA

The radiation-induced processes in the irradiated bilayer systems are taking into account over a period of time much greater than 10^{-8} s. At this time defect reaction by thermal migration is considered in the irradiated layers [41].

The radiation-induced excitation process relaxes into heating over this period of time. The influence of radiation-induced ionization process on the compound layer formation within this time frame is negligible due to a vast number of atoms that are diffusing almost at the same time in the irradiated layers. The influence of radiation-induced recombination process on the compound layer formation also may be ignored over this period of time due to the weak correlation (which arises from the spatial separation) between the vacancies and interstitial atoms in the irradiated systems. It takes much longer time for recombination process to takes place between the vacancy and the interstitial atom at a time greater than 10 *ns* than the period between 100 fs and 10 ps (for displacement cascade phenomenon).

Therefore, the radiation-induced heating and radiation-induced defects generation have a greater influence on the growth of the compound layer at a time $>10^{-8}$ s. These two processes are associated with thermal relaxation and diffusion phenomena in the irradiated layer. The investigation of these processes is considered at a low temperature. The reason for a low-temperature consideration in this study is because most of the silicides and other intermetallic compounds formation are observed empirically at low temperatures [11-15].

The role of both processes on atomic diffusion is examined independently. The temperature associated with heating in each irradiated layer is investigated in this work. Likewise, the effectiveness of radiation-induced interstitial and vacancy as transport mechanisms is independently investigated within the framework of the theoretical approach presented in this study.

© University of Pretoria

UNIVERSITEIT VAN PRETORIA
UNIVERSITY OF PRETORIA
YUNIBESITHI YA PRETORIA

3.2 Physical process for an *AB* compound layer formation under the influence of radiation-induced heating

Suppose that the *A* and *B* layers in the *A*-*B* bilayer system are irradiated with a low energetic particle beam. The energy transferred by the radiation particles to the target atoms *A* and *B* are assumed to be lower than the threshold displacement energies in their respective layers.
In other words, this interaction does not result in defect generation in the *A* and *B* irradiated layers. A vast amount of energy of radiation particles is transformed into heat due to its interaction with both layers.
However, the intensity of heat produced in each irradiated layer is not the same; since the energy deposited in the irradiated layers are different due to the difference in the particle penetration depth in both layers. The *A* and *B* layers are, therefore, heated up as a result of energy deposited by the radiation particles. Thermal vacancies are generated, and atomic bonds between target atoms are broken as a result of heating in the irradiated layers. The *A* and *B* atoms diffuse from their respective layers via thermal vacancies to the reaction interface(s); at the interface(s), the *A* species react chemically with *B* atoms to formed an *AB* compound layer. The new bond formed in the sublattices of an *AB* compound layer is not the same as the bonds in the *A* and *B* target layers; this makes the *AB* compound layer different from the *A* and *B* layers.
The *AB* layer is also heated by the energy deposited by radiation particles. The energy deposited in the *AB* layer is different from that of the *A* and *B* layers due to the particle penetration depth in the *AB* layer which is different in dimension from that of the *A* and *B* layers.
The geometry of the *A*-*B* bilayer system during the radiation-induced heating is shown in Figure 3-1. The *A*, *AB*, and *B* layer thicknesses are denoted by $h_{A(t)}, h_{AB(t)}$, and $h_{B(t)}$ respectively.

© University of Pretoria

where

h_A, h_{AB}, *and* h_B are the function of time t.

The temperature rise in the *A*, *AB*, and *B* layers due to radiation-induced heating are represented by ΔT_A, ΔT_{AB} and ΔT_B respectively.

T_e designates the environment temperature of the *A*-*B* bilayer system.

T_1, T_2, T_3, and T_4 are temperatures at points x_1, x_2, x_3, and x_4 respectively.

The heat fluxes in *A*, *AB*, and *B* irradiated layer are J_A, J_{AB}, and J_B respectively.

The volumetric heat generation rate (i.e., heat energy produced per unit volume in unit time) in the *A*, *AB*, and *B* layers are represented by Q_A, Q_{AB}, and Q_B respectively.

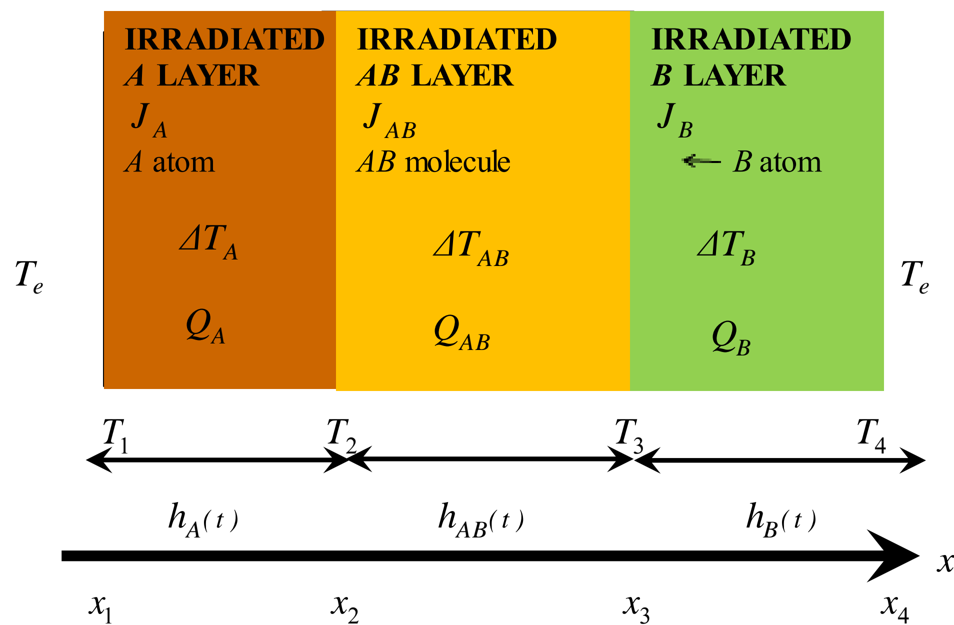

Figure 3-1: Schematic diagram of the *A*-*B* bilayer system during radiation heating process.

© University of Pretoria

3.2.1 Basic equations for an *AB* compound layer formation under the influence of radiation-induced heating

The equation for the stationary temperature distribution in the irradiated layers is described as thus:

$$C\rho\frac{\partial T}{\partial t} = \eta\frac{\partial^2 T}{\partial x^2} + Q \quad (3.1)$$

With the following boundary conditions:

$J_A(x_1) = -\xi_1(T_1 - T_e)$,

$J_A(x_2) = J_{AB}(x_2)$,

$J_{AB}(x_3) = J_B(x_3)$,

$J_B(x_4) = \xi_2(T_4 - T_e)$, and

$J(x) = -\eta\frac{dT(x)}{dx}$ (For heat flux in each layer).

Where

ξ_1 is the rate of heat transfer coefficient between the *A* layer and the environment,

ξ_2 is the rate of heat transfer coefficient between the *B* layer and the environment .

C, ρ, and η are the specific heat capacity, density, and thermal conductivity of the irradiated layers respectively.

We assume that $\xi_1 = \xi_2 = \xi$ (for a simple case).

© University of Pretoria

The solution of eqn. (3.1) is written as follows under a steady state condition $\left(\frac{\partial T}{\partial t}=0\right)$ for each of the irradiated layer:

$$T_{A}(x)=\frac{Q_A}{2\eta_A}\left(x^2-x(x_2+x_1)+x_1x_2\right)+\frac{T_2(x-x_1)+T_1(x_2-x)}{x_2-x_1} \tag{3.2.1}$$

$$T_{AB}(x)=\frac{Q_{AB}}{2\eta_{AB}}\left(x^2-x(x_3+x_2)+x_2x_3\right)+\frac{T_3(x-x_2)+T_2(x_3-x)}{x_3-x_2} \tag{3.2.2}$$

$$T_{B}(x)=\frac{Q_B}{2\eta_B}\left(x^2-x(x_4+x_3)+x_3x_4\right)+\frac{T_4(x-x_3)+T_3(x_4-x)}{x_4-x_3} \tag{3.2.3}$$

The heat fluxes $J_A(x_1)$ and $J_A(x_2)$ in the A layer at points x_1 and x_2 are:

$$J_A(x_1)=-\xi(T_1-T_e)=\frac{Q_A}{2}(x_2-x_1)-\frac{\eta_A(T_2-T_1)}{x_2-x_1} \tag{3.3.1}$$

$$J_A(x_2)=-\frac{Q_A}{2}(x_2-x_1)-\frac{\eta_A(T_2-T_1)}{x_2-x_1} \tag{3.3.2}$$

The heat fluxes $J_{AB}(x_2)$ and $J_{AB}(x_3)$ in the AB layer at points x_2 and x_3 are expressed as:

$$J_{AB}(x_2)=\frac{Q_{AB}}{2}(x_3-x_2)-\frac{\eta_{AB}(T_3-T_2)}{x_3-x_2} \tag{3.4.1}$$

© University of Pretoria

UNIVERSITEIT VAN PRETORIA
UNIVERSITY OF PRETORIA
YUNIBESITHI YA PRETORIA

$$J_{AB}(x_3) = -\frac{Q_{AB}}{2}(x_3 - x_2) - \frac{\eta_{AB}(T_3 - T_2)}{x_3 - x_2} \tag{3.4.2}$$

The heat fluxes $J_B(x_3)$ and $J_B(x_4)$ in the B layer at points x_3 and x_4 are delineated as:

$$J_B(x_3) = \frac{Q_B}{2}(x_4 - x_3) - \frac{\eta_B(T_4 - T_3)}{x_4 - x_3} \tag{3.5.1}$$

$$J_B(x_4) = \xi_2(T_4 - T_e) = -\frac{Q_B}{2}(x_4 - x_3) - \frac{\eta_B(T_4 - T_3)}{x_4 - x_3} \tag{3.5.2}$$

To solve for temperature rise $\Delta T_A, \Delta T_{AB}$ and ΔT_B we apply the boundary conditions

The first boundary condition is employed in eqn. (3.3.1) and the fourth boundary condition is applied in eqn. (3.5.2).

The second and third boundary conditions are employed, respectively, as follow:

$$\begin{aligned} J_A(x_2) = J_{AB}(x_2) &= -\frac{Q_A}{2}(x_2 - x_1) - \frac{\eta_A(T_2 - T_1)}{x_2 - x_1} \\ &= \frac{Q_{AB}}{2}(x_3 - x_2) - \frac{\eta_{AB}(T_3 - T_2)}{x_3 - x_2} \end{aligned} \tag{3.6.1}$$

$$\begin{aligned} J_{AB}(x_3) = J_B(x_3) = J_{AB}(x_3) &= -\frac{Q_{AB}}{2}(x_3 - x_2) - \frac{\eta_{AB}(T_3 - T_2)}{x_3 - x_2} \\ &= \frac{Q_B}{2}(x_4 - x_3) - \frac{\eta_B(T_4 - T_3)}{x_4 - x_3} \end{aligned} \tag{3.6.2}$$

© University of Pretoria

UNIVERSITEIT VAN PRETORIA
UNIVERSITY OF PRETORIA
YUNIBESITHI YA PRETORIA

Recall that

$x_2 - x_1 = h_{A(t)}$,

$x_3 - x_2 = h_{AB(t)}$,

$x_4 - x_3 = h_{B(t)}$,

$T_2 - T_1 = \Delta T_A$,

$T_3 - T_2 = \Delta T_{AB}$, and

$T_4 - T_3 = \Delta T_B$

We rewrite eqns. (3.3.1), (3.5.2), (3.6.1), and (3.6.2) in terms of the symbols of the temperature rise and thickness of the irradiated layers:

$$J_{A(x_1)} = -\xi(T_1 - T_e) = \frac{Q_A h_{A(t)}}{2} - \frac{\eta_A \Delta T_A}{h_{A(t)}} \tag{3.7}$$

$$J_{B(x_4)} = \xi(T_4 - T_e) = -\frac{Q_B h_{B(t)}}{2} - \frac{\eta_B \Delta T_B}{h_{B(t)}} \tag{3.8}$$

$$\begin{aligned} J_{A(x_2)} = J_{AB(x_2)} &= -\frac{Q_A h_{A(t)}}{2} - \frac{\eta_A \Delta T_A}{h_{A(t)}} \\ &= \frac{Q_{AB} h_{AB(t)}}{2} - \frac{\eta_{AB} \Delta T_{AB}}{x_3 - x_2} \end{aligned} \tag{3.9}$$

© University of Pretoria

$$J_{AB}(x_3) = J_B(x_3) = -\frac{Q_{AB}h_{AB(t)}}{2} - \frac{\eta_{AB}\Delta T_{AB}}{h_{AB(t)}}$$

$$= \frac{Q_B h_{B(t)}}{2} - \frac{\eta_B \Delta T_B}{h_{B(t)}} \tag{3.10}$$

We solve eqns. (3.7), (3.8), (3.9), and (3.10) simultaneously and the following results are obtained for ΔT_A, ΔT_{AB}, and ΔT_B

$$\Delta T_A = \frac{I_1 + I_2}{I_3} \tag{3.11}$$

Where

$$I_1 = 2\eta_{AB}\eta_B h_{A(t)} h_{AB(t)} \left(2Q_A h_{A(t)} + Q_B h_{B(t)} - Q_{AB} h_{AB(t)}\right),$$

$$I_2 = \xi h_A h_{AB(t)} \left[\left(Q_{AB} h^2_{AB(t)} \eta_B - Q_B h^2_{B(t)} \eta_{AB}\right) - Q_A h_{A(t)} \left(h_{AB(t)} \eta_B + h_{B(t)} \eta_{AB}\right)\right], \text{ and}$$

$$I_3 = 2\eta_{AB}\left[\eta_A h_{AB(t)}\left(\eta_B + \xi h_{B(t)}\right) - \xi \eta_B h_{A(t)} \left(\frac{h^2_{AB(t)}\eta_A}{\eta_{AB} h_{A(t)}} + \frac{\eta_{AB} h_{A(t)}}{\eta_A}\right)\right]$$

$$\Delta T_{AB} = \frac{M_1 + M_2}{M_3} \tag{3.12}$$

© University of Pretoria

where

$$M_1 = \eta_A \eta_{AB} h_{AB(t)} \left[2\eta_B h_{AB(t)} \left(Q_A h_{A(t)} - Q_B h_{B(t)} \right) - \xi h_{A(t)} h_{AB(t)} \left(Q_{AB} h_{AB(t)} + Q_B h_{B(t)} \right) \right],$$

$$M_2 = h_{A(t)} h_{AB(t)}^2 \left[(\eta_{AB}\eta_B + 2\xi\eta_B h_{AB(t)})(Q_{AB}\eta_{AB} + Q_A\eta_A) - \xi^2 h_{AB(t)}\eta_B \left(Q_{AB} h_{AB(t)} + Q_A h_{A(t)} \right) \right],$$

and $M_3 = 2\eta_{AB} h_{AB(t)} \left[\eta_A (\eta_{AB}\eta_B + \xi\eta_{AB} h_{B(t)} - \xi\eta_B h_{AB(t)}) - \xi\eta_B\eta_{AB} h_{A(t)} \right].$

$$\Delta T_B = \frac{V_1(V_2 + V_3(V_4 + V_5)) + V_6}{V_7} \tag{3.13}$$

where

$$V_1 = \eta_A h_{B(t)} h_{AB(t)},$$

$$V_2 = 2\eta_{AB}(\eta_B + \xi h_{B(t)})(Q_{AB} h_{AB(t)} + Q_A h_{A(t)}),$$

$$V_3 = \xi h_{AB(t)},$$

$$V_4 = 2\eta_B(3Q_A h_{A(t)} + Q_B h_{B(t)} - 2Q_{AB} h_{AB(t)}) - \xi h_{A(t)}(Q_{AB} h_{AB(t)} + Q_B h_{B(t)}),$$

$$V_5 = (Q_{AB} h_{AB(t)} + Q_A h_{A(t)}) \left(\eta_B + \xi \left(\frac{h_{AB(t)}\eta_B}{\eta_{AB}} + \frac{\eta_B h_{A(t)}}{\eta_A} \right) \right),$$

© University of Pretoria

UNIVERSITEIT VAN PRETORIA
UNIVERSITY OF PRETORIA
YUNIBESITHI YA PRETORIA

$$V_6 = \left(\xi h_A(t)\eta_{AB}h_B(t)h_{AB}(t)\right)\begin{pmatrix} Q_B h_B(t)\left(2\eta_B + \xi h_B\right) + 2\eta_B\left(Q_{AB}h_{AB}(t) + 2Q_A h_A(t)\right) \\ -\xi Q_A h_A(t) h_B(t) \end{pmatrix},$$

$$V_7 = 2\eta_A h_{AB}(t)\left(2\eta_B + \xi h_B(t)\right)\left(\eta_{AB}\eta_B + \xi\eta_{AB}h_B(t) - 2\xi\eta_B h_{AB}(t)\right).$$

The temperature associated with radiation induced heating process is described by:

$$T^{irr} = T_e + \Delta T^{irr} \tag{3.14}$$

where

ΔT^{irr} is the change in temperature in the irradiated layer due to radiation heating.

Therefore, ΔT^{irr} in the *A*, *AB*, and *B* layers are ΔT_A, ΔT_{AB} and ΔT_B respectively.

There are two important parameters for radiation heating calculation. These are the stopping power of the radiation particle and its depth of penetration in the target layer.

These two parameters are estimated based on the expressions given in eqns. (3.15) and (3.16) for the light particle irradiation and eqns. (3.19) and (3.21) for the heavy particle irradiation.

For a compound layer to form at the reaction interface during irradiation, the range of the radiation particle must be greater or equal to the thickness of the target layer [42]. Otherwise, no compound layer would form at the reaction site.

The radiation particles considered in this study are electron and ion.

The volumetric heat generation rate Q in each irradiated layer is determined in the following way:

At first, we estimate the stopping power for light particles radiation in each target layer in accordance with the model in [42]. The corresponding depth of penetration in each irradiated layer is estimated with the empirical data in [43].

© University of Pretoria

UNIVERSITEIT VAN PRETORIA
UNIVERSITY OF PRETORIA
YUNIBESITHI YA PRETORIA

The amount of light particle energy used during the collision process is calculated as the product of light particle radiation stopping power and thickness of the target layer.

The quantity Q, in turn, is determined by the product of defect generation rate, the density of atoms in the target layer and light particle radiation energy expended during the collision process.

The idea of incorporating defect generation rate into the equation that delineated Q is to transform the defect formation energy into radiation heating.

This notion would inhibit the chance of defect generation in each irradiated layer and circumscribe the formation of the compound layer exclusively to the contribution of heating under irradiation.

The light particle stopping power according to [42] is defined as follows:

$$S_l = \frac{0.1535\, Z\, \rho}{A R_f^2}\left[\ln\left(\frac{\mu^2(\mu+2)}{2\left(\frac{I}{E_0}\right)^2}\right) + 1 - R_f^2 + \frac{\frac{\mu^2}{8} - (2\mu+1)\,0.693}{(\mu+1)^2} - \frac{2\,\pi\, N_A}{A}\left(\frac{e^2}{E_0}\right)^2 + \Omega\right] \tag{3.15}$$

where

$$\Omega = \frac{5.8x10^{-28} N_A\, Z^2\, \omega\,(E_K + E_0)\,\rho}{A}$$

Z is the atomic number of the target atom,

ρ is the mass density of the target atom,

A is the mass number of the target atom,

© University of Pretoria

R_f is the relativistic factor $\left(R_f = \sqrt{1-\left(\frac{E_K}{E_0}\right)^2}\right)$ when $E_K < E_0$.

E_K is the light particle kinetic energy,

E_0 is the light particle rest energy,

μ is the ratio of light particle kinetic energy to its rest energy $\left(\mu = \frac{E_K}{E_0}\right)$,

I is the mean excitation energy,

N_A is the Avogadro's number,

ω is the slowly variation function of Z and E_K, and

e is the electronic charge.

The light particle penetration depth in the irradiated layer can be estimated using [43]:

$$d_l = \frac{6.7x10^{-11} E_K^{\frac{5}{3}}}{\rho} \tag{3.16}$$

The volumetric heat generation rate in the target layers A and B is described by:

$$Q^l_{a(b)} = S_l\, h(t)\, K\, n^0_{a(b)} \tag{3.17}$$

where

K is the defect generation rate,

n^0_a and n^0_b are the atomic densities of lattice atoms in the A and B layers, and

$h(t)$ is the thickness of the irradiated layer.

© University of Pretoria

Parameters like I and Z do not apply to AB layer. It is, therefore, difficult to estimate for Q_{ab}^{l} in the AB layer directly from the equation described above.

We, then look for an alternative way of obtaining an expression for Q_{ab}^{l}. This expression is described in terms of Q_a^l, Q_b^l, n_a^0, n_b^0, n_{ab}, v_a and v_b as shown in eqn. (3.18).

$$Q_{ab}^{l} = v_a Q_a^l \frac{n_{ab}}{n_a^0} + v_b Q_b^l \frac{n_{ab}}{n_b^0} \tag{3.18}$$

where

n_{ab} is the density of AB molecule in the AB layer.

On the other hand, the heavy particle stopping power and its penetration depth can be determined in the following way.

The stopping power of heavy particle in each irradiated layer according to [41] is described by:

$$S_h = \frac{8.462x10^{-15} N_A\, Z_t\, Z_h\, A_h\, \theta}{(A_h + A_t)\left(Z_h^{0.23} + Z_t^{0.23}\right)} + \frac{3.83x10^{-15} N_A\, Z_h^{\frac{7}{6}}\, Z_t\, E_K^{0.5}}{A_h^{0.5}\left(Z_h^{\frac{2}{3}} + Z_t^{\frac{2}{3}}\right)^{1.5}} \tag{3.19}$$

where

Z_t and Z_h are the atomic numbers of target atom and heavy particle respectively,

A_h and A_t are the corresponding atomic masses of target atom and heavy particle.

θ is defined in [44] as:

$$\theta = \frac{\ln \iota}{\iota} \quad \text{When } \iota > 30 \text{ keV}$$

and

© University of Pretoria

UNIVERSITEIT VAN PRETORIA
UNIVERSITY OF PRETORIA
YUNIBESITHI YA PRETORIA

$$\theta = \frac{\ln\left[1 + 1.1383\,\iota\right]}{2\left(\iota + 0.01321\,\iota^{0.21226} + 0.19593\,\iota^{0.5}\right)} \quad \text{When } \iota \leq 30 \text{ keV}$$

where

$$\iota = \frac{32.53\,A_t\,E_K}{Z_t\,Z_h\left(A_h + A_t\right)\left(Z_h^{0.23} + Z_t^{0.23}\right)} \tag{3.20}$$

The heavy particle penetration depth [41] in each layer can be determined by:

$$d_h = \frac{E_K\left(A_h + A_t\right)\left(Z_h^{0.23} + Z_t^{0.23}\right)}{8.462x10^{-15} N_A\,Z_t\,Z_h\,A_h\,\theta\,n_{a(b)}^0} \tag{3.21}$$

The volumetric heat generation rate in the *A* and *B* target layers is described by:

$$Q_{a(b)}^h = S_h\,h(t)\,K\,n_{a(b)}^0 \tag{3.22}$$

The volumetric heat generation rate in the *AB* layer is defined as:

$$Q_{ab}^h = v_a Q_a^h \frac{n_{ab}}{n_a^0} + v_b Q_b^h \frac{n_{ab}}{n_b^0} \tag{3.23}$$

3.2.2 Results and discussion on radiation-induced heating

The volumetric heat generation rate and the corresponding temperature rise in each irradiated layers of three bilayer systems are estimated under light and heavy particle irradiation. The bilayer systems under consideration are cobalt-silicon, nickel-silicon, and tungsten-silicon.

© University of Pretoria

These bilayer systems produced the same kinds of silicides as the one described under non-irradiation process in the previous chapter.

The temperature rise in the metal layer (A layer) is estimated with eqns. (3.11) and (3.14). While in silicon layer (B layer), the temperature rise is estimated with eqns. (3.13) and (3.14). The temperature rise in silicide layer (AB layer) is determined with eqns. (3.12) and (3.14). These estimations are done under both light and heavy particle irradiation.

The volumetric heat generation rates in metal and silicon layers are calculated with eqn. (3.17) under light particle irradiation and with eqn. (3.22) under heavy particle irradiation.

The volumetric heat generation rate in silicide layer under light and heavy particle irradiation is estimated with eqns. (3.18) and (3.23) respectively.

The light particles beam of 20 keV is used in our estimation for the irradiation of the three bilayer systems considered in this study. Electron is considered as light particle. The electron energy used in this work is the same as the one reported in [21]. The thickness of the irradiated layer is taken as 5 nm for each metal and silicon in the bilayer system. The thickness of silicide formed at the interface of each bilayer system is taken as 10 nm.

On the other hand, the heavy particles beam of 110 keV and 120 MeV energy is considered in this work. These energies are of the same magnitude as the one used in the experiments described in [12-14, 39]. Argon and gold ions are the heavy particles used for the irradiation of the metal-silicon bilayer systems in these experiments.

The thickness of the metal layer, silicon layer, and silicide layer in each bilayer system used under heavy particle irradiation (considered in this study) are as thus:

In cobalt-silicon system, a 120 MeV gold ion beam is used. The thickness of cobalt and silicon layer in this system is 50 nm each. The cobalt silicide layer formed from this irradiation has a thickness of 100 nm.

In tungsten-silicon system, a 120 MeV gold ion beam is used for irradiation. The thickness of tungsten and silicon layers in this bilayer system is 50 nm each. The tungsten disilicide layer formed from this irradiation has a thickness of 100 nm.

© University of Pretoria

UNIVERSITEIT VAN PRETORIA
UNIVERSITY OF PRETORIA
YUNIBESITHI YA PRETORIA

In nickel-silicon system, an 110 keV argon ion beam is used for irradiation. The thickness of nickel and silicon layers in this system is 45 nm each. The nickel silicide layer formed from this irradiation has a thickness of 90 nm.

The thickness of metal and silicon layers in each bilayer system is the same as the one reported in the experimental works [12-14, 39].

Atomic numbers of gold and argon ions are 79 and 18 respectively, and their mass numbers are 197 and 40 a.m.u.

The data for temperature rise estimation in each layer is depicted in Table 3-1 for both light and heavy particle irradiation. The estimated values of light particle stopping power, light particle penetration depth, volumetric heat generation rate, and temperature rise in each irradiated layer are presented in Table 3-2. Table 3-3 shows the estimated values of heavy particle stopping power, heavy particle penetration depth, volumetric heat generation rate and temperature rise in each target layer under irradiation.

Table 3-1. Useful parameters for estimation of temperature rise in the irradiated layers

(where $\xi = 100 \text{ W m}^{-2}\text{K}^{-1}$)

Irradiated layer	Mean excitation energy I (eV)	Thermal conductivity η (W/mK)	Density ρ (kg/m^3)	Thickness $h(t)$ (nm) under light particle irradiation	Thickness $h(t)$ (nm) under heavy particle irradiation	Atomic number Z	Atomic mass A (a.m.u)	Lattice constant a (10^{-10} m)	Estimated density of species in the irradiated layer (10^{28} m^{-3})
Si	171.2	150.000	2330	5	9, 45, and 50	14	28.0	5.4	5.0
Ni	306.3	91.0	8910	5	45	28	58.7	3.5	9.1
Co	298.6	100.0	8900	5	50	27	58.9	2.5	9.1
W	704.0	170.0	19250	5	50	74	183.8	3.2	6.3
Ni_2Si	-	18.2	7890	10	90	-	145.5	-	3.3
Co_2Si	-	34.0	4900	10	100	-	146.0	-	2.6
WSi_2	-	47.0	9300	10	100	-	240.0	-	2.3

© University of Pretoria

Table 3-2 Estimated values for light particle stopping power, light particle penetration depth, volumetric heat generation rate, and temperature rise in metal-silicon bilayer system at a given energy of 20 keV.

Irradiated layer	Light particle stopping Power S_l (10^{-11} J/m)	Light particle penetration depth d_l (µm)	Volumetric heat generation rate Q^l (10^7 J/m^{3}s)	Temperature rise ΔT^{irr} (10^{-12} K)
Si	2.2	4.2	0.6	6.9
Ni	6.8	1.1	3.1	4.3
Co	6.6	1.1	2.1	1.9
W	9.9	0.5	3.1	5.2
Ni_2Si	-	-	2.6	70
Co_2Si	-	-	2.0	23
WSi_2	-	-	1.6	27

© University of Pretoria

UNIVERSITEIT VAN PRETORIA
UNIVERSITY OF PRETORIA
YUNIBESITHI YA PRETORIA

Table 3-3. Estimated values for heavy particle stopping power, heavy particle penetration depth, volumetric heat generation rate, and temperature rise in metal- silicon bilayer system at a given energy of 110 keV and120 MeV.

Irradiated layer	Heavy particle stopping Power S_h (µJ/m)	Heavy particle penetration depth d_h (µm)	Volumetric heat generation rate Q^h (10^{12} J/m^{3}s)	Temperature rise ΔT^{irr} (10^{-4} K)
Si	0.25 - 46	0.04 - 220000	0.11 - 120	0.0013 - 350
Ni	3.7	8.4	150	1.50
Co	134	690000	600	125
W	170	44000	540	85
Ni_2Si	-	-	130	26
Co_2Si	-	-	410	710
WSi_2	-	-	310	450

Table 3-4. Estimated values for the diffusion coefficients of reactant species under the influence of radiation heating.

Atomic species in each irradiated layer	Vacancy migration energy E_v^m (eV)	Vacancy formation energy E_v^f (eV)	Activation energy for self-diffusion E_{SD} (eV) $E_{SD} = E_v^m + E_v^f$	Estimated irradiated temperature T^{irr} (K)	Lattice constant (10^{-10} m)	Diffusion coefficient D_{th} (m^2/s)
Si	1.06 [45]	2.32 [45]	3.40	298	5.43	1.74×10^{-23}
Ni	1.04 [46]	1.55 [47]	2.59	298	3.52	1.60×10^{-23}
Co	1.60 [47]	1.34 [47]	2.94	298	2.51	2.74×10^{-33}
W	1.70 [46]	3.60 [46]	5.30	298	3.16	8.85×10^{-35}

© University of Pretoria

UNIVERSITEIT VAN PRETORIA
UNIVERSITY OF PRETORIA
YUNIBESITHI YA PRETORIA

The results in Table 3-4 is estimated based on the Arrhenius equation of the form:

$$D_{\mathrm{th}} = a^2 f_v \, exp\left(\frac{-E_v^m}{K_B T}\right) \tag{3.24}$$

where

f_v (5 x 10^{13} s^{-1} [5]) is the jump frequency factor for vacancy.

The temperature rise in each irradiated layer at room temperature under light particle irradiation is extremely small as depicted in Table 3-2. This temperature is too low to activate the diffusion of atoms in the target layers. Therefore, it cannot make any significant contribution towards the layer growth during the irradiation process. Thus, the growth of the silicide must have taken place through other radiation induced processes.

The heavy particle stopping power in the silicon layer in Table 3-3 has estimated values that range from 0.25 – 46 µJ/m, this is due to different ion energies considered in different bilayer systems. For example, argon ion energy in the nickel-silicon system is 110 keV while in the cobalt-silicon system its energy is 120 MeV. Whereas under electron irradiation, a 20 keV electron energy is considered in all the bilayer systems. The same explanation holds for other parameters considered in silicon layer under heavy particle irradiation as shown in Table 3-3.

The temperature rise in each layer under heavy particle irradiation is depicted in Table 3-3. It shows that irradiation at low energy cannot account for silicide growth under the influence of radiation-induced heating. The same conclusion is deduced from the results obtained for the ion irradiation at high energy. However if we compared the results in Table 3-2 and Table 3-3 on the basis of temperature rise induced by the irradiation of light and heavy particles beams. We can see a wide gap between these two results; this shows that heavy particle deposited a greater amount of energy in the irradiated layers than light particles.

© University of Pretoria

The results presented in Table 3-4 shows that the irradiation temperature expressed in eqn. (3.14) cannot account for the diffusion coefficients of atomic species that are in the order of magnitude of 10^{-16} - 10^{-20} m^2/s reported in [2, 3].

This range of diffusion coefficients is the required interdiffusion coefficients for the silicide layer growth at the interfaces of metal-silicon systems.

This study shows that the influence of radiation heating has no significant impact on the layer growth of the thin film of the compound layer under both heavy and light particles irradiation. The reason for this may be ascribed to the nature of thickness of the irradiated layers. The amount of heat energy generated in each irradiated layer depends on the thickness of the layer. For example, the thicker the irradiated layer, the higher the chance for the radiation particle to penetrate to a greater depth in the layer and the more plausible it become to produce a greater amount of heat energy in the layer. The results obtained from this study is in good agreement with that of the experiment. In the experiment, it is observed that the temperature of the irradiated layers at a time greater than 10^{-8} s is approximately the same as that of the immediate surrounding [15, 48].

3.3 The influence of radiation-induced vacancies on the formation of an *AB* compound layer

Suppose the irradiation of *A* and *B* layers leads to the creation of vacancy and interstitial atoms. Let us not consider a very high rate of defect generation. For example, let us restrict our consideration exclusively to defect rates which correspond to reactor irradiation. In this case, the density of interstitial atoms is small, the correlation between fluxes of vacancy and interstitial atoms is weak, and contributions of vacancy and interstitial mechanisms of diffusion can be considered separately.

The number of vacancies in the *AB* layer increases as the radiation-induced vacancy add up to the thermally generated ones.

© University of Pretoria

We assume that *A* and *B* atoms diffuse via a vacancy mechanism from the *AB* layer to reaction interface *A/AB* and *AB/B* to formed an *AB* compound layer as shown in Figure 2-2. The thickness of the *AB* layer formed owing to chemical reaction at interfaces *A/AB* and *AB/B* are designated by $h_A(t)$ and $h_B(t)$ respectively. The total thickness of the compound layer is given by: $h(t) = h_A(t) + h_B(t)$.

Suppose the x-axis is perpendicular to all the layers under consideration and $h(t) = 0$ before irradiation.

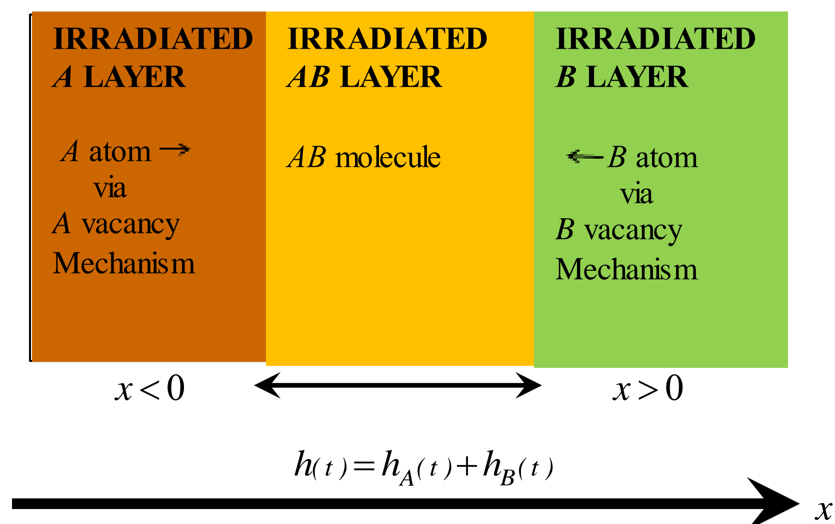

Figure 3-2: Schematic diagram showing the formation of an *AB* layer under a radiation-induced vacancy mechanism.

3.3.1 Basic equations for an *AB* compound layer formation due to radiation-induced vacancy mechanism

The diffusivity of *A* and *B* atoms through the vacancy mechanisms under irradiation are $D_a^{v,irr}$ and $D_b^{v,irr}$ respectively and the equation relating the diffusivity under irradiation to that of thermal diffusion is given by:

© University of Pretoria

$$D_a^{v,irr} = \frac{n_a^{v,irr} D_a^{v,th}}{n_a^{v,th}} \tag{3.25a}$$

and

$$D_b^{v,irr} = \frac{n_b^{v,irr} D_b^{v,th}}{n_b^{v,th}} \tag{3.25b}$$

where

$n_a^{v,irr}$ and $n_b^{v,irr}$ are the *A* and *B* vacancy densities under irradiation,

$D_a^{v,th}$ and $D_b^{v,th}$ are the diffusivities of *A* and *B* atoms via vacancy mechanisms due to thermal vacancies.

$n_a^{v,th}$ and $n_b^{v,th}$ are the thermal vacancy densities for *A* and *B* atom sites inside the *AB* layer.

Neglecting the recombination between vacancy and interstitial atoms, we can consider the change of densities of vacancy and interstitial atoms separately and obtain equations for two kinds of vacancy densities in the *AB* layer

$$\frac{dn_a^{v,irr}}{dt} = Kn_a^0 - \frac{\left(n_a^{v,irr} - n_a^{v,th}\right)}{\tau_a^v} \tag{3.26a}$$

and

$$\frac{dn_b^{v,irr}}{dt} = Kn_b^0 - \frac{\left(n_b^{v,irr} - n_b^{v,th}\right)}{\tau_b^v} \tag{3.26b}$$

where

τ_a^v and τ_b^v are the lifetimes for *A* and *B* vacancy.

© University of Pretoria

UNIVERSITEIT VAN PRETORIA
UNIVERSITY OF PRETORIA
YUNIBESITHI YA PRETORIA

Because the relaxation of vacancy distribution occurs more quickly than the growth of the *AB* layer, we assume that the vacancy distribution is homogeneous and stationary $\frac{dn_a^{v,irr}}{dt} = \frac{dn_b^{v,irr}}{dt} = 0$

Thus, for *A* and *B* vacancy densities we obtain:

$$n_a^{v,irr} = K n_a^0 \tau_a^v + n_a^{v,th} \tag{3.27a}$$

and

$$n_b^{v,irr} = K n_b^0 \tau_b^v + n_b^{v,th} \tag{3.27b}$$

Neglecting transient diffusion, we obtain equations for stationary density of *A* and *B* atoms inside the *AB* layer

$$D_a^{v,irr} \frac{\partial^2 n_a^{v,irr}(x)}{\partial x^2} = 0 \tag{3.28a}$$

and

$$D_b^{v,irr} \frac{\partial^2 n_b^{v,irr}(x)}{\partial x^2} = 0 \tag{3.28b}$$

With corresponding boundary conditions:

$J_a^v\left(x = h_{B(t)}\right) = R_a = \gamma n_b^0 v_a n_a^{v,irr}\left(x = h_{B(t)}\right)$,

$J_b^v\left(x = -h_{A(t)}\right) = R_b = \gamma v_b n_a^0 n_b^{v,irr}\left(x = -h_{A(t)}\right)$,

$n_a^{v,irr}\left(x = -h_{A(t)}\right) = n_a^0$, and

$n_b^{v,irr}\left(x = h_{B(t)}\right) = n_b^0$.

© University of Pretoria

UNIVERSITEIT VAN PRETORIA
UNIVERSITY OF PRETORIA
YUNIBESITHI YA PRETORIA

where

J_a^v and J_b^v are the fluxes of *A* and *B* atoms that diffuse via *A* and *B* vacancy mechanisms respectively,

R_a and R_b represent the chemical reaction rate at *A/AB* and *AB/B* interfaces, and

γ is the reaction rate constant.

The fluxes of *A* and *B* atoms is assumed to occur at the same rate as the chemical reaction in order to ensure that the reaction only occurs at the interface and not inside either the *A* or *B* layer.

The speed of growth of an *AB* layer by virtue of chemical reaction at *A/AB* interface is:

$$\frac{dh_{A(t)}}{dt} = \gamma V_{ab} n_a^0 n_b^{v,irr}\left(x = -h_{A(t)}\right) \tag{3.29a}$$

and at *AB/B,* the speed of growth is

$$\frac{dh_{B(t)}}{dt} = \gamma V_{ab}\left(n_b^0\right)^2 \tag{3.29b}$$

Therefore, the total speed of growth is

$$\frac{dh_{(t)}}{dt} = \frac{dh_{A(t)}}{dt} + \frac{dh_{B(t)}}{dt} \tag{3.29c}$$

© University of Pretoria

Solving eqn. (3.28a) and eqn. (3.28b) with given boundary conditions, we obtain an expression for the distribution of *A* and *B* atoms inside the *AB* compound layer:

$$n_a^{v,irr}(x,t) = -n_a^0 \left(n_b^0\right)^2 \left[\frac{\gamma\left(x + h_{a(t)}\right)}{D_a^{v,irr} n_a^0} - \frac{1}{\left(n_b^0\right)^2} \right] \tag{3.30a}$$

and

$$n_b^{v,irr}(x,t) = n_b^0 \left[\frac{\gamma\left(x - h_{B(t)}\right) v_b}{\frac{D_b^{v,irr}}{n_a^0} + \gamma v_b h_{(t)}} + 1 \right] \tag{3.30b}$$

The rate of chemical reaction at interfaces of solid layers depends on density of *A* and *B* atoms in a complex manner. However if there exist an excess of the *A* (or *B*) atoms, then the rate of reaction remain the same with a change of the density of the *A* (or *B*) atoms [26].

On the other hand, if densities of the *A* and *B* atoms are approximately equal. Then the rate of the *AB* compound formation can be represented in the first approximation as a product of *A* and *B* atom densities.

Thus, the rate of chemical reaction between the *A* and *B* atoms, at reaction interfaces *A/AB* and *AB/B* can be approximately expressed in two stages in the following ways:

$$R_a = \begin{cases} \gamma\left(n_a^0\right)^2 = \text{const} & n_b^{v,irr}\left(x = -h_{A(t)}\right) v_b \geq n_a^0 v_a \\ \gamma n_a^0 n_b^{v,irr}\left(x = -h_{A(t)}\right) & n_b^{v,irr}\left(x = -h_{A(t)}\right) v_b \leq n_a^0 v_a \end{cases} \tag{3.31a}$$

and

$$R_b = \begin{cases} \gamma\left(n_b^0\right)^2 = \text{const} & n_a^{v,irr}\left(x = h_{B(t)}\right) v_a \geq n_b^0 v_b \\ \gamma n_b^0 n_a^{v,irr}\left(x = h_{B(t)}\right) & n_a^{v,irr}\left(x = h_{B(t)}\right) v_a \leq n_b^0 v_b \end{cases} \tag{3.31b}$$

© University of Pretoria

UNIVERSITEIT VAN PRETORIA
UNIVERSITY OF PRETORIA
YUNIBESITHI YA PRETORIA

where

$n_b^{v,irr}\left(x=-h_{A(t)}\right)$ and $n_a^{v,irr}\left(x=h_{B(t)}\right)$ are the densities of B atoms at $x=-h_{A(t)}$ and A atoms at $x=h_{B(t)}$.

Owing to this, approximating the growth of the *AB* layer can have two stages. The first stage is when there is an excess of one kind of diffusing atoms. For example, an excess of *A* atoms near interface *AB/B* or an excess of *B* atoms near interface *A/AB*.

The second stage is when there is no excess of any kind of atoms near the corresponding interfaces. The second stage can take place independently of the first stage. However, if there is a first stage the second stage must follow suit.

Thus, for the first stage, the growth rate of the *AB* layer is determined by both the diffusion of *A* and *B* atoms inside the *AB* layer and also by the rate of reaction at the interfaces:

$$\frac{dh_{(t)}}{dt}=\frac{dh_{A(t)}}{dt}+\frac{dh_{B(t)}}{dt}=V_{ab}\left(\gamma\left(n_a^0\right)^2+\gamma n_b^0 n_a^{v,irr}\left(x=h_{B(t)}\right)\right) \tag{3.32}$$

The density of *A* atoms near interface *AB/B* and *B* atoms near interface *A/AB* at second stage are:

$$n_a^{v,irr}(h_{B(t)})=\frac{n_a^0}{n_b^0\left[\dfrac{1}{n_b^0}+\dfrac{\gamma v_a h_{(t)}}{D_a^{v,irr}}\right]} \tag{3.33a}$$

and

$$n_b^{v,irr}(-h_{A(t)})=\frac{n_b^0}{n_a^0\left[\dfrac{1}{n_a^0}+\dfrac{\gamma v_b h_{(t)}}{D_b^{v,irr}}\right]} \tag{3.33b}$$

© University of Pretoria

UNIVERSITEIT VAN PRETORIA
UNIVERSITY OF PRETORIA
YUNIBESITHI YA PRETORIA

If there is an excess of *A* atoms at reaction interface *AB/B* at time $t < t_c$, the *AB* layer at this interface grows under interfacial reaction controlled process. And at *A/AB* interface, the growth is controlled by diffusion. Therefore, the relationship between time and layer thickness is found by solving eqn. (3.32):

$$h(t) - \gamma V_{ab}\left(n_b^0\right)^2 t - \frac{D_b^{v,irr} v_a^2}{\gamma v_b^3 n_b^0} \ln\left[\frac{\gamma n_a^0 n_b^0 v_b^2 h(t)}{D_b^{v,irr}\left(n_a^0 v_a + n_b^0 v_a\right)} + 1\right] = 0 \tag{3.34}$$

However, if there is no excess of *A* atoms at reaction interface, no interfacial reaction controlled growth would occur at *AB/B* interface. And growth at both interfaces *A/AB* and *AB/B* would be mainly diffusion controlled.

At critical time t_c, $h(t) = h_c(t_c)$:

$$n_a^{v,irr}\left(h_B(t_c)\right) = \frac{n_a^0}{n_b^0\left[\frac{1}{n_b^0} + \frac{\gamma v_a h_c}{D_a^{v,irr}}\right]} = n_b^0 v_b \tag{3.35}$$

Critical thickness, h_c is obtained as:

$$h_c(t_c) = \frac{D_a^{v,irr}\left(\frac{n_a^0 v_a}{n_b^0 v_b} - 1\right)}{\gamma v_a n_b^0} \tag{3.36}$$

and for the critical time, substitute $t = t_c$, and $h(t) = h_c(t_c)$ in eqn. (3.34)

© University of Pretoria

$$t_c = \frac{1}{\gamma^2 V_{ab}\left(n_b^0\right)^3}\left[\frac{D_a^{v,irr}\left(n_a^0 v_a - n_b^0 v_b\right)}{n_b^0} - \frac{D_b^{v,irr}}{v_b^3}\ln\left(\frac{D_a^{v,irr} n_a^0 v_b\left(n_a^0 v_a - n_b^0 v_b\right)}{D_b^{v,irr} v_a n_b^0\left(n_a^0 v_a + n_b^0 v_b\right)}+1\right)\right] \quad (3.37)$$

Growth rate of an AB compound layer at $t > t_c$, is described by:

$$\frac{dh(t)}{dt} = \gamma V_{ab} n_a^0 n_b^0\left(\frac{n_b^{v,irr}\left(-h_{A(t)}\right)}{n_b^0} + \frac{n_a^{v,irr}\left(h_{B(t)}\right)}{n_a^0}\right) \quad (3.38)$$

By inserting eqns. (3.33a) and (3.33b) into eqn. (3.38) and integrate the resulting equation. A growth kinetics that describes the relation between time and layer thickness is obtained:

$$t = t_c + \alpha_1\left(h^2(t) - h_c^2(t)\right) + \alpha_2\left(h(t) - h_c(t)\right) - \alpha_3\ln\left[\frac{\alpha_4 h(t) + \alpha_5}{\alpha_4 h_c(t) + \alpha_5}\right] \quad (3.39)$$

© University of Pretoria

where

$$\alpha_1 = \left[2V_{ab}\left(D_b^{v,irr} n_b^0 + D_a^{v,irr} n_a^0 \right) \right]^{-1},$$

$$\alpha_2 = \left[\left(D_a^{v,irr} n_a^0 \right)^2 + \left(D_b^{v,irr} n_b^0 \right)^2 \right] \left[\gamma V_{ab} n_a^0 n_b^0 \left(D_b^{v,irr} n_b^0 + D_a^{v,irr} n_a^0 \right)^2 \right]^{-1},$$

$$\alpha_3 = D_a^{v,irr} D_b^{v,irr} \left(D_a^{v,irr} n_a^0 - D_b^{v,irr} n_b^0 \right)^2 \left[\gamma^2 V_{ab} n_a^0 n_b^0 \left(D_b^{v,irr} n_b^0 + D_a^{v,irr} n_a^0 \right)^3 \right]^{-1},$$

$$\alpha_4 = \gamma \left(D_b^{v,irr} n_b^0 + D_a^{v,irr} n_a^0 \right), \text{ and}$$

$$\alpha_5 = D_a^{v,irr} D_b^{v,irr}.$$

3.3.2 Results and discussion on radiation-induced vacancy mechanism

The model presented here gives a description of diffusion of two kinds of reactant species A and B by means of A and B vacancies during the compound layer formation process. The results that follow from this theoretical approach show a complex dependence of growth of the AB compound layer on layer thickness similar to layer growth kinetics under a non-irradiation process.

Suppose that only one kind of reactant species diffuse during irradiation by one sort of vacancy mechanism. If, for instance, only A atoms diffuse in the AB layer via A vacancies when $D_b^{v,irr} = 0$, equation (3.34) changes to a linear equation in the same form as the one expressed in eqn. (2.14a).

© University of Pretoria

UNIVERSITEIT VAN PRETORIA
UNIVERSITY OF PRETORIA
YUNIBESITHI YA PRETORIA

The eqn. (3.39) transform to parabolic under the same condition:

$$\gamma n_b^0 \left(h^2(t) - h_c^2(t_c) \right) + 2D_a^{v,irr} \left(h(t) - h_c(t_c) \right) - 2\gamma V_{ab} D_a^{v,irr} n_a^0 n_b^0 (t - t_c) = 0 \qquad (3.40)$$

A linear-parabolic growth kinetics relationship is obtained similarly to the one described under the result and discussion in chapter two. However, if only B atoms diffuse via B vacancies when $D_a^{v,irr} = 0$, linear growth would be absent only parabolic law would hold. Eqn. (3.39), therefore, becomes:

$$\gamma n_a^0 h^2(t) + 2D_b^{v,irr} h(t) - 2\gamma V_{ab} D_b^{v,irr} n_a^0 n_b^0 t = 0 \qquad (3.41)$$

Equation (3.41) is expressed in a similar form as eqn. (2.16b) but note that the diffusivity in both cases are not the same and, therefore, they are determined differently.

Irradiation influences the growth of the AB layer via a change of diffusivity due to the production of vacancy at defect rate K . Let us assume that the A atoms diffuse only via vacancies of A sublattice of the AB compound and B atoms via the B sublattice, accordingly. It means that we consider the diffusion of A and B atoms separately and diffusivity of A and B atoms via A and B vacancy mechanisms become:

$$D_{a(b)}^{v,th} = \frac{n_{a(b)}^{v,th}}{n_{a(b)}^0} D^{v,a(b)} \qquad (3.42a)$$

Taking into account that

$$\left(\tau_{a(b)} \right)^{-1} = D^{v,a(b)} \left(\rho d \right)_{a(b)} \qquad (3.42b)$$

and

$$n_a^0 = \nu_a n_{ab}; \quad n_b^0 = \nu_b n_{ab} \qquad (3.42c)$$

© University of Pretoria

where

$D^{v,a}$ and $D^{v,b}$ are diffusivities of A and B vacancies, $(\rho d)_a$ and $(\rho d)_b$ are dislocation densities of A and B crystals.

Substitute eqns. (3.42a), (3.42b) and (3.42c) into eqns. (3.25a) and (3.25b), we obtain:

$$D_{a(b)}^{v,irr} = D_{a(b)}^{v,th} + \frac{Kn_{a(b)}^{0}}{(\rho d)_{a(b)}\, v_{a(b)}\, n_{ab}} \tag{3.43}$$

Equation (3.43) shows that the diffusivities of the atomic species A and B are both directly proportional to the defect generation rate in both irradiated A and B layers. The defect generation rate enhances diffusion of reactant species from their respective layers to the reaction interfaces; this, in turn, enhances the growth of the compound layer at the interfaces.

The diffusivity of the reactant species, in this case, depends on both temperature and defect generation rate.

However, at extremely low-temperature irradiation where the influence of temperature on layer growth kinetics can be ignored. The defect generation rate plays a dominant role on the layer growth rate.

The rates of growth of the compound layer at the reaction interfaces are enhanced by the number of atomic species that are able to diffuse via the vacancy mechanism from the reactant layers to the reaction sites.

In as much as the densities of species transported to the reaction interfaces, are not the same, the growth of the compound layer would proceed at different speeds at the interfaces.

© University of Pretoria

UNIVERSITEIT VAN PRETORIA
UNIVERSITY OF PRETORIA
YUNIBESITHI YA PRETORIA

Table 3-5. Estimation of diffusivity of palladium and silicon species via vacancy mechanism in the Pd_2Si layer together with the speed of growth and reaction rate of the layer.

$D_a^{v,irr}$ (Pd) (10^{-20} m²/s)	$D_b^{v,irr}$ (Si) (10^{-16} m²/s)	$dh_{A(t)}/dt$ (10^{-9}m/s)	$dh_{B(t)}/dt$ (10^{-7}m/s)	R_a (10^{19}/m²s)	R_b (10^{21}/m²s)	K (dpa/s)	γ (10^{-36} m⁴/s)
0.047	0.021	0.290	0.120	0.690	0.275	10^{-9}	0.110
0.470	0.210	0.900	0.330	2.100	0.775	10^{-8}	0.310
4.700	2.100	3.200	1.200	7.600	2.750	10^{-7}	1.100

Table 3-6. Estimation of speed of growth and reaction rate of Ni_2Si layer with the diffusivity of nickel and silicon species via vacancy mechanism in the Ni_2Si layer.

$D_a^{v,irr}$ (Ni) (10^{-20} m²/s)	$D_b^{v,irr}$ (Si) (10^{-16} m²/s)	$dh_{A(t)}/dt$ (10^{-9} m/s)	$dh_{B(t)}/dt$ (10^{-8} m/s)	R_a (10^{19}/m²s)	R_b (10^{20}/m²s)	K (dpa/s)	γ (10^{-37} m⁴/s)
0.028	0.015	0.220	0.062	0.670	0.190	10^{-9}	0.075
0.280	0.150	0.770	0.190	2.300	0.575	10^{-8}	0.230
2.800	1.500	2.500	1.400	7.500	4.100	10^{-7}	1.640

Table 3-7. Estimation of reaction rate, growth speed, and diffusivity of platinum and silicon species via vacancy mechanism in the Pt_2Si layer.

$D_a^{v,irr}$ (Pt) (10^{-20} m²/s)	$D_b^{v,irr}$ (Si) (10^{-16} m²/s)	$dh_{A(t)}/dt$ (10^{-9} m/s)	$dh_{B(t)}/dt$ (10^{-7} m/s)	R_a (10^{19}/m²s)	R_b (10^{21}/m²s)	K (dpa/s)	γ (10^{-36} m⁴/s)
0.014	0.022	0.290	0.028	0.675	0.065	10^{-9}	0.026
0.140	0.220	0.960	0.240	2.200	0.550	10^{-8}	0.220
1.400	2.200	3.500	2.400	8.100	5.500	10^{-7}	2.200

© University of Pretoria

UNIVERSITEIT VAN PRETORIA
UNIVERSITY OF PRETORIA
YUNIBESITHI YA PRETORIA

Table 3-8. Estimation of diffusivity of cobalt and silicon species via vacancy mechanism in the *CoSi* layer together with the speed of growth and reaction rate of the layer.

$D_a^{v,irr}$ *(Co)* (10^{-20} m²/s)	$D_b^{v,irr}$ *(Si)* (10^{-16} m²/s)	$dh_{A(t)}/dt$ (10^{-9} m/s)	$dh_{B(t)}/dt$ (10^{-7}m/s)	R_a (10^{19} /m²s)	R_b (10^{21} /m²s)	K (dpa/s)	γ (10^{-36} m⁴/s)
0.175	0.019	0.035	0.022	0.323	0.036	10^{-9}	0.017
1.750	0.192	0.360	0.200	2.059	0.376	10^{-8}	0.200
17.500	1.92	3.455	2.125	7.611	4.250	10^{-7}	1.700

Table 3-9. Estimation of the speed of growth, reaction rate, the diffusivity of tungsten and silicon species via vacancy mechanism in the WSi_2 layer.

$D_a^{v,irr}$ *(W)* (10^{-20} m²/s)	$D_b^{v,irr}$ *(Si)* (10^{-16} m²/s)	$dh_{A(t)}/dt$ (10^{-9} m/s)	$dh_{B(t)}/dt$ (10^{-8} m/s)	R_a (10^{19} /m²s)	R_b (10^{20}/m²s)	K (dpa/s)	γ (10^{-37} m⁴/s)
0.090	0.017	0.400	0.108	0.900	0.351	10^{-9}	0.110
0.910	0.165	0.870	0.538	3.678	0.751	10^{-8}	0.500
9.100	1.650	3.162	1.835	8.703	5.751	10^{-7}	1.100

Based on the proposed model for radiation-induced vacancy mechanism, we estimate the speed of growth, reaction rate and layer thickness of five silicides at room temperature at defect generation rates of $K = 10^{-9}$, 10^{-8}, and 10^{-7} dpa/s.

This study shows that the speed of growth and reaction rates at the metal/silicide and silicide/silicon interfaces are not the same as shown in Tables 3-5 to 3-9.

The diffusivity of atomic species via vacancy mechanism is estimated for metal and silicon species in palladium silicide, nickel silicide, platinum silicide, cobalt silicide and tungsten disilicide using eqns. (3.25a) and (3.25b). The result obtained from the diffusivity of both *Pd* and *Si* atoms as diffusing species is shown in Table 3-5.

The diffusivity of silicon is estimated to be about 10^4 times faster than that of palladium, which makes silicon the dominant species in the Pd_2Si layer.

© University of Pretoria

Similar results are shown in Tables 3-6, 3-7, 3-8, and 3-9 for nickel silicide Ni_2Si, platinum silicide Pt_2Si, cobalt silicide $CoSi$, and tungsten disilicide WSi_2. This result is contrary to the report in [29-30] where palladium, nickel, cobalt in (Co_2Si) and platinum were reported as the dominant species under thermal diffusion. The same view holds for the other near noble metal silicides where the metals were seen as the main diffusing species during the silicide growth [29-30] in the first compound phase as mentioned in the previous chapter.

However, in tungsten disilicide WSi_2 and cobalt monosilicide $CoSi$ silicon is found as the dominant diffusing species in both layers under thermal diffusion [2, 49].

Table 3-11 contains useful data for the estimation of thermal self-diffusivity of Pd, Si, Ni, Pt, Co, and W in their respective silicide layers.

The estimated values of diffusivity of silicon in the five silicide layers at different defect generation rates at room temperature yielded results that lie within the range of integrated interdiffusion coefficients of these silicides at their formation temperatures. This strongly corroborates silicon as the active diffusing species in the silicide layer under irradiation. The formation temperatures of these silicides are shown in Table 3-10.

The results depicted in Tables 3-5, 3-6, 3-7, 3-8, and 3-9 show that the speed of growth and reaction rate increase as the defect generation rate rises in the irradiated layer.

This is as a result of the opening of several channels (i.e. creation of vacant sites) in the irradiated layers for a considerable amount of atoms to diffuse to the reaction interface.

The results also show that the reaction in each layer proceeds at a different rate, likewise the layer growth speed. The difference in layer growth speed and reaction rate can be attributed to the number of surface atoms present at the reaction interface during the layer formation process. The interface that has more surface atoms has a greater chance of producing the compound layer faster than one with fewer atoms.

The layer thickness depicted in Figure 3-3 to 3-7 show that the growth of the compound layer depends strongly on the defect generation rate. For instance, the temperature considered in this study is too low for silicide formation to take place in the absence of irradiation.

© University of Pretoria

In literature, it has been reported that silicide formation can occur at a temperature much lower than room temperature (-120^0 C) under irradiation [48].

The tendency of producing silicides at a temperature as low as room temperature is highly feasible since radiation enhanced diffusion depends strongly on a defect generation rate at such a low-temperature irradiation.

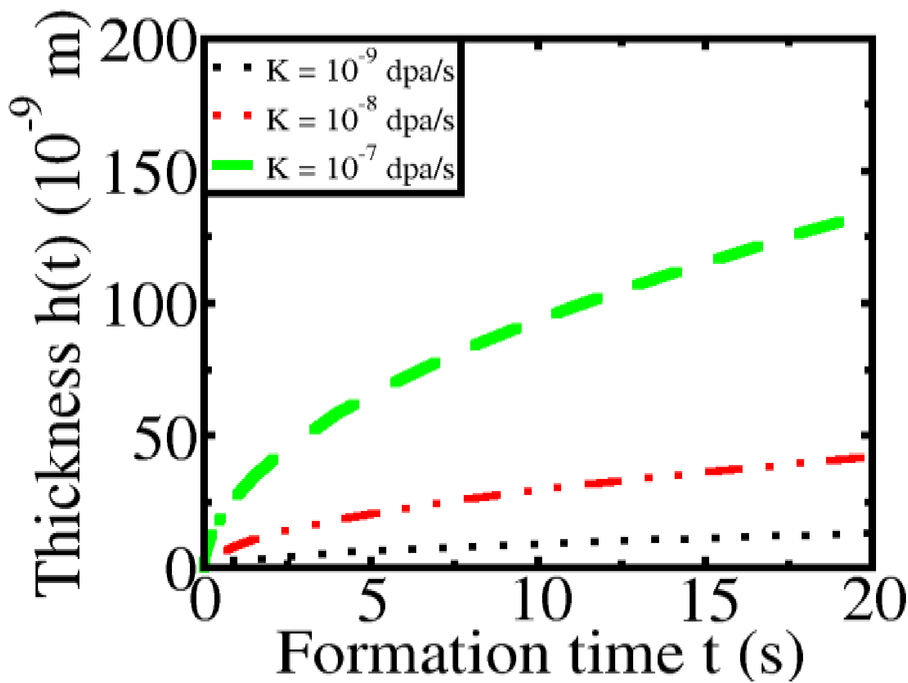

Figure 3-3: The growth kinetics of palladium silicide Pd_2Si at room temperature under the influence of radiation-induced vacancy at defect generation rates of $K = 10^{-9}$, 10^{-8} and 10^{-7} dpa/s.

© University of Pretoria

Table 3-10. Estimated density of silicide layers and their formation temperatures (Culled from [3]) under non-irradiation process.

Silicide layer	Formation temperature (K)	Estimated density of silicide layer (10^{28} molecules/m^3)
Pd_2Si	373	2.400
Ni_2Si	473	3.300
Pt_2Si	473	2.300
$CoSi$	648	2.600
WSi_2	923	2.300

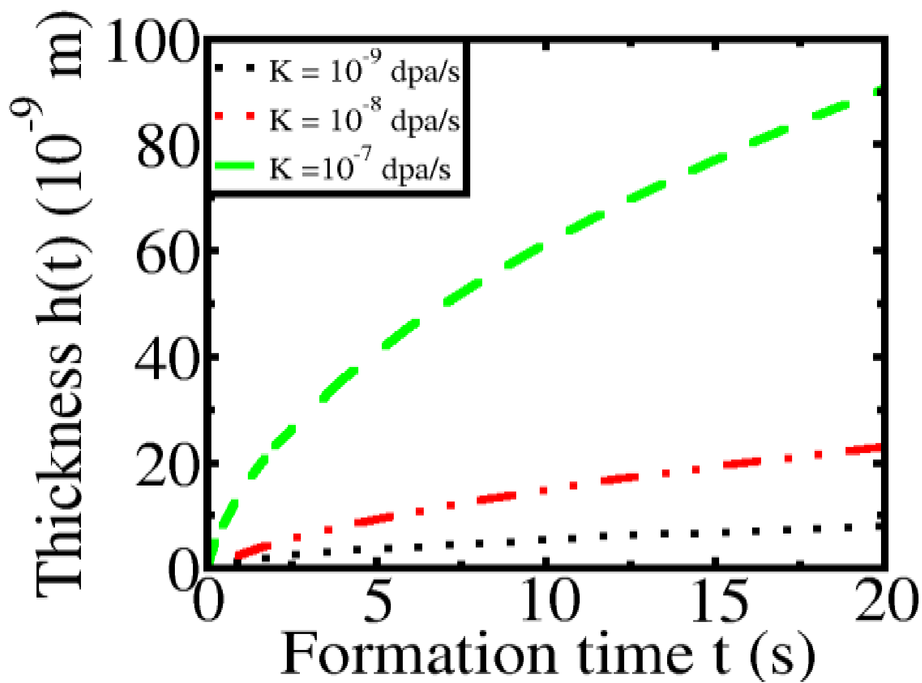

Figure 3-4: The growth kinetics of nickel silicide Ni_2Si at room temperature under the influence of radiation-induced vacancy at defect generation rates of $K = 10^{-9}$, 10^{-8} and 10^{-7} dpa/s.

© University of Pretoria

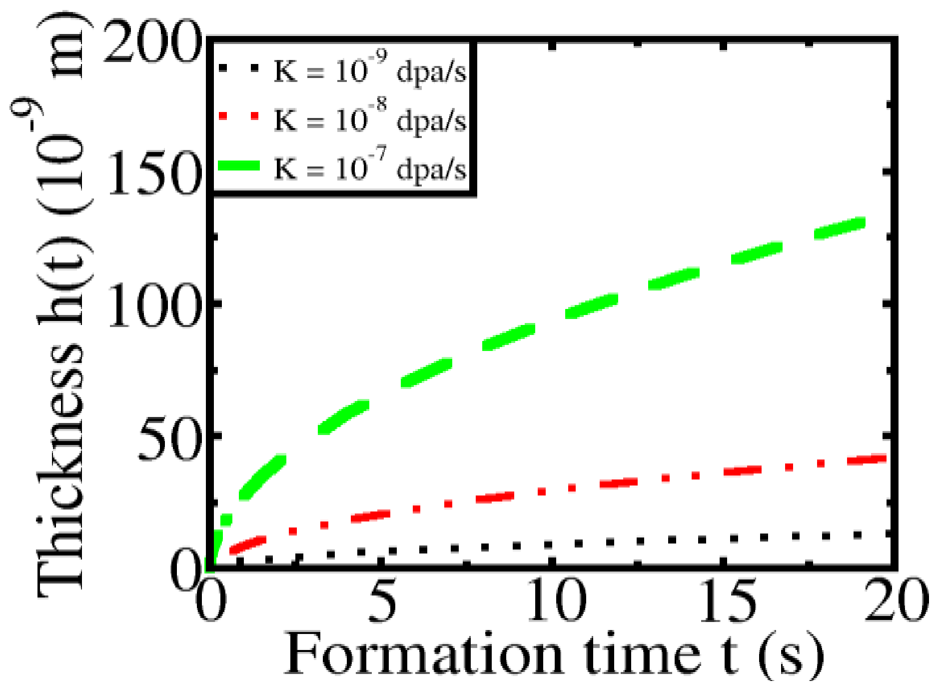

Figure 3-5: The growth kinetics of platinum silicide Pt_2Si at room temperature under the influence of radiation-induced vacancy at defect generation rates of $K = 10^{-9}$, 10^{-8} and 10^{-7} dpa/s.

© University of Pretoria

UNIVERSITEIT VAN PRETORIA
UNIVERSITY OF PRETORIA
YUNIBESITHI YA PRETORIA

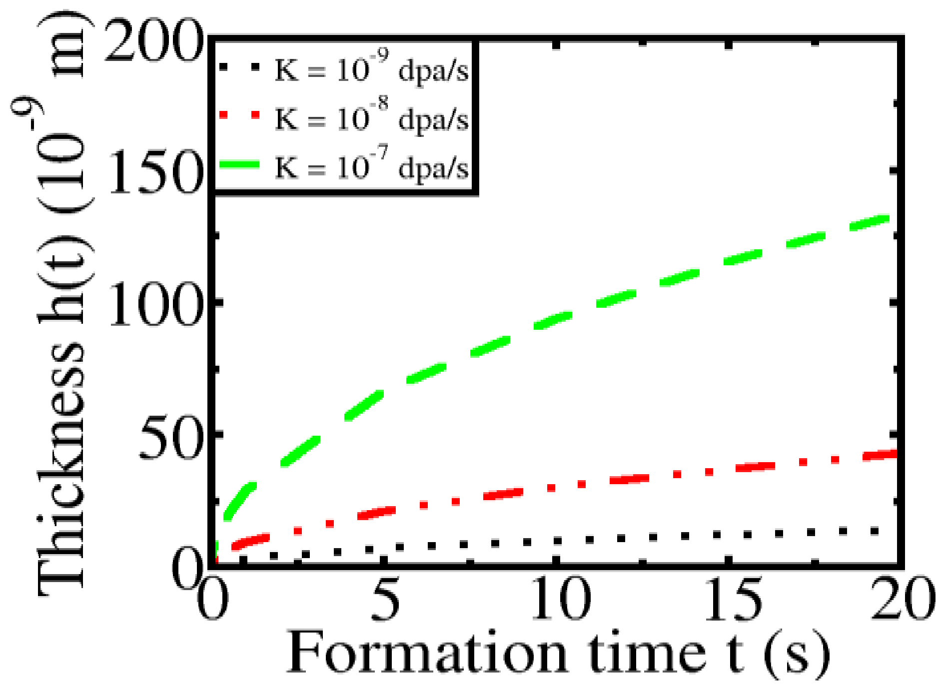

Figure 3-6: The growth kinetics of cobalt silicide *CoSi* at room temperature under the influence of radiation-induced vacancy at defect generation rates of $K = 10^{-9}$, 10^{-8} and 10^{-7} dpa/s.

© University of Pretoria

UNIVERSITEIT VAN PRETORIA
UNIVERSITY OF PRETORIA
YUNIBESITHI YA PRETORIA

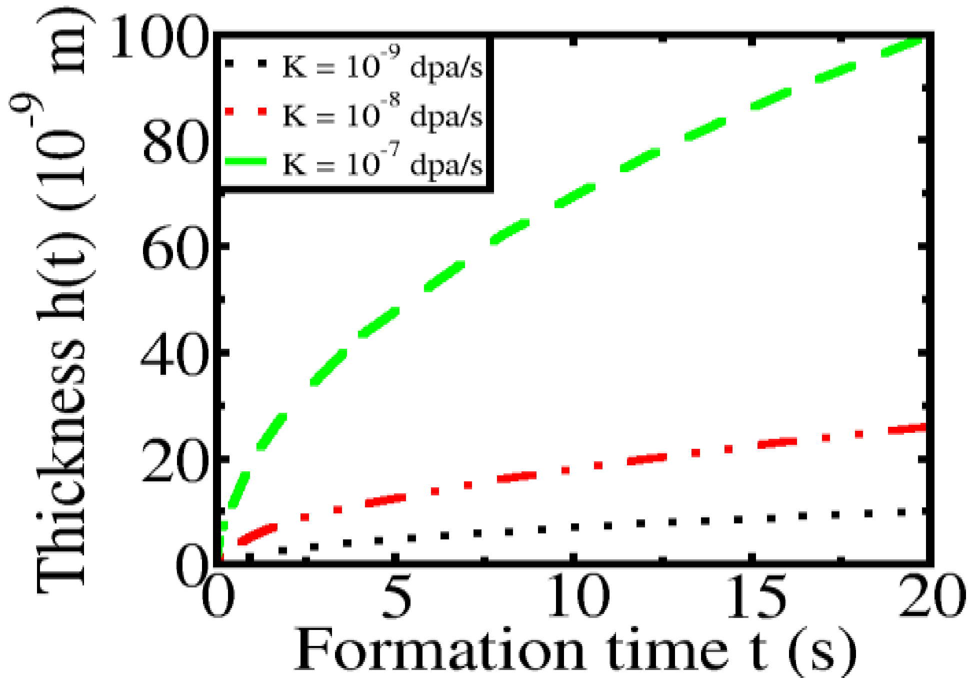

Figure 3-7: The growth kinetics of tungsten disilicide WSi_2 at room temperature under the influence of radiation-induced vacancy at defect generation rates of $K = 10^{-9}$, 10^{-8} and 10^{-7} dpa/s

The growth kinetics shown in Figures 3-3 to 3-7 depicts a parabolic dependence of layer thickness on time. This result can be explained in light of the first phase of silicide formed during the process of irradiation.

According to the model presented here, if 'majority atoms' are active (i.e. dominant) during the layer growth, a reaction controlled process would occur for a certain period of time and change to diffusion limited process after the growth kinetics has transformed to a parabolic growth. However, if the dominant atoms are the minority species, then the layer growth would begin and end as a diffusion limited process. Since minority species are the dominant atoms in the five silicide layers considered in this study.

© University of Pretoria

Therefore, only one stage of growth is plausible (i.e. the parabolic growth). The silicide thickness is estimated with eqn. (3.39) (when $h_c = 0$ and $t_c = 0$) over a period of 20 seconds at different defect generation rates in the Pd_2Si, Ni_2Si, Pt_2Si, $CoSi$ and WSi_2 silicide layers.

Table 3-11. Parameters used for estimation of thermal self-diffusion coefficients of *Pd*, *Si*, *Ni*, *Pt*, *Co* and *W* in their respective silicides.

Volume of Compound layer (10^{-29} m^3)	Diffusing species under non-irradiation process	Diffusing species under irradiation process	Pre-exponential factor D_0 (m^2/s) for non-irradiation condition for atomic species	Activation energy E_a (eV) for non- irradiation condition for atomic species
Pd_2Si, (4.200)	*Pd*, *Si* [4]	*Pd*, *Si* [5]	*Pd* (1.500 x 10^{-8}) [22] *Si* (6.240 x 10^{-5}) [22]	*Pd* (1.000) [22], *Si* (1.700) [22]
Ni_2Si, (3.200)	*Ni* [3]	*Ni*, *Si* present work	*Ni* (1.820 x 10^{-3}) [4] *Si* (8.950 x 10^{-9}) [50]	Ni (1.710) [4], *Si* (1.900) [50]
Pt_2Si, (4.300)	*Pt* [2]	*Pt*, *Si* present work	*Pt* (5.500 x 10^{-4}) [10] *Si* (3.590 x 10^{-5}) [50]	*Pt* (1.485) [10], *Si* (2.100) [50]
WSi_2, (4.300)	*Si* [3]	*W*, *Si* present work	*W* (1.400 x 10^{-3}) (estimated from [51]) *Si* (3.100 x 10^{-7}) (estimated from[51])	*W* (2.780), *Si* (1.570) (estimated from [51])
$CoSi$, (4.300)	*Si* [2]	*Co*, *Si* present work	*Co* (9.800 x 10^{-5}) [49] *Si* (3.200 x 10^{-6}) [50]	*Co* (2.930) [49], *Si* (2.140) [50]

© University of Pretoria

Table 3-12. Useful parameters for estimation of diffusivity via vacancy mechanism at temperature of 298 K. (Where K_B = 8.617 x 10^{-5} eV and f_i = 5 x 10^{12} s^{-1} [5]).

Reactant Species	Dislocation density $(\rho d)_{a(b)}$ (10^9 m^{-2})	Vacancy formation energy for reactant species (eV)
Pd	3000 [52]	1.700 [58]
Ni	5000 [53]	1.550 [47]
Pt	< 1000 [54]	1.350 [46]
Si	1.000 [55]	2.320 [45]
W	3000 [56]	3.560 [46]
Co	2000 [57]	1.340 [47]

3.4 The role of radiation-induced interstitial mechanism on the formation of an *AB* compound layer

Suppose that interstitial and vacancy pairs are created in both the *A* and *B* layers as a result of irradiation of the *A*-*B* bilayer system at low defect generation rates. The low rates of defect generation weaken the correlation between the interstitial and the vacancy fluxes such that the contribution of interstitial can be separated from that of the vacancy in both irradiated layers.

Let us assume that the *A* layer occupies space $x < 0$ and *B* layer occupies space $x > 0$ in the *A*-*B* bilayer system. Before irradiation, *AB* layer is absent between the *A* and *B* layers due to the absence of chemical interaction at the reaction interface at a time, $t = 0$. At $t > 0$, irradiation begins in the *A* and *B* layers. The *A* and *B* interstitial atoms produced as a result of irradiation diffuse via interstitial mechanisms in the *A*-*B* bilayer system as depicted in Figure 3-8. The *A* interstitial atom diffuses via an *A* interstitial mechanism to reaction interface *AB/B* where it chemically interacts with *B* surface lattice atoms to formed an *AB* compound.

© University of Pretoria

UNIVERSITEIT VAN PRETORIA
UNIVERSITY OF PRETORIA
YUNIBESITHI YA PRETORIA

In a similar fashion, the *B* interstitial atom traverse via a *B* interstitial mechanism to reaction interface *A/AB* where it also reacts with *A* surface lattice atom to formed an additional *AB* compound. The *AB* layer formed from this chemical transformation occupies the space from $x=-h_A(t)$ to $x=h_B(t)$. The *AB* layer thickness formed at interfaces *A/AB* and *AB/B* are denoted by $h_A(t)$ and $h_B(t)$ respectively.

The total *AB* compound layer thickness is, therefore, represented by $h(t)$;

$h(t)=h_A(t)+h_B(t)$. Where h_A, h_B and h are the function of time t.

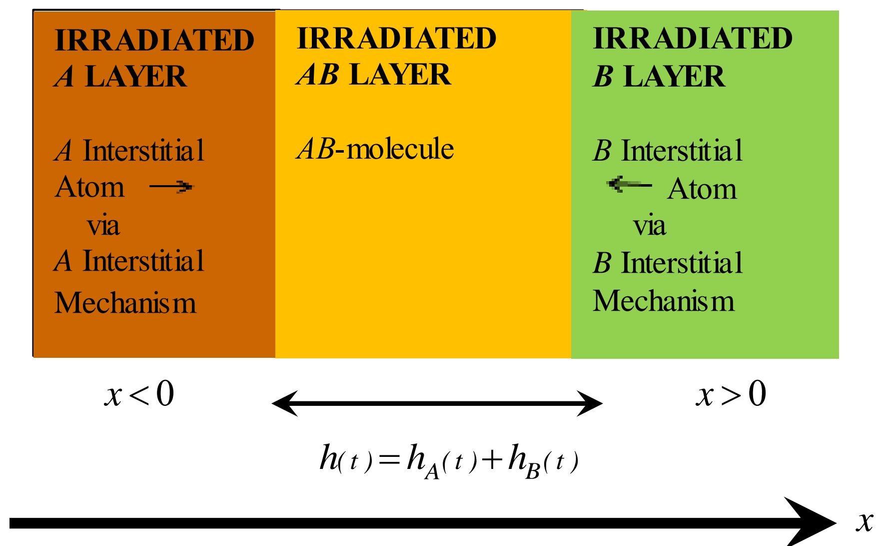

Figure 3-8: Schematic diagram showing the formation of an *AB* layer under a radiation-induced interstitial mechanism.

© University of Pretoria

3.4.1 Basic equations for an *AB* compound layer formation due to radiation-induced interstitial mechanism

The diffusivity of *A* and *B* interstitial atoms through the interstitial mechanisms via the *AB* layer under irradiation are $D_a^{i,irr}$ and $D_b^{i,irr}$.

Interstitial diffusivity is described by Arrhenius equation in the following way in agreement with the model proposed in [59]:

$$D_{a(b)}^{i,irr} = 0.1a^2 f_i \, exp\left(\frac{-E_i^m}{K_B T}\right) \tag{3.44}$$

where

a is the lattice constant,

f_i is the jump frequency factor for interstitial atom,

E_i^m is the interstitial migration energy,

Neglecting the recombination between interstitial atoms and vacancy, change of density of interstitial atoms and vacancy can be considered separately under both stationary and homogeneous distribution condition. The reason behind this condition is associated with the fact that relaxation of interstitial distribution occurs faster than the growth of an *AB* layer.

For a stationary condition:

$$\frac{dn_{i,irr}^{a(b)}}{dt} = Kn_{a(b)}^0 - \frac{n_{i,irr}^{a(b)}}{\tau_{i,a(b)}} = 0 \tag{3.45}$$

© University of Pretoria

Thus, A and B interstitial densities can be obtained in the A and B layers as follow:

$$n_{i,irr}^{a(b)} = Kn_{a(b)}^{0}\tau_{i,a(b)} = \frac{Kn_{a(b)}^{0}}{(\rho d)_{a(b)} D_{a(b)}^{i,irr}} \tag{3.46}$$

where

$n_{i,irr}^{a}$ and $n_{i,irr}^{b}$ are the interstitial densities in the A and B layers produced during irradiation,

$\tau_{i,a}$ and $\tau_{i,b}$ are the lifetimes of A and B interstitial atoms,

Neglecting transient diffusion, the Fick's equation for diffusion of A and B interstitial atoms inside the AB layer is given by:

$$D_{a(b)}^{i,irr}\frac{\partial^2 n_{i,irr}^{a(b)}(x)}{\partial x^2} = 0 \tag{3.47}$$

With respect to the following boundary conditions:

$$J_i^a(h_{B(t)}) = R_a = \gamma v_a n_b^0 n_{i,irr}^a(h_{B(t)}),$$

$$J_i^b(-h_{A(t)}) = R_b = \gamma v_b n_a^0 n_{i,irr}^b(-h_{A(t)}),$$

$$n_{i,irr}^a(-h_{A(t)}) = n_i^a = \frac{Kn_a^0}{(\rho d)_a\, D_a^{i,irr}},$$

$$n_{i,irr}^b(h_{B(t)}) = n_i^b = \frac{Kn_b^0}{(\rho d)_b\, D_b^{i,irr}}.$$

© University of Pretoria

UNIVERSITEIT VAN PRETORIA
UNIVERSITY OF PRETORIA
YUNIBESITHI YA PRETORIA

where

J_i^a and J_i^b are the fluxes of A and B interstitial atoms,

$n_{i,irr}^a\left(h_{B(t)}\right)$ and $n_{i,irr}^b\left(-h_{A(t)}\right)$ are the densities of A and B interstitial atoms which diffuse to interfaces AB/B and A/AB through the A and B interstitial mechanisms respectively.

The fluxes of A and B interstitial atoms are assumed to occur at the same rate as the chemical reaction rates at reaction interfaces.

This assumption is taken as a measure to ensure that reaction only takes place at reaction interfaces and not inside the reactant layers.

The rate of chemical reaction at the reaction interfaces of the A-B bilayer system is determined by the density of interstitial atoms and surface lattice species within the proximity of the interfaces.

The solution of eqn. (3.47) with respect to the boundary conditions stated above are expressed as follows:

$$n_{i,irr}^a(x,t) = -\frac{\gamma n_i^a n_b^0 v_a}{D_a^{i,irr} + \gamma v_a n_b^0 h(t)}\left(x + h_{A(t)}\right) + n_i^a \tag{3.48a}$$

and

$$n_{i,irr}^b(x,t) = \frac{\gamma n_a^0 n_i^b v_b}{D_b^{i,irr} + \gamma v_b n_a^0 h_{(t)}}\left(x - h_{B(t)}\right) + n_i^b \tag{3.48b}$$

where

$n_{i,irr}^a(x,t)$ and $n_{i,irr}^b(x,t)$ are the distribution densities of A and B interstitial atoms inside the AB compound layer respectively.

The growth rate of the AB compound layer occurs under diffusion controlled process. This is because the number of A and B atoms that diffuse from the interstitial sites as a result of irradiation are small compared to the number of surface lattice atoms at both interfaces AB/B and A/AB.

© University of Pretoria

UNIVERSITEIT VAN PRETORIA
UNIVERSITY OF PRETORIA
YUNIBESITHI YA PRETORIA

Therefore, the reaction rate depends on both atomic densities of interstitial atoms and surface lattice atoms at the reaction interfaces [26].

The rate of growth $\left(\frac{dh_{(t)}}{dt}\right)$ of an *AB* layer is described in terms of the chemical reaction rate at the interfaces *AB/B* and *A/AB* and also by interstitial diffusivity of *A* and *B* atoms inside the *AB* compound layer:

$$\frac{dh_{(t)}}{dt} = \frac{dh_{A(t)}}{dt} + \frac{dh_{B(t)}}{dt} = \gamma V_{ab}\left(n_a^0 n_{i,irr}^b\left(-h_{A(t)}\right) + n_b^0 n_{i,irr}^a\left(h_{B(t)}\right)\right) \qquad (3.49)$$

where

$$\frac{dh_{A(t)}}{dt} = \gamma V_{ab} n_a^0 n_{i,irr}^b\left(-h_{A(t)}\right),$$

$$\frac{dh_{B(t)}}{dt} = \gamma V_{ab} n_b^0 n_{i,irr}^a\left(h_{B(t)}\right),$$

$$n_{i,irr}^a(h_{B(t)}) = \frac{D_a^{i,irr} n_i^a}{D_a^{i,irr} + \gamma v_a n_b^0 h_{(t)}} \text{ and}$$

$$n_{i,irr}^b(-h_{A(t)}) = \frac{D_b^{i,irr} n_i^b}{D_b^{i,irr} + \gamma v_b n_a^0 h_{(t)}}.$$

$\frac{dh_{A(t)}}{dt}$ is the speed of growth of an *AB* layer at the interface *A/AB* and

$\frac{dh_{B(t)}}{dt}$ is the speed of growth of an *AB* layer at the interface *AB/B*

Substitute $n_{i,irr}^a(h_{B(t)})$ and $n_{i,irr}^b(-h_{A(t)})$ into eqn. (3.49) and solve the resulting equation.

© University of Pretoria

An expression relating time to thickness is obtained which has both parabolic and natural logarithmic functions:

$$t = \chi_1 h^2(t) + \chi_2 h(t) - \chi_3 \ln\left[\frac{\chi_4 h(t) + \chi_5}{\chi_5}\right] \qquad (3.50)$$

where

$$\chi_1 = \left[2V_{ab}\left(D_a^{i,irr} n_i^a + D_b^{i,irr} n_i^b\right)\right]^{-1},$$

$$\chi_2 = \left[\begin{matrix} D_a^{i,irr} D_b^{i,irr}\left(n_a^0 n_i^b + n_i^a n_b^0\right) + \\ 2\left(\left(D_a^{i,irr}\right)^2 n_a^0 n_i^a + \left(D_b^{i,irr}\right)^2 n_i^b n_b^0\right) \end{matrix}\right]\left[2\gamma V_{ab} n_a^0 n_b^0 \left(D_a^{i,irr} n_i^a + D_b^{i,irr} n_i^b\right)^2\right]^{-1},$$

$$\chi_3 = \frac{D_a^{i,irr} D_b^{i,irr}\left[\begin{matrix} D_a^{i,irr} D_b^{i,irr}\left(\left(n_i^a n_b^0\right)^2 + \left(n_a^0 n_i^b\right)^2 - 2 n_a^0 n_b^0 n_i^a n_i^b\right) \\ + 2 n_i^a n_i^b \left(\left(D_a^{i,irr}\right)^2 \left(n_a^0\right)^2 + \left(D_b^{i,irr}\right)^2 \left(n_b^0\right)^2\right) \end{matrix}\right]}{2\gamma^2 V_{ab} \left(n_a^0\right)^2 \left(n_b^0\right)^2 \left[D_a^{i,irr} n_i^a + D_b^{i,irr} n_i^b\right]^3},$$

$$\chi_4 = 2\gamma n_a^0 n_b^0 \left[D_a^{i,irr} n_i^a + D_b^{i,irr} n_i^b\right] \text{ and}$$

$$\chi_5 = D_a^{i,irr} D_b^{i,irr}\left[n_i^b n_a^0 + n_i^a n_b^0\right].$$

© University of Pretoria

UNIVERSITEIT VAN PRETORIA
UNIVERSITY OF PRETORIA
YUNIBESITHI YA PRETORIA

3.4.2 Results and discussion on radiation-induced interstitial mechanism

This study shows a detailed illustration of diffusion of two forms of atomic species *A* and *B* under radiation-induced interstitial mechanisms by means of two sorts of interstitial mediated processes.

The growth of an *AB* compound layer occurs under irradiation by means of contributions of the *A* and *B* interstitial species via the *A* and *B* interstitial mechanisms through the *AB* layer to the reaction interfaces. At the reaction interfaces, the *A* and *B* interstitial atoms react chemically with the *A* and *B* surface lattice atoms which result in the *AB* layer formation.

The growth kinetics of the compound layer under this consideration shows a complex dependence on layer thickness similar to those discussed previously.

The complex kinetics of the growth of an *AB* compound layer under radiation-induced interstitial mechanism can be attributed to two forms of interstitial mechanisms taking place simultaneously in the *AB* compound layer.

These are the *A* and *B* interstitial mechanisms which transport the *A* and *B* interstitial atoms from their respective layers to the reaction interfaces.

If a similar approach like the one used in the previous section is applied to eqn. (3.50). The complex layer growth kinetic reduces to parabolic under diffusion limited process.

For example, if only the *A* interstitial atoms diffuse via the *A* interstitial mechanism in the *AB* layer when $D_b^{i,irr} = 0$. Equation (3.50) transform to parabolic:

$$\gamma n_b^0 h^2(t) + 2D_a^{i,irr} h(t) - 2\gamma V_{ab} D_a^{i,irr} n_i^a n_b^0 t = 0 \qquad (3.51)$$

© University of Pretoria

In a similar manner, if only *B* interstitial atoms diffuse via *B* interstitial mechanism in the *AB* layer when $D_a^{i,irr} = 0$, eqn. (3.50) also changes to parabolic:

$$\gamma n_a^0 h^2(t) + 2D_b^{i,irr} h(t) - 2\gamma V_{ab} D_b^{i,irr} n_a^0 n_i^b t = 0 . \tag{3.52}$$

Equation (3.46) shows the importance of defect generation rate in the irradiated layer during radiation-induced interstitial mediated process. It is shown that the density of the *A* and *B* interstitial species generated by irradiation depend on the defect generation rates. In other words, the defect generation rates enhance the layer growth at the reaction interfaces via the number of interstitial species produced in the target layers. The interstitial diffusivity in this case only depends on irradiation temperature, but interstitial species are generally more mobile at lower temperatures than atoms diffusing via vacancy mechanism.
The rate of growth at the two interfaces, therefore, depends on the densities of interstitial atoms and interstitial diffusivities.

The formation of Pd_2Si, Ni_2Si, Pt_2Si, $CoSi$, and WSi_2 under radiation-induced interstitial mechanism are explained in terms of the results obtained in this study.
The estimated values of interstitial diffusivity of palladium, nickel, platinum, cobalt, tungsten, and silicon in their respective layers are depicted in the headings of Tables 3-14 to 3-18. These values are obtained with eqn. (3.44) using the data shown in Table 3-13; the results of the interstitial diffusivity show that both metal and silicon species actively contribute to the growth process of the silicide layer. This fact is supported by high diffusivity values of both silicon and metal species estimated in each metal-silicon system.
On the other hand, the interstitial densities are very different for these species in their respective layers. The interstitial densities of silicon and metal species are also shown in Tables 3-14 to 3-18.The result obtained from this study shows that the interstitial density of silicon species is higher than that of the metal atoms (palladium, nickel, platinum, cobalt, and tungsten) in their respective silicides.

© University of Pretoria

UNIVERSITEIT VAN PRETORIA
UNIVERSITY OF PRETORIA
YUNIBESITHI YA PRETORIA

The defect generation rate is proportional to the density of interstitial species produced in both metal and silicon layers. The higher the defect generation rate, the greater the number of silicon or metal species that diffuse from their respective interstices to the reaction interfaces. The reaction rate at interfaces metal/silicide and silicide/silicon depends on the density of interstitial species and surface lattice atom at the proximity of these interfaces. The rate limiting step at the interfaces is diffusion. The interfacial controlled growth is totally absent due to the limited number of interstitial atoms (in comparison with surface lattice atoms) at both reaction interfaces.

The silicide grows faster at metal/silicide interface than at the silicide/silicon interface. This is due to the high density of interstitial silicon species at the metal/silicide interface compared to the density of the interstitial metal species at silicide/silicon interface. This deduction is based on the result presented in Tables 3-14 to 3-18.

Table 3-13. Parameters used for estimation of interstitial diffusivity at a temperature of 298 K together with the density of atomic species and *AB* molecule. (Where K_B = 8.617 x 10^{-5} eV and f_i = 5 x 10^{12} s^{-1} [5]).

Atomic species	Interstitial migration energy for atomic species E_i^m (eV)	Estimated value for density of *AB* molecule (10^{28} molecule/m^3) n_{ab}	Density of atomic species (10^{28} atoms/m^3) $n^0_{a(b)}$	Lattice constant a (10^{-10} m)
Pd	0.148 [60]	Pd_2Si, (2.400)	*Pd*, (6.800)	3.890
Ni	0.150 [46]	Ni_2Si, (3.300)	*Ni*, (9.140)	3.520
Pt	0.063 [46]	Pt_2Si, (2.300)	*Pt*,(6.500)	3.920
Si	0.180 [61]		*Si*, (5.000)	5.430
W	0.054 [46]	WSi_2, (2.300)	*W*,(6.300)	3.160
Co	0.100 [60]	*CoSi*, (2.600)	*Co*, (9.100)	2.510

© University of Pretoria

Table 3-14. Estimation of speed of growth, the rate of reaction, and interstitial density of palladium and silicon species in their respective layers. (Interstitial diffusivities of palladium and silicon are estimated as 2.38 x 10^{-10} m²/s and 1.33 x 10^{-10} m²/s respectively using eqn. (3.44))

$dh_{A(t)}/dt$ (10^{-9} m/s)	$dh_{B(t)}/dt$ (10^{-12} m/s)	R_a (10^{19} /m²s)	R_b (10^{16}/m²s)	K (dpa/s)	γ (10^{-30} m⁴/s)	n_i^a (Pd) (10^{18}atoms/m³)	n_i^b (Si) (10^{22}atoms/m³)
0.267	0.578	0.636	1.375	10^{-9}	11.000	0.095	0.039
0.601	1.310	1.430	3.115	10^{-8}	6.430	0.952	0.390
1.736	3.780	4.133	9.000	10^{-7}	2.543	9.524	3.900

Table 3-15. Estimation of speed of growth and reaction rate of Ni_2Si layer with the interstitial density of nickel and silicon species in their respective layers. (Interstitial diffusivities of nickel and silicon are estimated as 1.8 x 10^{-10} m²/s and 1.33 x 10^{-10} m²/s respectively using eqn. (3.44))

$dh_{A(t)}/dt$ (10^{-10}m/s)	$dh_{B(t)}/dt$ (10^{-13} m/s)	R_a (10^{18}/m²s)	R_b (10^{15}/m²s)	K (dpa/s)	γ (10^{-30} m⁴/s)	n_i^a (Ni) (10^{19}atoms/m³)	n_i^b (Si) (10^{22} atoms/m³)
0.326	1.023	0.989	0.310	10^{-9}	18.850	0.010	0.039
0.832	2.650	2.520	0.802	10^{-8}	5.450	0.101	0.390
1.944	6.211	5.890	1.882	10^{-7}	2.278	1.011	3.900

© University of Pretoria

UNIVERSITEIT VAN PRETORIA
UNIVERSITY OF PRETORIA
YUNIBESITHI YA PRETORIA

Table 3-16. Estimation of interstitial density of platinum and silicon species in their respective layers together with the speed of growth and reaction rate of the Pt_2Si layer. (Interstitial diffusivities of platinum and silicon are estimated as 6.61 x 10^{-9} m^2/s and 1.33 x 10^{-10} m^2/s respectively using eqn. (3.44))

$dh_{A(t)}/dt$ (10^{-9} m/s)	$dh_{B(t)}/dt$ (10^{-12} m/s)	R_a (10^{19} /m^{2}s)	R_b (10^{16}/m^{2}s)	K (dpa/s)	γ (10^{-30}m^4/s)	n_i^a (Pt) (10^{18}atoms/m^3)	n_i^b (Si) (10^{22}atoms/m^3)
0.323	0.993	0.918	1.739	10^{-9}	15.93	0.098	0.039
0.866	1.715	1.862	5.678	10^{-8}	8.315	0.983	0.390
1.910	4.133	4.476	9.524	10^{-7}	2.832	9.834	3.900

Table 3-17. Estimation of interstitial density of cobalt and silicon species, the speed of growth and reaction rate of $CoSi$ layer. (Interstitial diffusivities of cobalt and silicon are estimated as 6.41 x 10^{-10} m^2/s and 1.33 x 10^{-10} m^2/s respectively using eqn. (3.44))

$dh_{A(t)}/dt$ (10^{-9} m/s)	$dh_{B(t)}/dt$ (10^{-12}m/s)	R_a (10^{19}/m^{2}s)	R_b (10^{16}/m^{2}s)	K (dpa/s)	γ (10^{-30}m^4/s)	n_i^a (Co) (10^{18} atoms/m^3)	n_i^b (Si) (10^{22}atoms/m^3)
0.260	0.734	0.850	1.468	10^{-9}	12.000	0.076	0.039
0.670	1.547	1.677	3.793	10^{-8}	5.900	0.760	0.390
1.800	3.890	4.290	9.342	10^{-7}	1.400	7.600	3.900

© University of Pretoria

UNIVERSITEIT VAN PRETORIA
UNIVERSITY OF PRETORIA
YUNIBESITHI YA PRETORIA

Table 3-18. Estimation of interstitial density of tungsten and silicon species in their respective layers together with the speed of growth and reaction rate of the WSi_2 layer. (Interstitial diffusivities of tungsten and silicon are estimated as 6.10×10^{-9} m²/s and 1.33×10^{-10} m²/s respectively using eqn. (3.44))

$dh_{A(t)}/dt$ (10^{-10} m/s)	$dh_{B(t)}/dt$ (10^{-13}m/s)	R_a (10^{18}/m²s)	R_b (10^{15}/m²s)	K (dpa/s)	γ (10^{-30} m⁴/s)	n_i^a (W) (10^{18} atoms/m³)	n_i^b (Si) (10^{22} atoms/m³)
0.538	1.248	1.127	0.646	10^{-9}	86.900	0.021	0.039
1.030	2.894	2.769	1.108	10^{-8}	36.000	0.210	0.390
2.211	6.583	7.816	2.153	10^{-7}	15.000	2.100	3.900

Reaction rate depends on defect generation rate. If the defect generation rate is high, more interstitial atoms leave their interstices and diffuse via the interstitial mechanism to the reaction interface. The defect generation rate, from this viewpoint, enhances the rate of silicide formation at both metal/silicide and silicide/silicon interfaces by increasing the chances of silicide formation at the two interfaces.

This theoretical study shows that interstitial diffusivity of metal and silicon species remain invariant at different defect generation rates in contrast to vacancy diffusivity. However, the density of interstitial species changes significantly as the defect generation rate rises in the irradiated layers.

© University of Pretoria

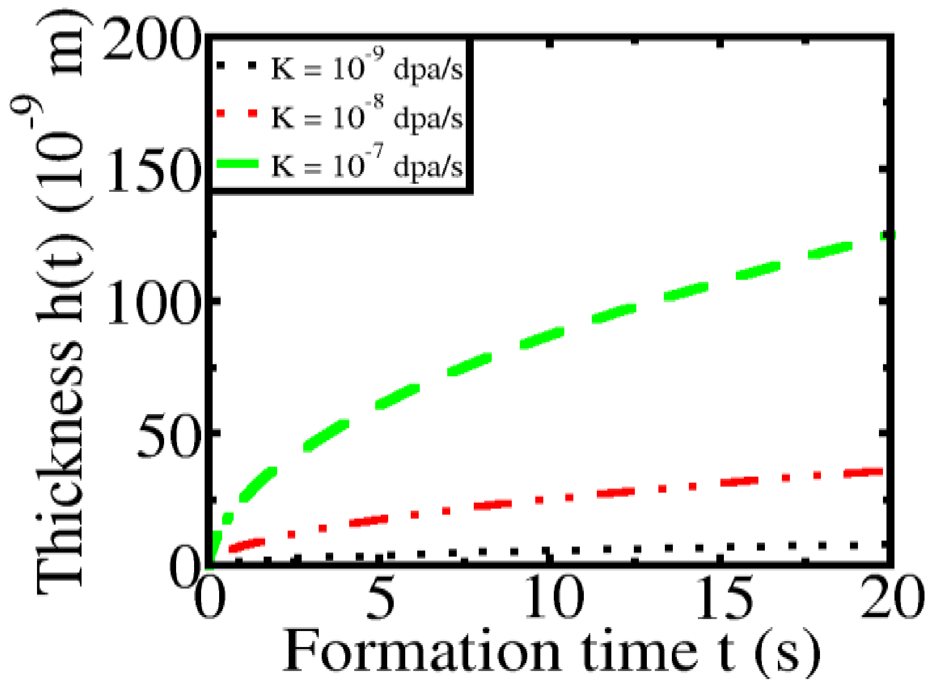

Figure 3-9: The growth kinetics of palladium silicide Pd_2Si at room temperature under the influence of radiation-induced interstitial at defect generation rates of $K = 10^{-9}$, 10^{-8} and 10^{-7} dpa/s.

© University of Pretoria

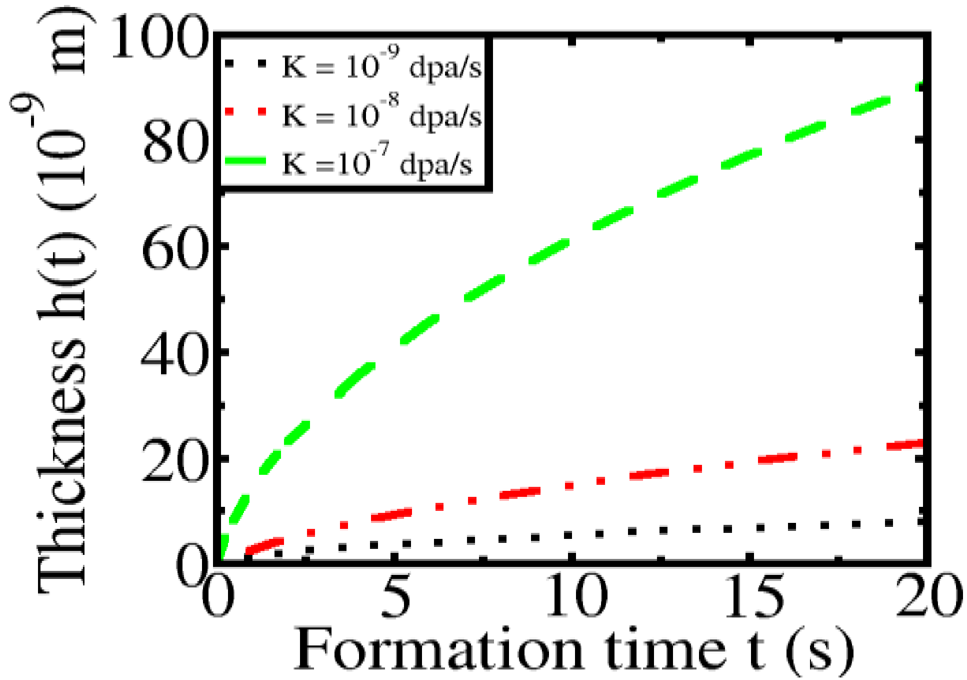

Figure 3-10: The growth kinetics of nickel silicide *Ni_2Si* at room temperature under the influence of radiation-induced interstitial at defect generation rates of K = 10^{-9}, 10^{-8} and 10^{-7} dpa/s.

© University of Pretoria

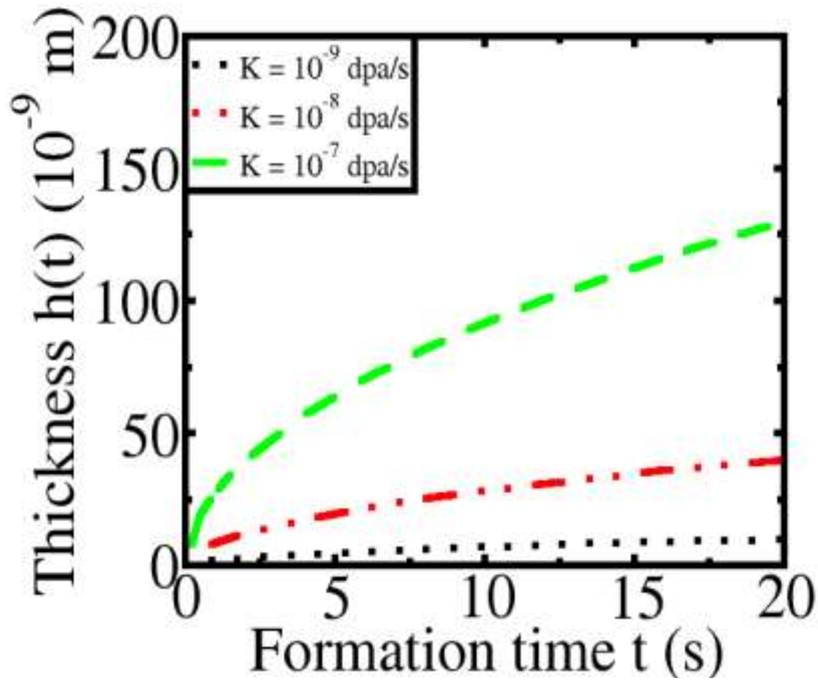

Figure 3-11: The growth kinetics of platinum silicide Pt_2Si at room temperature under the influence of radiation-induced interstitial at defect generation rates of $K = 10^{-9}$, 10^{-8} and 10^{-7} dpa/s.

© University of Pretoria

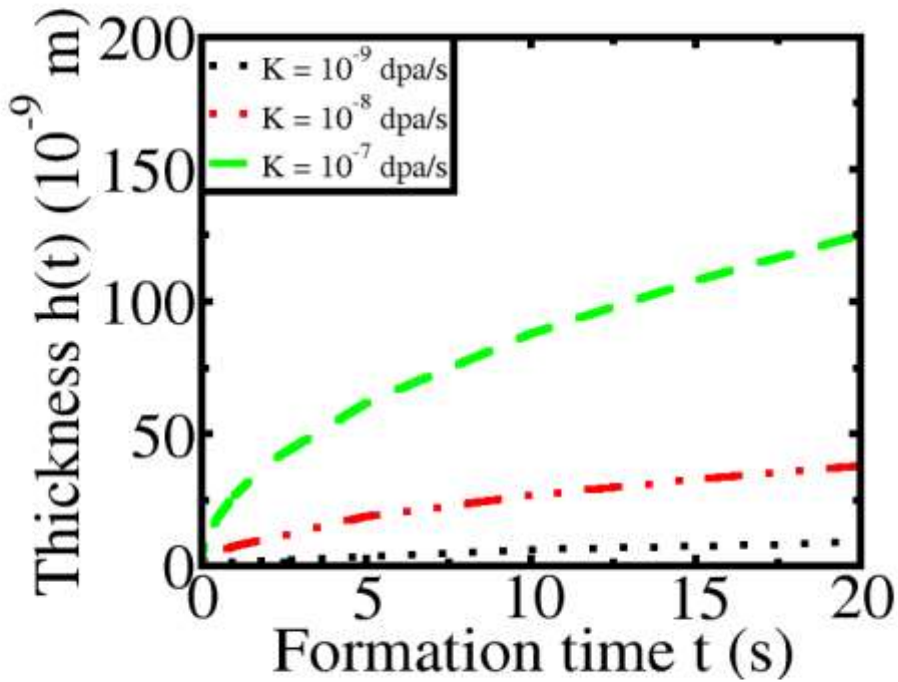

Figure 3-12: The growth kinetics of cobalt silicide *CoSi* at room temperature under the influence of radiation-induced interstitial at defect generation rates of $K = 10^{-9}$, 10^{-8} and 10^{-7} dpa/s.

© University of Pretoria

UNIVERSITEIT VAN PRETORIA
UNIVERSITY OF PRETORIA
YUNIBESITHI YA PRETORIA

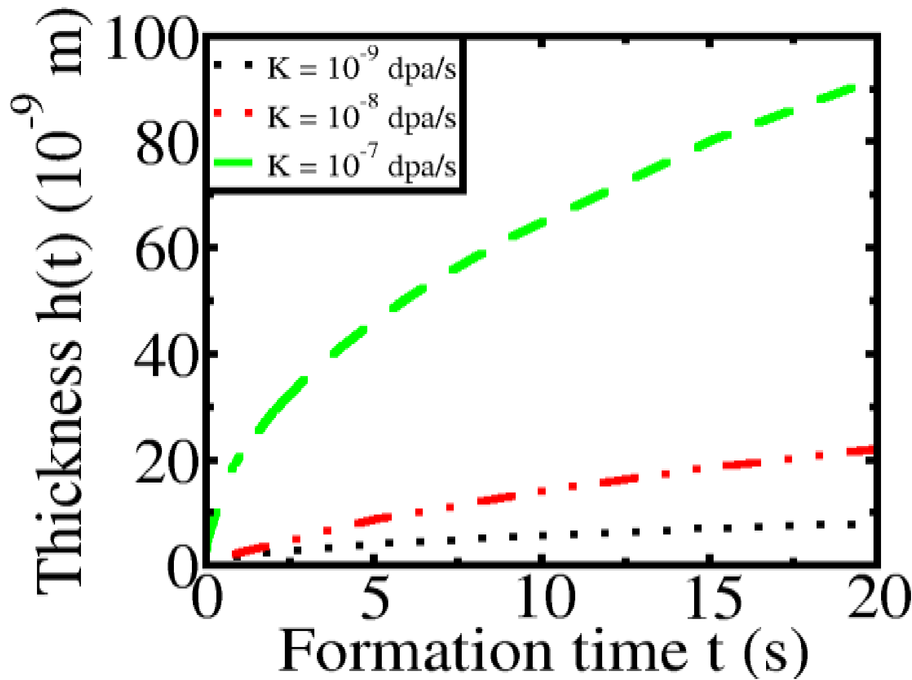

Figure 3-13: The growth kinetics of tungsten disilicide *WSi_2* at room temperature under the influence of radiation-induced interstitial at defect generation rates of $K = 10^{-9}$, 10^{-8} and 10^{-7} dpa/s.

The results that are shown in Figures 3-9 to 3-13 depict the dependence of silicide layer thickness on the defect generation rates. As we can clearly see that the higher the defect generation rate, the thicker the silicide layer become at constant temperature and at invariant interstitial diffusivity. The layer thickness is estimated with eqn. (3.50) together with the results presented in Tables 3-14 to 3-18. A parabolic growth relationship is shown between time and layer thickness and this is because the growth process is predominantly controlled by diffusion.

The room temperature considered in this work can neither provide sufficient thermal energy that can overcome the metallic bond in metal nor covalent bond in silicon for the silicide formation process to get started in the metal-silicon system.

© University of Pretoria

UNIVERSITEIT VAN PRETORIA
UNIVERSITY OF PRETORIA
YUNIBESITHI YA PRETORIA

In other words, this process would not have taken place in the absence of irradiation at such a low temperature as room temperature.

There are experimental reports that confirm the feasibility of silicide formation at such low-temperature irradiation for both near noble and refractory metal silicides [12, 15, 39, and 62]. It is experimentally confirmed in [14] that the dominant mechanism for the silicide formation under irradiation is radiation enhanced diffusion; this experimental fact corroborates the results presented in this work.

However, the actual type of radiation enhanced diffusion responsible for the silicide formation process was not identified in the report.

In this study, it is shown that radiation-induced interstitial is the dominant mechanism for the compound layer formation at a low-temperature under irradiation. The results in Tables 3-19 to 3-23 confirm this claim. We can see that the estimated interstitial diffusivity of palladium, nickel, platinum, cobalt, tungsten and silicon at room temperature is far greater than the interdiffusion coefficient of these silicides under a non-irradiation process. For example, interdiffusion coefficient for cobalt silicide is 2.3×10^{-17} m^2/s at 773 K [9] and tungsten disilicide has interdiffusion coefficient of 5.0×10^{-17} m^2/s at 1223 K [63].

With a beam of radiation particles overcoming the covalent bond in silicon and metallic bond in metal, metal and silicon species have a greater chance of diffusing fast under interstitial mechanisms to the reaction interfaces. At the reaction interfaces, these species can chemically interact with each other to formed silicide at low temperature.

3.5 Conclusion

The results of this theoretical study show that the influence of heating under irradiation cannot accelerate the growth of the compound layer in a bilayer system. The estimated temperatures associated with the heating process are extremely low to activate the diffusion of atoms inside the reactant layers. The diffusion coefficient of reactant species remains practically the same as diffusivity at immediate surrounding temperature, such as room temperature.

© University of Pretoria

If radiation heating cannot activate diffusion process in the irradiated layers, therefore, atoms remain in their respective layers. The chance of the compound layer formation at the reaction interfaces becomes zero. This study shows that radiation induced heating in the irradiated materials under consideration is not a viable process for the formation of thin film of the compound layer.

However, the radiation-induced defect generation is shown to be an effective mechanism for the compound layer formation under the thin film consideration. The results of this study show that the diffusivity of atoms is directly proportional to the defect generation rate in each irradiated layer under a vacancy induced mechanism.

The established relation between diffusivity and defect generation rate give room for a substantial number of atoms to diffuse via the vacant sites created by irradiation in the reactant lattices. The diffusion of atoms to the reaction interfaces via vacancy mechanism increases the chance of chemical transformation between the reactant species at the reaction sites; this evidently shows the feasibility of the compound layer growth at the interfaces of the bilayer system. It is shown in this work that the growth kinetics of the compound layer due to the radiation-induced vacancy mechanism at low temperature is practically the same as that of the non-irradiation process at high temperature.

The interstitial induced mechanism also shows the effectiveness of radiation-induced defect as a viable process for the formation of the thin film of the compound layer. The formation process is equally enhanced under extremely low-temperature condition by defect generation rate.

© University of Pretoria

UNIVERSITEIT VAN PRETORIA
UNIVERSITY OF PRETORIA
YUNIBESITHI YA PRETORIA

CHAPTER 4

SUMMARY, CONCLUSION, AND RECOMMENDATION

In this research study, we conduct a theoretical study on the formation of an AB compound layer at the interface(s) of two immiscible solid materials under irradiation and non-irradiation process. The influence of irradiation is being examined under the most important aspects of irradiation process, such as radiation heating and defects production (vacancies and interstitial atoms).

To describe the formation of an *AB* compound layer under irradiation, a new theoretical model is developed via kinetics of diffusion and chemical reaction. Unlike previous models, this one gives a unified approach to the phenomenon discussed in this study. Our approach allows us to examine the growth of *AB* layer as under and without irradiation.

It has been shown that irradiation accelerates the growth of an *AB* layer by enhancing all the thermo-activated processes and creates new diffusion mechanisms via defect production.

It has been determined that there are joint properties of the kinetics of an *AB* layer growth under and without irradiation. Namely, the growth of *AB* compound layer can occur in qualitatively different ways (regimes) each of them consist of different stages. This is a consequence of dependence of chemical transformation rate on reactant densities. The number of growth stages and sort of each of them depends on the ratio between reactant densities at interfaces and on the number of kind of diffusing atoms.

It has been shown that if there are mobile atoms of one kind, there can be two different regimes of *AB* layer growth. The necessary condition for the first regime of the growth stages is the presence of an excess of diffusing atoms at the respective interfaces.

© University of Pretoria

The first growth regime always starts as a linear function of time and continues as long as there is an excess of diffusing atoms at the interface. After that, the linear stage is changed to parabolic. The second growth regime has only a parabolic stage.

We have obtained explicit expressions for the distribution of *A* and *B* atoms, the rate of *AB* compound growth, and for the dependence of the thickness of *AB* layer on time. The time, at which the linear stage is changed to parabolic, as well as the corresponding thickness of this time has been found. For example, the thickness of cobalt silicide layer (Co_2Si) is found to be 66 nm at the moment the growth stage changes from linear to parabolic at a time of 44 s.

Depending on conditions (parameters of the model), the duration of the linear stage is in the range of few tens of seconds. The thickness of AB layer obtained within this time interval ranges within several tens of nanometers during the linear stage.

It has been shown that contribution of two kinds of mobile atoms does not change the number of growth regimes and the number of stages in each regime. However, the functions that describe the change of the AB layer thickness with time, become more complex. These functions have been obtained as implicit ones for each stage. They turn into linear or parabolic as limiting cases. Duration of the first stage decreases. The thickness of AB layer reaches hundreds of nanometers at the end of this stage.

The influence of radiation heating accelerates all thermo-activated processes and change of diffusion fluxes because heating of different materials under irradiation are different. The influence of radiation heating on the growth of the AB layer is significant when the irradiated sample size is in the order of several thousand of nanometers. In few tens of nanometers, its contribution is negligible.

Irradiation gives growth new mechanisms of diffusion due to the production of different kind of mobile defects. This results in an increase of the rate of AB layer growth. Influence of defect production is especially important under low temperature when thermal diffusivity is “frozen”.

© University of Pretoria

The obtained theoretical results are compared with the experimentally observed dependence of the AB layer growth on time. Theoretical and experimental results are in good agreement.

Thus the obtained results show that qualitative diversity (changes) of growth kinetics of AB layer is determined by the dependence of chemical transformation rate on reactant densities.

At the same time, the diffusion of A and (or) B atoms through the AB layer is a necessary condition for its growth. Irradiation accelerates growth and makes its kinetics more complex due to the generation of new mechanisms of diffusion due to radiation-induced defects.

In future, we plan to include the simultaneous formation of two or more compound layers at the interfaces of two immiscible solid layers under both irradiation and non-irradiation process into our study. The influence of complex radiation-induced process, such as the interstitial and vacancy cluster generation process on the formation of thin film of the compound layer will also be investigated. The growth kinetics of the compound layers formed from these processes will be compared with that of the experiment in order to establish a concrete agreement between the theoretical approach and empirical evidence.

© University of Pretoria

UNIVERSITEIT VAN PRETORIA
UNIVERSITY OF PRETORIA
YUNIBESITHI YA PRETORIA

REFERENCES

[1] VLSI Electronics Microstructure Science Volume 6 Materials and Process Characterization, Edited by N.G. Einspruch and G.B. Larrrabee, Academic Press, A subsidiary of Harcourt Brace Jovanovich, Publishers New York, America 1983, p. 599. ISBN: 978-0-122-34106-9.

[2] S.P. Murarka, "Silicides for VLSI Applications." Academic Press, New York, 1983. ISBN: 9780125112208.

[3] V.E. Borisenko and P.J. Hesketh, "Rapid Thermal Processing of Semiconductors," Plenum, New York, Chapt. 6, 1997, p. 194.

[4] A. Portavoce, K. Hoummada, and F. Dahlem, *Surf. Sci.* **624**, 135 (2014). Doi: 10.1016/j.susc.2014.02.011.

[5] C.N. Whang, H.K. Kim, R.Y. Lee, and R.J. Smith, *J. Mater. Sci.* **24**, 270 (1989).

[6] V. Sisodia, K.B. Sapnar, and S. Dhole, *Arch. Phy. Res.* **2**, 54 [2011].

[7] R.W. Bower and D. Sigurd, *Solid State Electron*. **16,** 1461 (1973).

[8] F. Nemouchi, D. Mangelinck, C. Bergman, and P. Gas, *Appl. Phys. Lett.* **86**, 041903 (2005). Doi: 10.1063/1.1852727.

[9] T. Barge, P. Gas, F.M. d'Heurle, *J. Mater. Res.* **10**, 1134 (1995). Doi: 10.1557/JMR.1995.1134.

[10] T. Stark, H. Grunleitner, M. Hundhausen, and L. Ley, *Thin Solid Films* **358**, 73 (2000). Doi: 10.1016/S0040-6090(99)00699-9.

[11] M. Matsuoka, J.F.D. Chubaci, J.P. Biersack, S. Watanabe, N. Kuratani, and K. Ogata, *Radiat. Eff. Defects Solids* **143**, 65 (1997). Doi: 10.1080/10420159708212949.

[12] B.R. Chakraborty, S.K. Halder, N. Karar, D. Kabiraj, and D.K. Avasthi, *J. Phys. D: Appl. Phys.* **38**, 2836 (2005).

[13] G. Agarwal, V. Kulshrestha, P. Sharma, and L.P. Jain, *J. Colloid Interface Sci.* **351**, 570 (2010). Doi: 10.1016/j.jcis.2010.07.055.

© University of Pretoria

[14] A. Arranz, C. Palacio, *Thin Solid Films* **517**, 2656 (2009).

[15] S.Tamulevicius, L.Pranevicius , Budinavicius *J. Appl. Surf. Sci.* **53,** 159 (1991).

[16] F.M. d'Heurle and P. Gas, *J. Mater. Res.* **1**, 205 (1986).

[17] J. Philibert, *Appl. Surf. Sci.* **53**, 74 (1991).

[18] U. Gosele and K.N. Tu, *J. Appl. Phys.*, **53,** 3252 (1982).

[19] V.I. Dybkov, '*Solid State Reaction Kinetics'.* IPMS Publication, Kyiv 2013. ISBN: 978-966-02-6762-6.

[20] A.S. Wakita, T.W. Sigmon, and J.F. Gibbons, *J. Appl. Phys.* **54**, 2711 (1983). Doi: 10.1063/1.332296.

[21] G. Majni, F. Nava, G. Ottaviani, A. Luches, V. Nassisi, G. Celotti, *Vacuum* **32**, 11 (1982).

[22] E.C. Zingu, J.W. Mayer, C.M. Comrie, and R. Pretorious, *Phys. Rev. B* **30**, 5916 (1984). Doi: 10.1103/PhysRevB.30.5916.

[23] L.S. Hung, J.W. Mayer, C.S. Pai, and S.S. Lau, *J. Appl. Phys.* **58**, 1527 (1985). Doi: 10.1063/1.336086.

[24] J.P. Ponpon and A. Saulnier, Semicond. *Sci. Technol.* **4**, 526 (1989). Doi: 10.1088/0268-1242/4/7/005.

[25] C.Y. Ting, "Silicide for Contact and Interconnects" in IEDM, 1984, pp. 110-113.

[26] R. Schmid and V.N. Sapunov, "*Non-formal kinetics."* Verlag Chemie GmbH, Weinheim, Germany, 1982, p 264.

[27] J. Lajzerowicz, Jr., J. Torres, G. Goltz, and R. Pantel, *Thin Solid Films* **140**, 23 (1986). Doi: 10.1016/0040-6090(86)90155-0.

[28] K.N. Tu, J.F. Ziegler, and C.J. Kircher, *Appl. Phys. Lett.* **23**, 493 (1973).

[29] D. Mangelinck, K. Hoummada, F. Panciera, M. El Kousseifi, I. Blum, M. Descoins, M. Bertoglio, A. Portavoce, C. Perrin, and M. Putero, *Phys. Status Solidi A* **211**,152 (2014). Doi: 10.1002/Pssa.201300167.

[30] D. Mangelinck, K. Hoummada, and I. Blum, *Appl. Phys. Lett.* **95**, 1902 (2009).

© University of Pretoria

UNIVERSITEIT VAN PRETORIA
UNIVERSITY OF PRETORIA
YUNIBESITHI YA PRETORIA

[31] W.K. Chu, S.S. Lau, J.W. Mayer, H. Muller, and K.N. Tu, *Thin Solid Film* **25**, 393 (1975). Doi: 10.1063/1.1655546.

[32] H. Foll and P.S. Ho, *J. Appl. Phys.* **52**, 5510 (1981). Doi: 10.1063/1.329533.

[33] R. Pretorius, C.L. Ramiller, and M.A, *Nucl. Instrum. Methods* **149**, 629 (1978). Doi: 10.1016/0029-554X (78)90941-2.

[34] Wittmer and K.N. Tu, *Phys. Rev. B* **27**, 1173 (1983). Doi: 10.1103/Phys. RevB.27.1173.

[35] J.E.E. Baglin, F.M. d'Heurle, W.N. Hammer, and S. Petersson, *Nucl. Instrum. Methods* **168**, 491 (1980).

[36] A.P. Botha and R. Pretorius, *Thin Solid Films* **93**, 127 (1982).

[37] J. Farmer, M.A.E. Wandt and R. Pretorious, *Appl. Phys. Lett*. **56,** 17 (1990).

[38] L.J. Qiang, W.Z. Lie, D.X. Liang, and C.F. Zhai, *Vacuum* **39,** 275 (1989). Doi: 10.1016/0042-207X(89)90217-0.

[39] N. Boussaa, A. Guittoum, S. Tobbeche, *Vacuum*. **77,** 125 (2005).

[40] E. D'anna, G. Leggieri, and A. Luches, *Thin Solid Films* **140**, 163 (1986).

[41] G. S. Was, "*Fundamentals of Radiation Materials Science*." Springer Berlin Heidelberg New York 2010, p.827. ISBN: 978-3-540-49471-3.

[42] F.H. Attix, "*Introduction to Radiological Physics and Radiation Dosimetry*." Wiley-VCH Verlag GmbH & Co. KGaA, Weinheim Germany 2004, p. 624. 1SBN-13: 978-0-471-01146-0

[43] B. Bogdanovitch, V. Senioukov, A. Koroliov, and K. Simonov, Proceedings of the 1999 Particle Accelerator Conference, New York 1999, pp. 2570-2572. ISBN: 0-7803-5573-3

[44] J.P. Biersack, J.F. Ziegler, U. Littmark, J.F. Ziegler (Ed.). The Stopping and Range of Ions in Solids, Series in Electrophysics, Vol. 10, Springer, Berlin (1982), p. 122.

[45] R.A. Swalin, *J. Phys. Chem. Solids* **23**, 154 (1962).

[46] W. Pfeiler, "*Alloy Physics: A comprehensive Reference*" Technology and Engineering, 2008, p. 1003. J. Wiley and Sons, ISBN: 978-3527313214.

© University of Pretoria

[47] H. Matter, J. Winter, and W. Triftshauser, *Appl. Phys.* **20**, 135 (1979).

[48] R.Y. Lee, C.N. Whang, H.K. Kim, and R.J. Smith, *Nucl. Instrum. Methods Phys. Res.* B **33**, 661 (1988). Doi: 10.1016/0168-583X(88)90654-4.

[49] M.J.H. van Dal, D.G.G.M. Huibers, A.A. Kodentsov, F.J.J. van Loo, *Intermetallics* **9**, 409 (2001). Doi: 10.1016/50966-9795(01)00018-8.

[50] A.P. Botha and S. Kritzinger, *Thin Solid Films* **141**, 41 (1986).

[51] R. Soumitra, P. Aloke, *Intermetallics* **37**, 83 (2013).

[52] A.D. Vasilyev, *Thin Solid Films.* **289**, 205 (1996).
Doi: 10.1016/S0040-6090(96)08932-8

[53] D.A. Hughes and N. Hansen, *Acta Mater.* **48**, 2993 (2000).

[54] A. Cizek, F. Parizek, A. Orlova, and J. Tousek, *Czech. J. Phys.* B **20**, 56 (1970).

[55] J.M. Po, D.M. Pera, M.C. Brito, J.M. Alves, and A.M. Vallera, *EU PVSEC Proceedings*, 722-724 (www.eupvsec-proceedings.com/proceedings?paper=30804).

[56] G.K. Williamson, R.E. Smallman, *Phil Mag.* **1**, 34 (1956).
Doi: 10.1080/14786435608238074.

[57] P.C. Riedi and T. Dumelow, *Phys. B* **36**, 4595 (1987).

[58] T.R. Mattsson and A.E. Mattsson, *Phys. Rev. B* **66**, 214110 (2002).
Doi: 10.1103/PhysRevB.66.214110.

[59] N.Q. Lam, K. Janghorban and A.J. Ardell, *Ibid* **101,** 314 (1981).
Doi: 10.1016/0022-3115(81)90173-2.

[60] Physical Metallurgy Volume 1 5th Edition, Edited by D.E. Laughlin and K. Hono, Elsevier Amsterdam, Netherland 2014, p. 566. ISBN: 978-0-444-59598-0.

[61] W.K. Leung, R.J. Needs, G. Rajagopol, S. Itoh, S. Ihara, *Phys. Rev. Lett.* **83**, 2351 (1999). Doi: 10.1103/PhysRevLett.83.2351.

[62] G. Gawlik, J. Jagielski, *Vacuum* **83**, S111 (2009).
Doi: 10.1016/j.vacuum.2009.01.038.

© University of Pretoria

[63] H. Jehn, Gmelin Handbook of Inorganic and Organometallic Chemistry 8th Edition, Tungsten Supplement Volume A 5b Metal, Chemical Reaction with Non-metals, Edited by J. Von Jouanne, E. Koch, and E. Koch, Springer-Verlag Berlin Heidelberg GmbH, 1993, p. 189.

© University of Pretoria

UNIVERSITEIT VAN PRETORIA
UNIVERSITY OF PRETORIA
YUNIBESITHI YA PRETORIA

Appendix

Articles

© University of Pretoria

UNIVERSITEIT VAN PRETORIA
UNIVERSITY OF PRETORIA
YUNIBESITHI YA PRETORIA

Results in Physics 6 (2016) 43–47

Contents lists available at ScienceDirect

Results in Physics

journal homepage: www.journals.elsevier.com/results-in-physics

Kinetics of growth of thin-films of Co_2Si, Ni_2Si, WSi_2 and VSi_2 during a reactive diffusion process

S.O. Akintunde *, P.A. Selyshchev

Department of Physics, University of Pretoria, Private Bag X20, Hatfield 0028, South Africa

ARTICLE INFO

Article history:
Received 16 December 2015
Accepted 14 January 2016
Available online 22 January 2016

Keywords:
Thin-film
Reaction controlled
Diffusion limited
Critical thickness
Critical time

ABSTRACT

A theoretical approach is developed which describes the growth kinetics of thin films of near noble metal silicide (especially of cobalt silicide (Co_2Si) and nickel silicide (Ni_2Si)) and refractory metal silicide (particularly of tungsten disilicide (WSi_2) and vanadium disilicide (VSi_2)) at the interfaces of *metal–silicon* system. In this approach, metal species are presented as *A*-atoms, silicon as *B*-atoms, and silicide as *AB*-compound. The *AB*-compound is formed as a result of chemical transformation between *A*- and *B*-atoms at the reaction interfaces *A*/*AB* and *AB*/*B*. The growth of *AB*-compound at the interfaces occurs in two stages. The first growth stage is reaction controlled stage which takes place at the interface with excess *A* or *B*-atoms and the second stage is diffusion limited stage which occurs at both interfaces. The critical thickness of *AB*-compound and the corresponding time is determined at the transition point between the two growth stages. The result that follows from this approach shows that the growth kinetics of any growing silicides depends on the number of kinds of dominant diffusing species in the silicide layer and also on their number densities at the reaction interface. This result shows a linear-parabolic growth kinetics for WSi_2, VSi_2, Co_2Si, and Ni_2Si and it is in good agreement with experiment.

© 2016 The Authors. Published by Elsevier B.V. This is an open access article under the CC BY-NC-ND license (http://creativecommons.org/licenses/by-nc-nd/4.0/).

Introduction

The thin film of near noble and refractory metal silicides gained wide attention in solid state reaction because of their applicability as low resistance contacts, gate electrodes, and interconnect materials in integrated circuit technology [1–3].

A number of works in the literature report the formation and growth kinetics of these silicides [4–7]. Silicide formation can be explained from two approaches: diffusion approach (which is considered as the conventional approach) and physicochemical approach (alternative approach to the former). From diffusion approach silicides are formed as a result of intermixing of silicon with metal species after the diffusion of either silicon atoms into the metal layer or metal atoms into the silicon layer. This intermixing is initiated by heat treatment process. Diffusion approach usually leads to loss of reaction controlled stage [8] due to lack of consideration for chemical reaction between metal and silicon species.

Unlike diffusion approach, physicochemical approach incorporates two processes: diffusion and chemical reaction. It describes metal and silicon layers as two immiscible layers with interface(s) separating them. Chemical reaction takes place between silicon and metal atoms at the interface(s). The metal atoms or silicon atoms or both are brought to the interface(s) by means of diffusion. This approach creates room for the possibility of accounting for chemical reaction contributions to the silicide growth during reaction controlled stage.

It is shown that the growth kinetics of silicides of near noble metals (for example, palladium, platinum, and cobalt) obey parabolic law [4–6] and the dominant atomic species in the first silicide phase (such as Ni_2Si, Pt_2Si, and Co_2Si) are unanimously identified as metal [2,7]. Metal species are reported as dominant species because the silicide is a metal rich silicide. However, there are different viewpoints on dominant species in the Pd_2Si phase [9–13].

In refractory metal silicides (such as molybdenum disilicide ($MoSi_2$), titanium disilicide ($TiSi_2$), tungsten disilicide (WSi_2), and vanadium disilicide (VSi_2)) the dominant diffusing species is reported as silicon [2–7]. This is due to the richness of this silicide phase in silicon. There are different growth kinetics exhibited by silicide in this phase [2,6–7]. For instance, in VSi_2 and WSi_2 growth kinetics are described as linear and parabolic, in $TiSi_2$ it's delineated as parabolic, and in $MoSi_2$ and $CrSi_2$ it is shown to be linear.

* Corresponding author.
E-mail addresses: samuel.akintunde@up.ac.za (S.O. Akintunde), selyshchev@gmail.com (P.A. Selyshchev).

http://dx.doi.org/10.1016/j.rinp.2016.01.006
2211-3797/© 2016 The Authors. Published by Elsevier B.V.

This is an open access article under the CC BY-NC-ND license (http://creativecommons.org/licenses/by-nc-nd/4.0/).

© University of Pretoria

UNIVERSITEIT VAN PRETORIA
UNIVERSITY OF PRETORIA
YUNIBESITHI YA PRETORIA

UNIVERSITEIT VAN PRETORIA
UNIVERSITY OF PRETORIA
YUNIBESITHI YA PRETORIA

Department of Physics

In this paper, we present a model that describes the growth kinetics of the *AB*-compound layer based on the first approximation of reaction rate as product of reactant number densities. This approximation is in accord with mass action law. The speed of growth is proportional to reaction rate during the reaction controlled and diffusion limited stages. The *AB*-compound layer growth kinetics that follow from this approach show that the growth behavior of the growing layer can be explained from the viewpoint of the number of kinds of atomic species actively diffusing into the *AB*-layer during their formation process.

Model and result

Suppose that the *A*-layer occupies space $x < 0$ and the *B*-layer occupies space $x > 0$ in *A*–*B* system.

At time $t > 0$ heat treatment process commences in *A*- and *B*-layers. The interfaces *A*/*AB* and *AB*/*B* spatially separates *A*- and *B*-layers. *A*-atoms diffuse from the *A*-layer via *AB*-layer into interface *AB*/*B* and *B*-atoms diffuse from the *B*-layer via *AB*-layer into interface *A*/*AB*. At interface *AB*/*B*, diffuse *A*-atoms chemically react with surface *B*-atom to form *AB*-compound. Likewise, at interface *A*/*AB*, diffuse *B*-atoms interact chemically with surface *A*-atoms to form additional *AB*-compound. The *AB*-layer occupies space from $x = -h_a$ to $x = h_b$. The thickness of the compound layer formed at interface *A*/*AB* is denoted by $h_a(t)$ and at interface *AB*/*B* by $h_b(t)$. The total thickness of the *AB*-compound layer formed between *A*- and *B*-layers is designated by $h(t)$; $h(t) = h_a(t) + h_b(t)$ where h_a, h_b, and h are function of time t.

The rate of chemical transformation at interfaces of solid layers depends on number densities of *A* and *B* atoms. If there are excess *A*- or *B*-atoms at the interface, the rate of reaction remains the same with change of number density of *A*-or *B*-atoms [14]. On the other hand if number densities of *A*- and *B*-atoms are approximately equal ($\nu_b n_b \approx \nu_a n_a^0$ or $\nu_a n_a \approx \nu_b n_b^0$), then the rate of *AB*-compound formation can be represented in the first approximation as product of *A*- and *B*-atomic number densities. Where n_a^0 and n_b^0 are number densities of *A*- and *B*-atoms in *A*- and *B*-layers respectively, n_a and n_b are number densities of *A*- and *B*-atoms inside the *AB*-layer, ν_a and ν_b are stoichiometric coefficients of *A*- and *B*-atoms.

Thus the rate of chemical reaction between *A*- and *B*-atoms, at reaction interfaces *A*/*AB* and *AB*/*B* can be approximately expressed in two stages as follows:

$$R_a = \begin{cases} \gamma (n_a^0)^2 = const & \nu_b n_b(-h_a(t)) \geq \nu_a n_a^0 \\ \gamma n_a^0 n_b(-h_a(t)) & \nu_b n_b(-h_a(t)) \leq \nu_a n_a^0 \end{cases}$$
$$R_b = \begin{cases} \gamma (n_b^0)^2 = const & \nu_a n_a(h_b(t)) \geq \nu_b n_b^0 \\ \gamma n_b^0 n_a(h_b(t)) & \nu_a n_a(h_b(t)) \leq \nu_b n_b^0 \end{cases} \tag{1}$$

where $n_b(-h_a(t))$ and $n_a(h_b(t))$ are the number densities of *B*- and *A*-atoms which diffuse into reaction interfaces *A*/*AB* and *AB*/*B*, γ is the reaction rate constant, R_a and R_b are the reaction rates at interfaces *A*/*AB* and *AB*/*B*.

Due to this approximation, the growth of the *AB* layer can be described in two stages. The first growth stage occurs when there are excess of one kind of diffusing atoms, for example, excess *A*-atoms at interface *AB*/*B* or excess *B*-atoms at interface *A*/*AB* and the second growth stage takes place when there are no excesses of any kind of atoms at the corresponding interfaces.

The growth rate of the *AB*-layer is determined by both diffusion of *A*- and *B*-atoms inside the *AB*-layer and rate of reaction at interfaces:

$$\frac{dh}{dt} = \frac{dh_a}{dt} + \frac{dh_b}{dt} = V_{ab}\left(\gamma n_a^0 n_b(-h_a(t)) + \gamma (n_b^0)^2\right). \tag{2a}$$

Eq. (2a) holds only if *A*-atoms are in excess at interface *AB*/*B* or

$$\frac{dh}{dt} = \frac{dh_a}{dt} + \frac{dh_b}{dt} = V_{ab}\left(\gamma (n_a^0)^2 + \gamma n_b^0 n_a(h_b(t))\right). \tag{2b}$$

Eq. (2b) holds only if *B*-atoms are in excess at interface *A*/*AB*, where V_{ab} is the volume of one molecule of *AB*-compound.

Suppose that all *A*-atoms at *AB*/*B* interface and all *B*-atoms at *A*/*AB* interface reacted at once. Therefore the growth of the *AB*-compound layer is determined by flux of *A*-atom toward the *B*-layer and flux of *B*-atom toward the *A*-layer. Thus we consider the diffusion of *A*- and *B*-atoms inside the *AB*-compound layer.

Diffusion of *A*- and *B*-atoms inside the *AB*-layer is described by Fick's second law under a stationary condition thus:

$$D_{a(b)} \frac{\partial^2 n_{a(b)}(x)}{\partial x^2} = 0. \tag{3}$$

With corresponding boundary conditions:

$$J_a(h_b(t)) = -D_a \nabla n_a(x) = \nu_a \gamma n_b^0 n_a(h_b(t)); \quad J_b(-h_a(t)) = -D_b \nabla n_b(x) = \nu_b \gamma n_a^0 n_b(-h_a(t));$$

$$n_a(-h_a(t)) = n_a^0; \quad n_b(h_b(t)) = n_b^0.$$

where J_a and J_b are fluxes of *A*- and *B*-atoms, D_a and D_b are diffusivities of *A*- and *B*-atoms.

Solving Eq. (3) with boundary conditions for the first stage of layer growth (before critical time), we obtain an expression for the distribution of *A*- and *B*-atoms inside the *AB*-compound layer when *A*-atom is in excess at *AB*/*B* interface:

$$n_a(x) = -\frac{\gamma (n_b^0)^2}{D_a}(x + h_a) + n_a^0 \quad \text{and}$$
$$n_b(x,t) = \frac{\gamma n_a^0 n_b^0 \nu_b}{D_b + \gamma n_a^0 \nu_b h(t)}(x - h_b) + n_b^0 \tag{4a}$$

And for excess *B*-atoms at *A*/*AB* interface, the distribution of *A*- and *B*-atoms in the *AB*-layer is described by:

$$n_a(x,t) = \frac{\gamma n_a^0 n_b^0 \nu_a}{D_a + \gamma n_b^0 \nu_a h(t)}(x + h_a) + n_a^0 \quad \text{and}$$
$$n_b(x) = -\frac{\gamma (n_a^0)^2}{D_b}(x - h_b) + n_b^0. \tag{4b}$$

Number densities of *A*-atoms at interface *AB*/*B* and *B*-atoms at interface *A*/*AB* during the second growth stage are:

$$n_a(h_b(t)) = \frac{D_a n_a^0}{D_a + \gamma n_b^0 \nu_a h(t)} \quad \text{and}$$
$$n_b(-h_a(t)) = \frac{D_b n_b^0}{D_b + \gamma n_a^0 \nu_b h(t)}. \tag{5}$$

If there are excess *A*-atoms at reaction interface *AB*/*B* at time $t < t_c$, (t_c, is the critical time), the *AB*-layer at this interface grows under reaction controlled process and at *A*/*AB* interface the growth is diffusion limited and vice versa for excess *B*-atoms at interface *A*/*AB*; therefore, the relationship between time and layer thickness can be found by solving either Eq. (2a) or (2b)

$$t = \frac{h(t)}{\gamma V_{ab} (n_b^0)^2} - \frac{D_b \nu_a^2}{\gamma^2 \nu_b^2 V_{ab} (n_b^0)^3} \ln\left[\frac{\gamma n_a^0 n_b^0 \nu_b^2 h(t)}{D_b (n_a^0 \nu_a + n_b^0 \nu_b)} + 1\right] \tag{6a}$$

or

$$t = \frac{h(t)}{\gamma V_{ab} (n_a^0)^2} - \frac{D_a \nu_b^2}{\gamma^2 \nu_a^2 V_{ab} (n_a^0)^3} \ln\left[\frac{\gamma n_a^0 n_b^0 \nu_a^2 h(t)}{D_a (n_a^0 \nu_a + n_b^0 \nu_b)} + 1\right]. \tag{6b}$$

© University of Pretoria

UNIVERSITEIT VAN PRETORIA
UNIVERSITY OF PRETORIA
YUNIBESITHI YA PRETORIA

UNIVERSITEIT VAN PRETORIA
UNIVERSITY OF PRETORIA
YUNIBESITHI YA PRETORIA

Corresponding solutions to Eqs. (2a) and (2b) are expressed in Eqs. (6a) and (6b) respectively.

However, if there are no excess *A*- or *B*-atoms at the reaction interfaces no reaction controlled growth would occur at either *AB*/*B* or *A*/*AB*-interface and growth at both interfaces would be predominantly diffusion limited at all time.

At critical time t_c, $h(t) = h_c$; $v_a n_a(h_b(t_c)) = v_b n_b^0$ or

$$v_b n_b(-h_a(t_c)) = v_a n_a^0 \tag{7}$$

where $n_a(h_b(t_c)) = \frac{\cdots}{\cdots}$ and $n_b(-h_a(t_c)) = \frac{\cdots}{\cdots}$

Critical thickness, h_c is obtained as follows:

$$h_c = \frac{D_a(n_a^0 v_b - n_b^0 v_b)}{\gamma v_a v_b (n_b^0)^2} \tag{8a}$$

or

$$h_c = \frac{D_b(n_b^0 v_b - n_a^0 v_a)}{\gamma v_a v_b (n_a^0)^2} \tag{8b}$$

Eq. (8a) holds at interface *AB*/*B* under reaction controlled process or Eq. (8b) at *A*/*AB* under the same process. It is worth noting that critical thickness cannot takes place at two interfaces at the same time. It can only occur at the interface that has excess atomic species.

For critical time, substitute $t = t_c$, and $h = h_c$ in Eq. (6a) or (6b)

$$t_c = \frac{h_c}{\gamma V_{ab}(n_b^0)^2} - \frac{D_b v_a^2}{\gamma^2 v_b^2 V_{ab}(n_b^0)^3} \ln\left[\frac{\gamma n_a^0 n_b^0 v_b^2 h_c}{D_b(n_a^0 v_a + n_b^0 v_b)} + 1\right] \tag{9a}$$

or

$$t_c = \frac{h_c}{\gamma V_{ab}(n_a^0)^2} - \frac{D_a v_b^2}{\gamma^2 v_a^2 V_{ab}(n_a^0)^3} \ln\left[\frac{\gamma n_a^0 n_b^0 v_a^2 h_c}{D_a(n_a^0 v_a + n_b^0 v_b)} + 1\right]. \tag{9b}$$

Eq. (9a) is the corresponding critical time of Eqs. (8a) and (9b) is the corresponding critical time of Eq. (8b).

The growth rate of the *AB*-compound layer after critical time (second stage of growth) is described by:

$$\frac{dh(t)}{dt} = \gamma V_{ab}(n_a^0 n_b(-h_a(t)) + n_b^0 n_a(h_b(t))). \tag{10}$$

Substitute Eq. (5) into Eq. (10) and integrate the resulting equation; a connection between time and layer thickness is established:

$$t = t_c + \phi_1(h^2(t) - h_c^2) + \phi_2(h(t) - h_c) - \phi_3 \ln\left[\frac{\phi_4 h(t) + \phi_5}{\phi_4 h_c + \phi_5}\right]. \tag{11}$$

where

$$\phi_1 = \left[2V_{ab}\left[D_b n_b^0 + D_a n_a^0\right]\right]^{-1},$$

$$\phi_2 = \left[(D_a n_a^0)^2 + (D_b n_b^0)^2\right]\left[\gamma V_{ab} n_a^0 n_b^0 \left[D_b n_b^0 + D_a n_a^0\right]^2\right]^{-1},$$

$$\phi_3 = D_a D_b \left[D_a n_a^0 - D_b n_b^0\right]^2 \left[\gamma^2 V_{ab} n_a^0 n_b^0 \left[D_b n_b^0 + D_a n_a^0\right]^3\right]^{-1},$$

$$\phi_4 = \gamma\left[D_b n_b^0 + D_a n_a^0\right], \quad \phi_5 = D_a D_b.$$

The kinetics of the first stage of the growth of the *AB*-compound layer expressed in Eqs. (6a) and (6b) shows time as both partly linear and partly natural logarithmic functions of layer thickness and Eq. (11) depicts time as partly parabolic and partly natural logarithmic functions of thickness. The natural logarithmic function in Eqs. (6a), (6b) and (11) is attributed to the simultaneous diffusion of *A* and *B*-atomic species in the *AB*-compound layer.

It is important to mention that the layer growth kinetic would be linear under reaction controlled process and parabolic under diffusion limited process, if only one kind of atomic species diffuses into the *AB*-compound layer. If, for example, only *A*-atoms diffuse into the *AB*-layer when there are excess of *A*-atom at *AB*/*B* interface during the first stage of growth (reaction controlled growth).

Equation (6a) transforms to a linear equation when $D_b = 0$

$$h(t) = V_{ab}\gamma(n_b^0)^2 t \tag{12a}$$

And Eq. (11) reduces to parabolic equation

$$\gamma v_a n_b^0\left(h^2(t) - h_c^2\right) + 2D_a(h(t) - h_c) - 2\gamma V_{ab} D_a n_a^0 n_b^0 (t - t_c) = 0. \tag{12b}$$

Likewise if only *B*-atom diffuses into the *AB*-layer when there are excess of *B*-atoms at *A*/*AB* interface during the same stage of growth, Eq. (6b) also changes to linear equation when $D_a = 0$

$$h(t) = V_{ab}\gamma(n_a^0)^2 t \tag{13a}$$

And Eq. (11) reduces to parabolic equation

$$\gamma v_b n_a^0\left(h^2(t) - h_c^2\right) + 2D_b(h(t) - h_c) - 2\gamma V_{ab} D_b n_a^0 n_b^0 (t - t_c) = 0. \tag{13b}$$

However, if there are no excess *A*- or *B*-atoms at either *AB*/*B* or *A*/*AB* interface, the first growth stage would be absent. In other words there would be no reaction controlled process and linear growth would not take place. Thus only parabolic growth (diffusion limited growth) would be feasible. Eq. (14a) would hold if there are only *A*-atoms diffusing into the *AB*-layer and Eq. (14b) would also hold if there are only *B*-atoms diffusing into the *AB*-layer under the second stage of growth.

$$\gamma v_a n_b^0 h^2(t) + 2D_a h(t) - 2\gamma V_{ab} D_a n_a^0 n_b^0 t = 0, \tag{14a}$$

$$\gamma v_b n_a^0 h^2(t) + 2D_b h(t) - 2\gamma V_{ab} D_b n_a^0 n_b^0 t = 0. \tag{14b}$$

The growth kinetics of four silicides (WSi_2, VSi_2, Co_2Si, and Ni_2Si) are studied based on the result of this model. The experimental data are taken from the literature [15–18] to determine the inter-diffusion coefficients of silicide layers under conventional furnace annealing process. We assume that the diffusivity of dominant species is the same as that of inter-diffusion coefficient of the growing silicides (since only one kind of species diffuses into the silicide layer). The diffusing species in each silicide layer are shown in Table 1.

The results of inter-diffusion coefficients for four silicides are depicted in Table 2 and they are obtained from Arrhenius equation

Table 1
Useful information on growth kinetics of silicides considered in this study.

AB-compound layer	Diffusing species under annealing condition in *AB*-layer	Formation temperature (K) used in this work	Growth kinetics (from this study)	Growth kinetics (from experiment)
WSi_2	Si [2,7]	1033 [15]	Linear and parabolic	Linear and parabolic [2,7]
VSi_2	Si [2,7]	873 [16]	Linear and parabolic	Linear and parabolic [7]
Co_2Si	Co [2,7]	763 [17]	Linear and parabolic	Parabolic [2,6–7]
Ni_2Si	Ni [2,7]	573 [18–19]	Linear and parabolic	Linear and parabolic [18]

© University of Pretoria

UNIVERSITEIT VAN PRETORIA
UNIVERSITY OF PRETORIA
YUNIBESITHI YA PRETORIA

Department of Physics

Table 2
Data used for silicide layer thickness estimation.

AB-compoundlayer	Inter-diffusion coefficient of *AB*-layer (10^{-17} m²/s)	Reaction rate constant (10^{-38} m⁴/s)	Volume of *AB*-compound per molecule (10^{-29} m³)	Number density of *A*- and *B*-atoms in *A*- and *B*-layers (10^{28} atoms/m³)
WSi_2	1.000 [15]	4.700	4.300	W (6.3), Si (5.0)
VSi_2	0.029 [16]	0.910	4.000	V (5.2), Si (5.0)
Co_2Si	3.000 [17]	1.200	5.000	Co (9.1), Si (5.0)
Ni_2Si	1.100 (estimated)	0.620	3.300	Ni (9.14), Si (5.0)

Table 3
Critical thickness and time of *AB*-layer.

AB-layer	h_c (10^{-9} m)	t_c (s)
WSi_2	0.980	0.124
VSi_2	0.280	0.285
Co_2Si	66.000	44.000
Ni_2Si	47.000	92.000

Table 4
Activation energy and pre-exponential factor.

AB-layer	E_a (eV)	D_0 (m²/s)
WSi_2	3.4 [15]	0.40 (estimated)
VSi_2	2.9 [16]	0.016 (estimated)
Co_2Si	–	–
Ni_2Si	1.5 [18,19]	0.000167 [18,19]

described in Eq. (15) based on the data available on D_0 and E_a in Table 4 at formation temperatures shown in Table 1

$$D_{int} = N_{A(B)} D_{A(B)} = N_{A(B)} D_0 \exp\left(\frac{-E_a}{K_B T}\right). \tag{15}$$

where D_{int} is the inter-diffusion coefficient of the *AB*-layer, $N_{A(B)}$ is the atomic fraction of *A*- or *B*-atoms (which is equal to unity in case of one kind of diffusing species) in the *AB*-layer, D_0 is the pre-exponential factor, E_a is the activation energy, K_B (8.617×10^{-5} eV) is the Boltzmann constant, and T is the absolute temperature.

The layer thickness of WSi_2 and VSi_2 is estimated with Eq. (13a) (for reaction controlled growth) and Eq. (13b) (for diffusion limited growth). The critical thickness between the two growth stages is obtained with Eq. (8b) and the corresponding critical time, t_c (when $D_a = 0$) is estimated with Eq. (9b). In a similar vein, the thickness of Co_2Si and Ni_2Si is obtained from Eq. (12a) (for reaction controlled growth) and Eq. (12b) (for diffusion limited growth). The critical thickness and time are estimated with Eqs. (8a) and (9a) respectively when $D_b = 0$. The results of critical thickness and time of the silicide layers are shown in Table 3. The results show that critical thickness is strongly dependent on the diffusivity of the active moving species in the silicide layer. The higher the diffusing rate of the active species the thicker the thickness becomes at the transition point.

The growth kinetics of four silicides considered in this study reveals a linear-parabolic relationship between layer thickness and time. The linear growth in both WSi_2 and VSi_2 layers is due to the reaction rate dependence on tungsten atomic density at W/WSi_2 interface and vanadium number density at V/VSi_2 interface during reaction controlled stage, while parabolic growth on the other hand is due to reaction rate dependence on both number densities of tungsten and silicon atoms at both interfaces in tungsten–silicon system. The same explanation applies to vanadium–silicon system. Linear growth in the Co_2Si layer occurs as a result of excess cobalt atoms at Co_2Si/Si interface during reaction controlled stage and parabolic growth arises in the Co_2Si layer due to the active diffusion of cobalt as the only moving atoms during diffusion limited stage in the Co_2Si layer. The same explanation holds for linear-parabolic growth in the Ni_2Si layer where nickel is the only active diffusing species.

Due to the small magnitude of layer thickness formed over a very short period of time during reaction controlled growth as shown in Table 3, the linear section of this curve is correspondingly

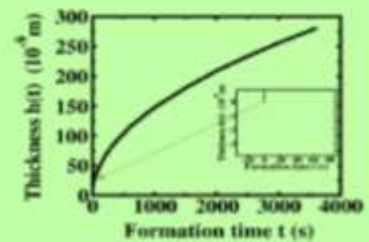

Fig. 1. The growth kinetics of tungsten disilicide (WSi_2) at 1033 K. The dotted arrow shows the linear growth regime of WSi_2 under a reaction controlled process. The estimated time for the linear growth of WSi_2 is 0.124 s. The inserted graph shows the linear section of the curve.

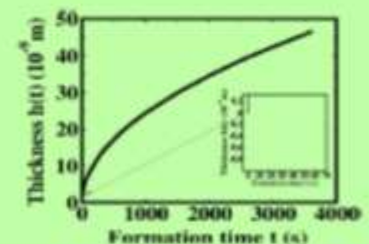

Fig. 2. The growth kinetics of vanadium disilicide (VSi_2) at 873 K. The dotted arrow shows the linear growth region of VSi_2 over an estimated period of 0.285 s. The inserted graph also shows the linear section of the curve which appears parallel to the time axis due to short time involved during the growth process.

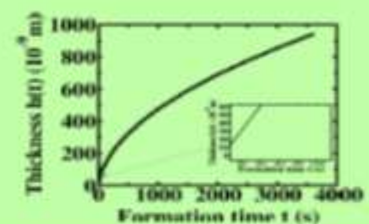

Fig. 3. The growth kinetics of cobalt silicide (Co_2Si) at 763 K. The thin arrow shows the linear growth regime of Co_2Si over a period of 44 s. The inserted graph as well shows the linear section of the curve under a reaction controlled process.

© University of Pretoria

UNIVERSITEIT VAN PRETORIA
UNIVERSITY OF PRETORIA
YUNIBESITHI YA PRETORIA

UNIVERSITEIT VAN PRETORIA
UNIVERSITY OF PRETORIA
YUNIBESITHI YA PRETORIA

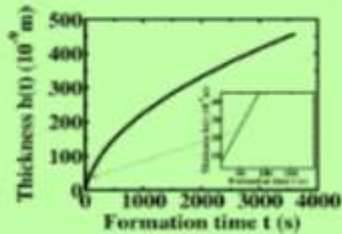

Fig. 4. The growth kinetics of nickel silicide (Ni_2Si) at 573 K. The dotted arrow indicates the linear growth of Ni_2Si over a period of 92 s under a reaction controlled process. The inserted graph also shows the linear section of the curve.

small that the growth kinetics appear to be predominantly parabolic in Figs. 1–4. The silicide growth is considered over a period of 3600 s in all the layers.

Conclusions

The theoretical approach presented here shows that the growth kinetics of any growing silicides can be described in terms of reaction rate between silicon and metal species at the reaction interfaces. This study shows that chemical reaction rate can either depend on silicon density or metal species density or both during the reactive diffusion process. This dependence determines the number of possible growth stages and also responsible for the correlation that arises between time and layer thickness during the growth stages. For example, reaction controlled growth occurs when the reaction rate depends on either silicon or metal species density and the relationship between time and layer thickness during this stage can either be linear or more complex than linear depending on the number of kinds of diffusing species in the silicide layer, however, in diffusion limited growth stage chemical reaction rate relies on both metal and silicon densities at the reaction interface and the link between time and thickness can either be parabolic or more complex than parabolic which also depends on the number of kinds of active moving species in the silicide growing layer.

Acknowledgment

This research work is funded by NRF South Africa.

References

[1] Connetable D, Thomas O. J Alloy Compd 2011;509:2639. [illegible]
[2] Murarka SP. Silicide for VLSI application. New York: Academic Press; 1983. p. 15.
[3] Chen LJ. An integral part of microelectronics, vol. 57. JOM; 2005. p. 24.
[4] Abbes O, Hoummada K, Mangelinck D, Carron V. Thin Solid Films 2013;542:174. [illegible]
[5] Portavoce A, Hoummada K, Dahlem F. Surf Sci 2014;624:135. [illegible]
[6] Mangelinck D, Hoummada K, Blum I. Appl Phys Lett 2009;95:1902.
[7] Borisenko V. Semiconducting silicide. Berlin Heidelberg: Springer Publication; 2011. ISBN 978-3540661115.
[8] Dybkov VI. Solid state reaction. Kyiv: IPMS Publication; 2013. ISBN 978-966-02-6762-6.
[9] Chu WK, Lau SS, Mayer JW, Muller H, Tu KN. Thin Solid Films 1975;25:393. [illegible]
[10] Foll H, Ho PS. J Appl Phys 1981;52:5510. [illegible]
[11] Pretorius R, Ramiller CL, Nicolet MA. Nucl Instrum Methods Phys Res 1978;149:629. [illegible]
[12] Wittmer M, Tu KN. Phys Rev B 1983;27:1173. [illegible]
[13] Baglin JEE, d'Heurle FM, Hammer WN, Petersson S. Nucl Instrum Methods Phys Res 1980;168:491.
[14] House JE. Principle of chemical kinetics. 2nd ed. America: Academic Press; 2015. ISBN: 978-0-12-356787-1.
[15] Lajzerowicz Jr J, Torres J, Goltz G, Pantel R. Thin Solid Films 1986;140:23. [illegible]
[16] Tu KN, Ziegler JF, Kircher CJ. Appl Phys Lett 1973;23:493.
[17] Barge T, Gas P, d'Heurle FM. J Mater Res 1995;10:1134. [illegible]
[18] Nemouchi F, Mangelinck D, Bergman C, Gas P. Appl Phys Lett 2005;86:041903. [illegible]
[19] Mangelinck D, Hoummada K, Panciera F, El Kousseifi M, Blum I, Descoins M, Bertoglio M, Portavoce A, Perrin C, Putero M. Phys Status Solid A 2014;211:152. [illegible]

© University of Pretoria

UNIVERSITEIT VAN PRETORIA
UNIVERSITY OF PRETORIA
YUNIBESITHI YA PRETORIA

UNIVERSITEIT VAN PRETORIA
UNIVERSITY OF PRETORIA
YUNIBESITHI YA PRETORIA

Journal of Physics and Chemistry of Solids 92 (2016) 64–69

Contents lists available at ScienceDirect

Journal of Physics and Chemistry of Solids

journal homepage: www.elsevier.com/locate/jpcs

Review

The influence of radiation-induced vacancy on the formation of thin-film of compound layer during a reactive diffusion process

S.O. Akintunde *, P.A. Selyshchev

Department of Physics, University of Pretoria, Private Bag X20, Hatfield, Pretoria 0028, South Africa

ARTICLE INFO

Article history:
Received 16 October 2015
Received in revised form
23 December 2015
Accepted 25 January 2016
Available online 26 January 2016

Keywords:
Radiation-induced vacancy
Interfacial reaction
Diffusion
Critical thickness
Thin-film of *AB*-compound layer

ABSTRACT

A theoretical approach is developed that describes the formation of a thin-film of *AB*-compound layer under the influence of radiation-induced vacancy. The *AB*-compound layer is formed as a result of a chemical reaction between the atomic species of *A* and *B* immiscible layers. The two layers are irradiated with a beam of energetic particles and this process leads to several vacant lattice sites creation in both layers due to the displacement of lattice atoms by irradiating particles. *A*- and *B*-atoms diffuse via these lattice sites by means of a vacancy mechanism in considerable amount to reaction interfaces *A*/*AB* and *AB*/*B*. The reaction interfaces increase in thickness as a result of chemical transformation between the diffusing species and surface atoms (near both layers). The compound layer formation occurs in two stages. The first stage begins as an interfacial reaction controlled process, and the second as a diffusion controlled process. The critical thickness and time are determined at a transition point between the two stages. The influence of radiation-induced vacancy on layer thickness, speed of growth, and reaction rate is investigated under irradiation within the framework of the model presented here. The result obtained shows that the layer thickness, speed of growth, and reaction rate increase strongly as the defect generation rate rises in the irradiated layers. It also shows the feasibility of producing a compound layer (especially in near-noble metal silicide considered in this study) at a temperature below their normal formation temperature under the influence of radiation.

© 2016 Elsevier Ltd. All rights reserved.

Contents

1. Introduction 64
2. Model and basic equations 65
3. **The growth of the *AB*-layer** 65
4. Results and discussion 66
5. Conclusion 68
Acknowledgment 68
References 69

1. Introduction

It is a well-established fact that irradiation creates defects in solid materials [1]. These defects are called radiation-induced defects and the simplest of them is termed a Frenkel pair (vacancy–interstitial pair). By means of radiation-induced defects many new channels are created for atomic diffusion in the target material. Atomic diffusion is very important for layer formation in solid-state reaction. The growth of a compound layer at the reaction interface requires both diffusion and a chemical reaction. This process is termed reactive diffusion.

The phenomenon of reactive diffusion is observed experimentally under both non-irradiation [2–5] and irradiation [6–9] conditions. The compound layer growth is shown to obey parabolic law (thickness is proportional to square root of time) in both cases.

In this paper the influence of radiation-induced vacancy is

* Corresponding author.
E-mail addresses: samuel.akintunde@up.ac.za (S.O. Akintunde), selyshchev@gmail.com (P.A. Selyshchev).

http://dx.doi.org/10.1016/j.jpcs.2016.01.020
0022-3697/© 2016 Elsevier Ltd. All rights reserved.

© University of Pretoria

considered on the growth of the compound layer during a reactive diffusion process. Although both vacancy and interstitial defects are created at the same time during irradiation, we take into consideration the situation whereby the contribution of interstitial defect is separated from that of vacancy. With this approach, we are able to determine the contribution of vacancy defects to the growth of a compound layer. We begin by considering the chemical reaction rate as the approximation of product of reactants' atom number densities and assume that the growth rate of the compound layer is proportional to the reaction rate during both interfacial-reaction- and diffusion-controlled stages. Different defect generation rates are taken into account in each irradiated layer in order to determine how it influences the speed of growth, reaction rate, and thickness of a compound layer at a temperature below the compound layer formation under normal heat treatment processes such as conventional furnace and rapid thermal processing.

2. Model and basic equations

Suppose the irradiation of *A*- and *B*-layers leads to the creation of vacancy and interstitial atoms. Let us not consider a very high rate of defect generation; for example, which corresponds to reactor irradiation. In this case, the concentration of interstitial atoms is small, the correlation between fluxes of vacancy and interstitials is weak, and contributions of vacancy and interstitial mechanisms of diffusion can be considered separately. The vacancy mechanism is investigated in the present work.

The number of vacancies in the *AB*-layer increases as the radiation-induced vacancy adds up to the thermally generated ones. We assume that *A*- and *B*-atoms diffuse via a vacancy mechanism through the *AB*-compound layer to reaction interfaces *A/AB* and *AB/B* to form *AB*-compound layer. The thickness of the *AB*-layer formed owing to chemical reaction at interfaces *A/AB* and *AB/B* are designated by $g_a(t)$ and $g_b(t)$ respectively. The total thickness of the compound layer is given by $g(t)=g_a(t)+g_b(t)$. Let the *x*-axis be perpendicular to all the layers under consideration and $g(t)=0$ before irradiation.

The diffusivity of *A*- and *B*-atoms through the vacancy mechanism under irradiation are $D_a^{v,irr}$ and $D_b^{v,irr}$ respectively, and the equation relating the diffusivity under irradiation to that of thermal diffusion is given by:

$$D_a^{v,irr}=\frac{n_a^v D_a^{v,th}}{n_a^{v,th}} \text{ and } D_b^{v,irr}=\frac{n_b^v D_b^{v,th}}{n_b^{v,th}}. \qquad (1)$$

where n_a^v and n_b^v are vacancy concentrations under irradiation, $D_a^{v,th}$ and $D_b^{v,th}$ are diffusivities of *A*-and *B*-atoms via vacancy mechanism due to thermal vacancies, and $n_a^{v,th}$ and $n_b^{v,th}$ are thermal vacancy concentrations for *A*- and *B*-atom sites inside the *AB* layer.

Neglecting the recombination between vacancy and interstitial atoms, we can consider the change of densities of vacancy and interstitial atoms separately and obtain equations for two kinds of vacancy concentrations in the *AB* layer:

$$\frac{dn_a^v}{dt}=Kn_a^0-\frac{\left(n_a^v-n_a^{v,th}\right)}{\tau_a^v} \text{ and } \frac{dn_b^v}{dt}=Kn_b^0-\frac{\left(n_b^v-n_b^{v,th}\right)}{\tau_b^v}. \qquad (2)$$

where *K* is the defect generation rate, n_a^0 and n_b^0 are the number densities of *A*- and *B*-lattice atoms in their respective layers, and τ_v^a and τ_v^b are life-times for *A*- and *B*-vacancy. Because the relaxation of vacancy distribution occurs more quickly than the growth of the *AB*-layer, we assume that the vacancy distribution is homogeneous and stationary: $dn_a^v/dt=0$ and $dn_b^v/dt=0$.

Thus, for *A*- and *B*-vacancy concentrations we obtain:

$$n_a^v=Kn_a^0\tau_a^v+n_a^{v,th} \text{ and } n_b^v=Kn_b^0\tau_b^v+n_b^{v,th}. \qquad (3)$$

Neglecting transient diffusion, we obtain equations for stationary concentration of *A* and *B* atoms inside the *AB* layer:

$$D_a^{v,irr}\frac{\partial^2 n_a(x)}{\partial x^2}=0 \text{ and } D_b^{v,irr}\frac{\partial^2 n_b(x)}{\partial x^2}=0 \qquad (4)$$

with corresponding boundary conditions:
$J_a(x=g_b)=R_a=\nu_a\gamma n_a^0 n_b(x=g_b)$; $J_b(x=-g_a)=R_b=\nu_b\gamma n_b^0 n_a(x=-g_a)$; $n_a(x=-g_a)=n_a^0$; $n_b(x=g_b)=n_b^0$ where J_a and J_b are the fluxes of *A*- and *B*-atoms, R_a and R_b represent the chemical reaction rate at *A/AB* and *AB/B* interfaces and they are not exactly the same, ν_a and ν_b are the stoichiometric coefficients of *A*- and *B*-atoms, and γ is the reaction rate constant. The fluxes of *A*- and *B*-atoms are assumed to occur at the same rate as the chemical reaction in order to ensure that the reaction only occurs at the interface and not inside either the *A*- or *B*-layer bulk.

The speed of growth of the *AB*-layer by virtue of chemical reaction at *A/AB* interface is
$dg_a/dt=V_{ab}R_a=V_{ab}\gamma\, n_a^0 n_b\,(x=-g_a)$ and at *AB/B* is $dg_b/dt=V_{ab}R_b=V_{ab}\gamma\,(n_b^0)^2$, therefore the total speed is $dg/dt=dg_a/dt+dg_b/dt$, and V_{ab} is the volume of one molecule of the *AB*-layer.

By solving (4) with the given boundary conditions, we obtain an expression for the distribution of the *A*- and *B*-atoms inside the *AB*-compound layer:

$$n_a(x)=-\frac{\gamma\left(n_a^0\right)^2}{D_a^{v,irr}}(x+g_a)+n_a^0 \text{ and } n_b(x,t)=\frac{\gamma n_a^0 n_b^0 \nu_b}{D_b^{v,irr}+\gamma n_a^0 \nu_b g(t)}(x-g_b)+n_b^0. \qquad (5)$$

3. The growth of the AB-layer

The rate of chemical reaction at interfaces of solid layers depends on the number densities of the *A* and *B* atoms in a complex manner. However, if there exists an excess of *A*- (or *B*-) atoms, then the rate of reaction remain the same with a change of the number density of *A*- (or *B*-) atoms [10]. On the other hand, if number densities of the *A*- and *B*-atoms approximately equal $\nu_a n_a \approx \nu_b n_b^0$, then the rate of the *AB*-compound formation can be represented in the first approximation as a product of *A*- and *B*-atom number densities.

Thus the rate of chemical reaction between the *A*- and *B*-atoms, at reaction interfaces *A/AB* and *AB/B*, can be approximately expressed in two stages in the following ways:

$$R_a=\begin{cases}\gamma\left(n_a^0\right)^2=\text{const} & \nu_b n_b(x=-g_a)\geq \nu_a n_a^0\\ \gamma n_a^0 n_b(x=-g_a) & \nu_b n_b(x=-g_a)\leq \nu_a n_a^0\end{cases}$$

$$R_b=\begin{cases}\gamma\left(n_b^0\right)^2=\text{const} & \nu_a n_a(x=g_b)\geq \nu_b n_b^0\\ \gamma n_b^0 n_a(x=g_b) & \nu_a n_a(x=g_b)\leq \nu_b n_b^0\end{cases}. \qquad (6)$$

Where $n_b\,(x=-g_a)$ and $n_a\,(x=-g_b)$ are number densities of the *B*-atoms at $x=-g_a$ and the *A*-atoms at $x=-g_b$.

Owing to this, approximating the growth of the *AB* layer can have two stages. The first stage is when there is an excess of one kind of diffusing atom; for example, an excess of the *A*-atoms near interface *AB/B* or an excess of the *B*-atoms near interface *A/AB*. The second stage is when there is no excess of any kind of atoms near the corresponding surface; the second stage can take place

© University of Pretoria

independently of the first stage. However, if there is a first stage, the second stage must follow suit.

Thus, for the first stage, the growth rate of the *AB*-layer is determined by both the diffusion of the *A*- and *B*-atoms inside the *AB*-layer and also by the rate of reaction at the interface:

$$\frac{dg}{dt}=\frac{dg_a}{dt}+\frac{dg_b}{dt}=V_{ab}(R_a+R_b)=V_{ab}\left(\gamma\left(n_a^0\right)^2+\gamma n_b^0 n_a(x=g_b)\right) \quad (7)$$

The number density of the *A*-atom near interface *AB*/*B* and the *B*-atom near interface *A*/*AB* at second stage are:

$$n_a(g_b(t))=\frac{D_a^{v,irr}n_a^0}{D_a^{v,irr}+\gamma n_b^0 v_a g(t)} \text{ and } n_b(-g_a(t))=\frac{D_b^{v,irr}n_b^0}{D_b^{v,irr}+\gamma n_a^0 v_b g(t)} \quad (8)$$

If there is an excess of *A*-atom at the reaction interface, *AB*/*B* at time $t<t_c$, (t_c is the critical time), the *AB*-layer at this interface grows under the interfacial-reaction-controlled process, and at the *A*/*AB* interface, the growth is controlled by diffusion; therefore the relationship between time and layer thickness is found by solving (7):

$$t=\frac{v_a g(t)}{\gamma v_a V_{ab}\left(n_a^0\right)^2}-\frac{D_b^{v,irr}v_a^2}{\gamma^2 v_b^3 V_{ab}\left(n_a^0\right)^3}\ln\left[\frac{\gamma n_a^0 n_b^0 v_b^2 g(t)}{D_b^{v,irr}\left(n_a^0 v_a+n_b^0 v_b\right)}+1\right] \quad (9)$$

However, if there is no excess of *A*-atoms at the reaction interface, no interfacial-reaction-controlled growth would occur at the *AB*/*B* interface, and the growth at both interfaces *A*/*AB* and *AB*/*B* would be predominantly diffusion controlled at all time.

At critical time $t_c\,g(t)=g_c$: $v_a n_a(g_b(t_c))=v_b n_b^0 n_a$; where n_a

$$(g_b(t_c))=\frac{D_a^{v,irr}n_a^0}{D_a^{v,irr}+\gamma n_b^0 v_a g_c} \quad (10)$$

Critical thickness, g_c, is obtained as follows:

$$g_c=\frac{D_b^{v,irr}(n_a^0 v_a-n_b^0 v_b)}{\gamma v_a v_b\left(n_a^0\right)^2} \quad (11a)$$

And for critical time substitute $t=t_c$, and $g=g_c$ in (9)

$$t_c=\frac{v_a g_c}{\gamma v_b V_{ab}\left(n_a^0\right)^2}-\frac{D_b^{v,irr}v_a^2}{\gamma^2 v_b^3 V_{ab}\left(n_a^0\right)^3}\ln\left[\frac{\gamma n_a^0 n_b^0 v_b^2 g_c}{D_b^{v,irr}\left(n_a^0 v_a+n_b^0 v_b\right)}+1\right] \quad (11b)$$

The growth rate of the compound layer at $t>t_c$ is described by:

$$\frac{dg(t)}{dt}=\gamma V_{ab}\left(n_a^0 n_b(-g_a(t))+n_b^0 n_a(g_b(t))\right) \quad (12)$$

By inserting (8) into (12) and integrating the resulting equation, a connection between time and layer thickness is established:

$$t=t_c+\alpha_1(g^2(t)-g_c^2)+\alpha_2(g(t)-g_c)-\alpha_3\ln\left[\frac{\alpha_4 g(t)+\alpha_5}{\alpha_4 g_c+\alpha_5}\right] \quad (13)$$

where

$$\alpha_1=\left[2\gamma V_{ab}\left[D_a^{v,irr}n_a^0+D_b^{v,irr}n_b^0\right]\right]^{-1},\ \alpha_2=\left[\left(D_a^{v,irr}n_a^0\right)^2+\left(D_b^{v,irr}n_b^0\right)^2\right]\left[\gamma V_{ab}n_a^0 n_b^0\left[D_a^{v,irr}n_a^0+D_b^{v,irr}n_b^0\right]^2\right]^{-1},\ \alpha_3=D_a^{v,irr}D_b^{v,irr}\left[D_a^{v,irr}n_a^0-D_b^{v,irr}n_b^0\right]^2\left[\gamma^2 V_{ab}n_a^0 n_b^0\left[D_a^{v,irr}n_a^0+D_b^{v,irr}n_b^0\right]^3\right]^{-1},\ \alpha_4=\gamma\left[D_a^{v,irr}n_a^0+D_b^{v,irr}n_b^0\right],\ \alpha_5=D_a^{v,irr}D_b^{v,irr}.$$

4. Results and discussion

The growth kinetics of the thin-film of *AB*-compound layer expressed in (9) shows time as a linear and natural logarithmic function of thickness, and in (13) as a parabolic and natural logarithmic function of compound layer thickness. The natural logarithmic function in both (9) and (13) is ascribed to the simultaneous diffusion of both the *A* and *B*-atomic species via vacancy mechanisms during the compound layer growth.

If, for instance, only *A*-atoms diffuse in *AB*-layer when $D_b^{v,irr}=0$ Eq. (9) becomes a linear equation:

$$g(t)=V_{ab}\gamma\left(n_a^0\right)^2(v_a)^{-1}v_b t. \quad (14)$$

and (13) reduces to parabolic equation:

$$\gamma n_b^0(g^2(t)-g_c^2)+2D_a^{v,irr}(g(t)-g_c)-2\gamma V_{ab}D_a^{v,irr}n_a^0 n_b^0(t-t_c)=0 \quad (15)$$

and if only *B*-atoms diffuse when $D_a^{v,irr}=0$, linear growth will be absent, only the parabolic law will hold Eq. (13), therefore, becomes:

$$\gamma n_a^0 g^2(t)+2D_b^{v,irr}g(t)-2\gamma V_{ab}D_b^{v,irr}n_a^0 n_b^0 t=0 \quad (16)$$

Irradiation influences the growth of the *AB*-layer via change of diffusivity due to the production of the vacancy at rate *K*. Let us assume that the *A*-atoms diffuse only via vacancies of the *A*-sub-lattice of the *AB* compound and *B*-atoms via the *B*-sub-lattice, accordingly. This means that we consider diffusion of the *A*- and *B*-atoms separately and $D_{a(b)}^v=(n_{a(b)}^v D^{v,a(b)})/n_{a(b)}$; taking into account that

$(\tau_{v,a(b)}^{AB})^{-1}=(\rho d)_{a(b)}D_a^{v,a(b)}$ and $n_a^0=v_a\ n_0$, $n_b^0=v_b\ n_0$. Where $(\rho d)_a$ and $(\rho d)_b$ are the dislocation densities of *A*- and *B*-crystals, $D^{v,a}$ and $D^{v,b}$ are diffusivities of *A*-and *B*-vacancies, n_a and n_b are number densities of *A*- and *B*-atoms inside the *AB* layer. D_a^v and D_b^v are diffusivities of the *A*- and *B*-atoms via vacancy-mediated process; from (1) we obtain:

$$D_{a(b)}^{v,irr}=D_{a(b)}^{v,th}+\frac{K}{\rho_d V_{a(b)}n_0} \quad (17)$$

Where n_0 is the density of the *AB*-molecule. Thus, diffusivity is a linear function of the defect generation rate and we can estimate influence of irradiation using (9), (11), (13)–(16).

Based on the model described above, we estimate the speed of growth, reaction rate, and layer thickness of three near-noble metal silicides at room temperature under irradiation with a defect generation rate of $K=10^{-3}$, 10^{-4}, and 10^{-7} dpa/s. The reason for selecting this set of values was stated in the model and basic equation section. The thin-film of near-noble metal silicides is considered in this study because of their technological application and importance in integrated circuits [11].

The diffusivity under irradiation is estimated for the *A*- and *B*-atoms in A_2B-layers of palladium silicide, nickel silicide, and platinum silicide using (17) where *A*-atom represents near noble metal and *B*-atom denotes silicon. The result obtained from the diffusivity of both Pd- and Si- atoms as diffusing species under irradiation is shown in Table 1. The diffusivity of silicon is estimated to be about 10^4 times faster than that of palladium, which makes silicon the dominant species in the Pd_2Si layer. Similar results are shown in Tables 2 and 3 for nickel silicide, Ni_2Si, and platinum silicide, Pt_2Si. This result is contrary to the report in [12–14] where palladium, nickel, and platinum were reported as the dominant species under thermal diffusion. The same view holds for the other near-noble metal silicides where the metals were seen as the main diffusing species during the silicide growth [2,12–13] in the first compound phase. Tables 5 and 6 contain data for the estimation of thermal self-diffusivity of Pd, Si, Ni, and Pt in

© University of Pretoria

UNIVERSITEIT VAN PRETORIA
UNIVERSITY OF PRETORIA
YUNIBESITHI YA PRETORIA

Table 1
Estimation of diffusivity of palladium and silicon in Pd_2Si layer under irradiation together with speed of growth and reaction rate of the layer.

D_a^{irr} (Pd) (10^{-20} m^2/s)	D_b^{irr} (Si) (10^{-20} m^2/s)	dg_a/dt (10^{-8} m/s)	dg_b/dt (10^{-7} m/s)	R_a ($10^{20}/m^2s$)	R_b ($10^{21}/m^2s$)	K (dpa/s)	γ (10^{-16} m^4/s)
0.047	0.021	0.290	0.120	0.680	0.275	10^{-9}	0.110
0.470	0.210	0.900	0.330	2.100	0.775	10^{-8}	0.310
4.700	2.100	3.200	1.200	7.600	2.750	10^{-7}	1.100

Table 2
Estimation of speed of growth and reaction rate of Ni_2Si layer with diffusivity of nickel and silicon in Ni_2Si layer under irradiation.

D_a^{irr} (Ni) (10^{-20} m^2/s)	D_b^{irr} (Si) (10^{-20} m^2/s)	dg_a/dt (10^{-9} m/s)	dg_b/dt (10^{-8} m/s)	R_a ($10^{19}/m^2s$)	R_b ($10^{20}/m^2s$)	K (dpa/s)	γ (10^{-17} m^4/s)
0.028	0.015	0.220	0.062	0.670	0.190	10^{-9}	0.075
0.280	0.150	0.770	0.190	2.300	0.575	10^{-8}	0.230
2.800	1.500	2.500	1.400	7.500	4.100	10^{-7}	1.640

Table 3
Estimation of diffusivity of platinum and silicon in Pt_2Si layer under irradiation and also the speed of growth and reaction rate of the layer.

D_a^{irr} (Pt) (10^{-20} m^2/s)	D_b^{irr} (Si) (10^{-20} m^2/s)	dg_a/dt (10^{-8} m/s)	dg_b/dt (10^{-7} m/s)	R_a ($10^{20}/m^2s$)	R_b ($10^{21}/m^2s$)	K (dpa/s)	γ (10^{-16} m^4/s)
0.014	0.022	0.290	0.028	0.675	0.065	10^{-9}	0.026
0.140	0.220	0.960	0.240	2.200	0.550	10^{-8}	0.220
1.400	2.200	3.500	2.400	8.100	5.500	10^{-7}	2.200

Table 4
Near-noble metal silicide formation temperature under non-irradiation condition (culled from [12]).

Compound layer	Temperature (K)
Pd_2Si	373
Ni_2Si	473
Pt_2Si	473

their respective silicides. However, the growth of silicides under irradiation from our theoretical study indicate a view different from thermal diffusion in terms of the predominant diffusing species during the silicide formation, especially for the three silicides considered in this work. The estimated values of diffusivity of silicon in the three silicide layers under different defect generation rates at room temperature yielded results that lie within the range of integrated inter-diffusion coefficients of these silicides at their formation temperatures [2–5,15] and this also strongly corroborates silicon as the active diffusing species in the silicide layer under irradiation. The formation temperature of these silicides are shown in Table 4.

The results depicted in Tables 1–3 show that the speed of growth and reaction rate increase as the defect creation rate rises in the irradiated layer. This is as a result of opening of several channels (i.e. creation of vacant sites) in the irradiated layers for a considerable amount of atoms to diffuse to the reaction interface. The result also shows that the reaction in each layer proceeds at a different rate; likewise the layer growth speed. This difference can be attributed to the number of surface atoms present at the reaction interface during the layer formation. The interface that has more surface atoms has a greater chance of producing the compound layer faster than one with fewer atoms.

The layer thickness depicted in Figs. 1–3 show that the growth of the compound layer depends strongly on the defect generation rate. For instance, the temperature considered in this study is too low for silicide formation to take place in the absence of radiation. In the literature it has been reported that silicide formation can occur at a temperature much lower than room temperature (−120 °C) [16]. The tendency of producing silicides at a temperature as low as room temperature is highly feasible since radiation-enhanced diffusion depends strongly on a defect generation rate at such a low irradiation temperature.

The growth kinetics shown in Figs. 1–3 depict a parabolic dependence of layer thickness on time. This result can be explained in light of the first phase of near-noble metal silicide.

In metal-rich silicide, metal is the majority species while silicon is the minority atoms. According to the model presented here, if 'majority atoms' (metal in this case) are active (i.e. dominant) during the layer growth, a reaction-controlled process would occur for a certain period of time and change to diffusion controlled process after which the growth kinetics has transformed to parabolic. However, if the dominant atoms are the minority species, then the layer growth would begin and end as a parabolic growth under a diffusion-controlled process. In a similar manner, silicon is presented as the minority and dominant species in the first

Table 5
Parameters used for estimation of thermal self-diffusion coefficients of Pd, Ni, Pt, and Si in their respective silicides.

Volume of compound layer (10^{-29} m^3)	Diffusing species under non-irradiation condition	Diffusing species under irradiation condition	Pre-exponential factor D_0 (m^2/s) for non-irradiation condition for atomic species	Activation energy E_a (eV) for non- irradiation condition for atomic species
Pd_2Si, (4.2)	Pd, Si [2]	Pd, Si [17]	Pd (1.5×10^{-5}) [14], Si (6.24×10^{-4}) [14]	Pd (1.0) [14], Si (1.7) [14]
Ni_2Si, (3.2)	Ni [12]	Ni, Si Present work	Ni (1.82×10^{-5}) [2], Si (8.95×10^{-4}) [18]	Ni (1.71) [2], Si (1.9) [18]
Pt_2Si, (4.3)	Pt [13]	Pt, Si Present work	Pt (5.5×10^{-5}) [19], Si (3.59×10^{-4}) [18]	Pt (1.485) [19], Si (2.1) [18]

© University of Pretoria

UNIVERSITEIT VAN PRETORIA
UNIVERSITY OF PRETORIA
YUNIBESITHI YA PRETORIA

UNIVERSITEIT VAN PRETORIA
UNIVERSITY OF PRETORIA
YUNIBESITHI YA PRETORIA

Table 6
Parameters used for estimation of diffusion coefficient under irradiation at temperature of 298 K.

Atomic species	Dislocation density (10^8 m^{-2})	Vacancy formation energy for atomic species (eV)	Estimated value for number density of *AB*-molecule (10^{28} molecule/m^3)	Number density of atomic species (10^{28} atoms/m^3)
Pd	3000 [20]	1.70 [24]	Pd_2Si, (2.4)	Pd, (6.80)
Ni	5000 [21]	1.55 [25]	Ni_2Si, (3.3)	Ni, (9.14)
Pt	< 1000 [22]	1.35 [26]	Pt_2Si, (2.3)	Pt (6.50)
Si	1.0 [23]	2.32 [27]		Si (5.00)

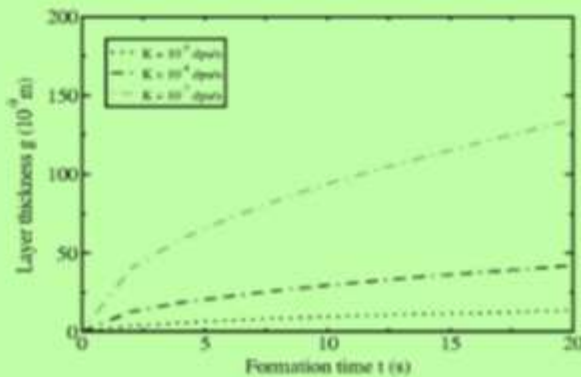

Fig. 1. The growth kinetics of palladium silicide Pd_2Si at room temperature under the influence of radiation-induced vacancy at defect generation rate of $K = 10^{-6}$, 10^{-8}, and 10^{-7} dpa/s.

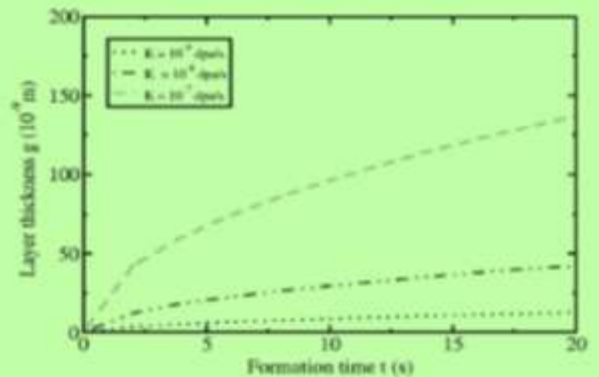

Fig. 3. The growth kinetics of platinum silicide Pt_2Si at room temperature under the influence of radiation-induced vacancy at defect generation rate of $K = 10^{-6}$, 10^{-8}, and 10^{-7} dpa/s.

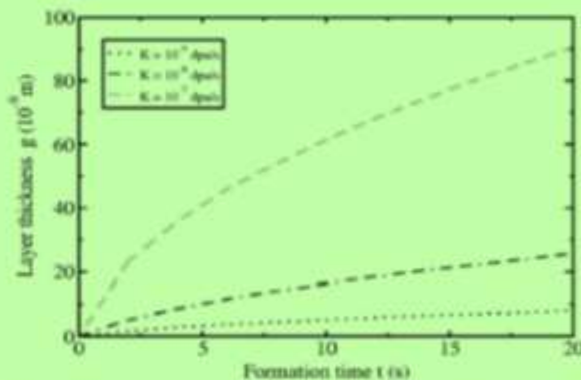

Fig. 2. The growth kinetics of nickel silicide Ni_2Si at room temperature under the influence of radiation-induced vacancy at defect generation rate of $K = 10^{-6}$, 10^{-8}, and 10^{-7} dpa/s.

compound phase of these silicides. Therefore, only one stage of growth is plausible (i.e. the parabolic growth). The silicide thickness is estimated with (13) (when $g_c = 0$ and $t_c = 0$) over a period of 20 s at different defect generation rates in the three silicide layers.

5. Conclusion

The results that follow from this study indicate that a thin-film of *AB*-compound layer is feasible under radiation-enhanced diffusion (radiation-induced vacancy type) for an *AB*-compound layer at a temperature lower than the formation temperature. The reason for this feasibility can be attributed to the dependence of diffusivity of atom, via vacancy mechanism, on defect generation rate at a low irradiation temperature. At such a low temperature, irradiation creates a number of vacant lattice sites in the *A*- and *B*- solid layers via which a substantial amount of *A*- and *B*- atoms are transported to the reaction interfaces, where they chemically react with surface atomic species that are close to the interfaces, thereby forming an *AB*-compound. The influence of room temperature on atomic diffusivity via vacancy is insignificant and cannot possibly enhance any growth at the reaction interfaces.

The results of this study also indicate that time dependence of layer thickness, i.e. growth kinetics, has both linear and natural logarithmic functions during the interfacial-reaction-controlled stage and parabolic and natural logarithmic functions during the diffusion-controlled stage. The reason for this result is ascribed to two forms of vacancy mechanisms in the *AB*-compound layer; one is an *A*-vacancy mechanism for the transport of *A*-atoms, and the other is the *B*-vacancy mechanism for transport of *B*-atoms. Lastly, we are able to show that defect generation rate enhances speed of growth, reaction rate and thickness of compound layer at low irradiation temperature.

Acknowledgment

This research work is financially motivated by the National Research Foundation (NRF) of South Africa.

© University of Pretoria

References

[1] H. Schmalzried, Chemical Kinetics of Solids, VCH, Weinheim, New York, Basel, Cambridge, Tokyo (1995), p. 433, ISBN: 3-527-29094-X.
[2] A. Portavoce, K. Hoummada, F. Dahlem, Surf. Sci. **624** (2014) 135, http://dx.doi.org/10.1016/j.susc.2014.02.011.
[3] L.S. Hung, J.W. Mayer, C.S. Pai, S.S. Lau, J. Appl. Phys. **58** (1985) 1527, http://dx.doi.org/10.1063/1.336086.
[4] D. Levy, A. Grob, J.J. Grob, J.P. Ponpon, Appl. Phys. A **35** (1984) 141, http://dx.doi.org/10.1007/BF00616966.
[5] J.P. Ponpon, A. Saulnier, Semicond. Sci. Technol. **4** (1989) 526, http://dx.doi.org/10.1088/0268-1242/4/7/005.
[6] G.J. Dienes, A.C. Damask, J. Appl. Phys. **29** (1713) (1958) 1958, http://dx.doi.org/10.1063/1.1723032.
[7] R.L. Myers, D.G. Nelson, J.F. Gibbons, J. Appl. Phys. **43** (1972) 3468.
[8] S.M. Myers, D.E. Amos, D.K. Brice, J. Appl. Phys. **47** (1976) 1812, http://dx.doi.org/10.1063/1.322897.
[9] H. Niehus, R. Spitzl, Surf. Int. Anal. **17** (1991) 287.
[10] R. Schmid, V.N. Sapunov, Non-Formal Kinetics, Verlag Chemie GmbH, Weinheim, Germany (1982), p. 264.
[11] L.J. Chen, An Integral Part of Microelectronics, JOM **57** (2005) 24, http://dx.doi.org/10.1007/s11837-005-0111-4.
[12] V.E. Borisenko, P.J. Hesketh, Micro Device (1977) 149–191.
[13] S.P. Murarka, Silicides for VLSI Applications, Academic Press, New York, 1983, ISBN: 9780125112208.
[14] E.C. Zingu, J.W. Mayer, C. Comrie, R. Pretorius, Phys. Rev. B **30** (1984) 5916, http://dx.doi.org/10.1103/PhysRevB.30.5916.
[15] F. Nemouchi, D. Mangelinck, C. Bergman, P. Gas, Appl. Phys. Lett. **86** (2005) 041903, http://dx.doi.org/10.1063/1.1852727.
[16] R.Y. Lee, C.N. Whang, H.K. Kim, R.J. Smith, Nuclear Instrum. Methods Phys. Res. B **33** (1988) 661, http://dx.doi.org/10.1016/0168-583X(88)90654-4.
[17] C.N. Whang, H.K. Kim, R.Y. Lee, R.J. Smith, J. Mater. Sci. **24** (1989) 270, http://dx.doi.org/10.1007/BF00660965.
[18] A.P. Botha, S. Kritzinger, Thin Solid Films **141** (1986) 41, http://dx.doi.org/10.1016/0040-6090(86)90317-2.
[19] T. Stark, H. Grunleitner, M. Hundhausen, L. Ley, Thin Solid Films **358** (2000) 73, http://dx.doi.org/10.1016/S0040-6090(98)00699-0.
[20] A.N. Bekrenev, A.D. Vasiliev, Russ. Phys. J **39** (1996) 502.
[21] D.A. Hughes, N. Hansen, Acta Mater. **48** (2000) 2993, http://dx.doi.org/10.1016/S1359-6454(00)00082-3.
[22] A. Cizek, F. Parizek, A. Orlova, J. Tousek, Czech. J. Phys. B **20** (1970) 56, http://dx.doi.org/10.1007/BF01698107.
[23] J.M. Po, D.M. Pera, M.C. Brito, J.M. Alves, and A.M. Vallera, EU PVSEC Proceedings, 722–724 (//www.eupvsec-proceedings.com/proceedings?paper=30804)), http://dx.doi.org/10.4229/EUPVSEC20142014-2AV.3.19.
[24] T.R. Mattsson, A.E. Mattsson, Phys. Rev. B **66** (2002) 214110, http://dx.doi.org/10.1103/PhysRevB.66.214110.
[25] H. Mattes, J. Winter, W. Triftshauser, Appl. Phys. **20** (1979) 135, http://dx.doi.org/10.1007/BF00885934.
[26] W. Pfeiler, Alloy Physics: A comprehensive Reference, Technology and Engineering, J. Wiley and Sons, Hoboken, New Jersey USA (2008), p. 1003, ISBN: 978-3527313214.
[27] R.A. Swalin, J. Phys. Chem. Solids **23** (1962) 154.

© University of Pretoria